NASA TECHNICAL REPORT

NASA TR R-423

CALIBRATION OF THE LANGLEY 16-FOOT TRANSONIC TUNNEL WITH TEST SECTION AIR REMOVAL

by Blake W. Corson, Jr., Jack F. Runckel, and William B. Igoe

Langley Research Center
Hampton, Va. 23665

NATIONAL AERONAUTICS AND SPACE ADMINISTRATION • WASHINGTON, D. C. • AUGUST 1974

CONTENTS

CALIBRATION OF THE LANGLEY 16-FOOT TRANSONIC TUNNEL

WITH TEST SECTION AIR REMOVAL

By Blake W. Corson, Jr., Jack F. Runckel,
and William B. Igoe
Langley Research Center

SUMMARY

The Langley 16-foot transonic tunnel with test section air removal (plenum suction) has been calibrated to a Mach number of 1.3. The results of the calibration, including the effects of slot shape modifications, test section wall divergence, and water vapor condensation, are presented. A complete description of the wind tunnel and its auxiliary equipment is included.

The relatively wide slot, which was near optimum without test section air removal, did not yield uniform distributions of static pressure in the test section at the higher Mach numbers obtained with test section air removal. After some experimentation, this wide (13.5 percent open periphery) slot was subsequently replaced by a relatively narrow (3.9 percent open periphery) slot which permitted the achievement of acceptably uniform flow at Mach numbers to 1.3. For most operating conditions, increased wall divergence angle caused a positive increment in the test section static-pressure gradient; this increment permitted cancellation of the negative static-pressure gradient caused by water vapor condensation effects due to operation with moist air at near maximum speeds.

The wind-tunnel drive power required at subsonic speeds was reduced by about 10 percent with the narrow slot. At supersonic speeds, operation of the tunnel with moist air required 3 to 5 percent more power than was required with relatively dry air, and operation of the tunnel with test section air removal required less power than would be required if all the power were expended through the main drive fans.

INTRODUCTION

The 16-foot transonic tunnel at the Langley Research Center of the National Aeronautics and Space Administration is a single-return atmospheric wind tunnel having a slotted transonic test section with a Mach number range from 0.2 to 1.3. Because the configuration of the present wind tunnel is the result of several major revisions, a brief résumé of this development is presented.

The original wind tunnel was designed and built in the expansion period of the National Advisory Committee for Aeronautics (NACA) prior to World War II and was put into operation in November 1941 as the Langley 16-foot high-speed tunnel. The original tunnel had a closed circular test section 4.88 m (16 ft) in diameter and was driven by two 5.97-MW (8000 hp) electric motors mounted in the return passage. The drive motors were directly coupled to counterrotating fans operating in tandem at the extremities of the motor nacelle. The wind tunnel was cooled by air exchange, the control room was operated at test section pressure, and the maximum test section Mach number was 0.71. The facility was designed and used primarily for aircraft engine cooling and cowling tests and for investigation of the aerodynamic characteristics of full-scale propellers, as typified by the work of references 1 and 2. No description and calibration report was prepared for the original wind tunnel.

The need for increased air speed capability led to major revision of the original tunnel, and this redesign and alteration proceeded for several years prior to 1950. During this time the development of the slotted-wall transonic test section by the NACA was reduced to practice (refs. 3 and 4) and this type of test section was selected for the revised tunnel. The major revisions which were incorporated in the modification consisted of a 44.76-MW (60 000 hp) drive system, the installation of air filters in the air exchange system, acoustical treatments, a new control room, and an octagonal slotted transonic test section. The repowered facility, designated the "Langley 16-foot transonic tunnel," was placed in operation on December 6, 1950. (See ref. 5 for description of the wind tunnel and its calibration to a Mach number of 1.10.) Work planned for the repowered tunnel pertained to the extension of propeller aerodynamic data to supersonic speeds (ref. 6) and to extensive study of jet effects on aircraft performance For the jet-exit research, a special hydrogen peroxide monopropellant system, described in reference 7, was developed.

After the repowering of the tunnel in 1950, several factors combined to indicate the need for a further increase in maximum speed. In tests of models of moderate size in the Mach number range from 1.03 to 1.10, flow disturbances generated at the nose of a model and reflected from the test section walls back to the model afterbody frequently resulted in force measurements, especially drag, which were not representative of free-flight conditions. The uncertainty involved in the application of aerodynamic theory in the transonic speed range made desirable the attainment of a low but clearly supersonic speed from which there might be a tie-in with data obtained at higher speeds in supersonic wind tunnels. Also, the rapid development of aircraft and missiles having supersonic speed capability and the necessity for these and reentry vehicles and spacecraft to negotiate the transonic speed regime emphasized the importance of experimental aerodynamic research at transonic speeds. Design studies, based on work of which reference 8

2

is typical, indicated that the application of test section air removal was the most economical method for extending the test section air speed to a low supersonic value.

The most recent repowering of the Langley 16-foot transonic tunnel, which is the subject of this paper, required primarily the provision of a 26.86-MW (36 000 hp) compressor capable of removing about 4.5 percent of the tunnel mass flow by way of the test section wall slots and surrounding plenum, the removed air being exhausted to the atmosphere. The wind tunnel with this test section air removal system was placed in operation on March 9, 1961. The maximum test section Mach number is slightly greater than 1.30.

This report presents a description of the Langley 16-foot transonic tunnel and its auxiliary equipment, a description of the calibration procedures, and the results of the initial wind-tunnel calibration with test section air removal. Inasmuch as the attainment of a satisfactory axial distribution of Mach number within the test section required the investigation of 11 additional slot configurations, the results of these studies are also included.

SYMBOLS

Values are given in both the International System of Units (SI) and U.S. Customary Units. The measurements and calculations were made in the U.S. Customary Units.

A   cross-sectional area

A_p cross-sectional area of surge control valve pipe

A_v area of sonic surface between valve disk and pipe wall of surge control valve

A_{107} test section cross-sectional area at station 107, 18.502 m^2 (199.15 ft^2)

a   surge control valve inlet loss, fraction of total pressure, $\Delta p_t/p_t$

b   function of surge control valve position, $(1 - \cos \theta)\left(A_p/A_{v,max}\right)$

c   a function of the ratio of motor operating speed to synchronous speed (see fig. 7 of ref. 9)

H   equivalent pressure altitude

M   Mach number

dM/dx	Mach number gradient
$\dot{m}$	mass flow at wind-tunnel throat
$\dot{m}_c$	mass flow through air removal compressor, $\dot{m}_s + \dot{m}_v$
$\dot{m}_s$	secondary mass flow (mass flow scavenged from plenum surrounding test section)
$\dot{m}_v$	mass flow through surge control valve (bypass air)
N	compressor rotational speed
P	power
p	static pressure
p_a	atmospheric pressure
$p_{a,o}$	standard atmospheric pressure, 10.13 N/cm^2 (2116 lb/ft^2)
p_t	stagnation pressure
p_{107}	tunnel wall static pressure at station 107 (throat)
q	dynamic pressure
R	gas constant; for air, 287 (m/sec)^2/K (1716 (ft/sec)^2/$^\circ$R)
r/R	fraction of radial distance from tunnel center line to slot center line
T_t	stagnation temperature
$T_{t,A}$	average stagnation temperature at given Mach number on or near tunnel center line
x	axial distance
γ	ratio of specific heats, 1.4 for air

4

δ test section wall divergence angle with respect to tunnel center line

θ surge control valve disk angle (valve closed at $\theta = 0^O$; valve full open at $\theta = 90^{\,\gamma})$

μ relative mass flow through surge control valve, $\dot{m}_V/\dot{m}_{V,\max}$

τ plenum valv· setting, percent open

Subscripts:

e   compressor exit

corr   corrected

i   compressor inlet

l local

max   maximum

meas   measured

ref   reference

WIND TUNNEL AND EQUIPMENT

Wind Tunnel

Arrangement.- The Langley 16-foot transonic tunnel is a single-return atmospheric wind tunnel having a slotted transonic test section. An exterior view of the facility is shown in figure 1, a phantom view (without air removal equipment) in figure 2, and a schematic diagram in figure 3. Starting at station 0 (fig. 3), the major components are the quiescent chamber, entrance cone, test section, diffuser, power section, return passage, and air exchange section. There are four sets of turning vanes located at the respective 90° elbows in the tube and two antiturbulence screens, one in the air exchange section and another in the quiescent chamber. The length of the tunnel circuit along the center line is 283.46 m (930 ft), the maximum inside diameter of the large end of the tunnel is 17.68 m (58.0 ft), and the test section is a regular octagonal cylinder having a cross-sectional area slightly less than that of a 4.88-m-diameter (16 ft) circle. The test

section air removal equipment is located outside the tunnel between the diffuser and the return passage. The axial locations and dimensions of the major components of the wind tunnel are given in table I.

Quiescent chamber and entrance cone.- The dimensions of these components provide a contraction ratio of 13.31 between the large end of the wind tunnel and the test section. At test section Mach numbers above 1.0, the average air speed in the quiescent chamber is 16.46 m/sec (54 ft/sec). This low velocity region downstream of the antiturbulence screen permits further decay of residual turbulence prior to acceleration of the airstream through the entrance cone and into the test section. The entrance cone incorporates a transition from circular to octagonal cross sections and includes a slowly converging accurately finished entrance liner which terminates at the upstream end of the test section.

Test section.- The test section is an octagonal cylinder vented to a surrounding plenum through slots at the corners of the octagon. This component is described in detail in a subsequent section of this report.

Diffuser.- The overall diffuser extends from the downstream end of the test section to the power section. Because the diffuser entrance, which begins at station 42.06 m (138 ft), includes the diffuser entrance vanes, the cross section of the tunnel in this region has 16 sides and is of variable geometry. Downstream of station 46.94 m (154 ft), the diffuser geometry is fixed except for expansion joints. The function of the diffuser is to decelerate the airstream after its passage through the test section and thereby to convert as much as possible of its kinetic energy into pressure energy.

Power section and drive fans.- The wind-tunnel tube at the drive end has a constant diameter of 10.36 m (34 ft), and the power section includes two 90° elbows which incorporate, respectively, the first and second sets of turning vanes. The arrangement of the major components of the tunnel drive end is indicated in figures 2 and 3. The two main drive motors, housed outside the tunnel, are each connected directly to one of the drive fans through a shaft about 18.29 m (60 ft) long. The enclosure which houses the fan hubs, jack shafts, and bearing pedestals for both units has a streamlined shape with a maximum diameter of 6.10 m (20 ft) in the vicinity of the fan stations. The leading edge of this enclosure at station 107.90 m (354 ft) is just downstream of the first set of turning vanes. Downstream of the fans, however, the requirement of a gradual tapering of the afterbody resulted in an enclosure length extending downstream of the second set of turning vanes. The enclosure afterbody has a 90° elbow at the turning vanes to maintain its alinement with the airstream and terminates at station 152.49 m (500.3 ft). The drive shafts are enclosed in a streamlined fairing between the tunnel wall and the enclosure, and quick access to the shafts and hubs is provided by rail cart (prone) through these fairings.

The two main drive electric motors are of the wound rotor type and each is rated for continuous operation at 17.16 MW (23 000 hp) at a rotational speed of 340 rpm, for

6

2 hr of operation at 22.38 MW (30 000 hp) at 366 rpm, and for 1/2 hr of operation at 25.36 MW (34 000 hp) at 372 rpm. The rotational speed of the motors is controlled by a modified Kramer system which permits essentially continuous variation of speed from 60 rpm to 372 rpm.

The drive fans constitute a two-stage axial-flow compressor having two sets of counterrotating blades with no stator blades. A photograph of the drive fans and of the tunnel interior in this region is shown as figure 4. The fans are 10.36 m (34.0 ft) in diameter less 5.1 mm (0.2 in.) radial clearance between blade tip and tunnel wall. The fan blades are made of laminated spruce. The upstream fan has 25 blades and the downstream unit has 26 blades. The blades have Clark Y airfoil sections and the average solidity of each fan is about 0.8. The adiabatic efficiency of the fan system is 96 percent. The aerodynamic design is based on the procedures outlined in reference 10, with blade interference corrections obtained from reference 11. The axial space between the two fan hubs is occupied by a floating spinner 2.44 m (8.0 ft) long and 6.10 m (20 ft) in diameter which represents a continuation of the shaft enclosure contour. This spinner is supported on bearings housed in the ends of the fan drive shafts and is restrained from rotating by two small cables.

Return passage.- The return passage upstream of the air exchange section is a large conical diffuser and downstream, a cylinder. Dimensions of these components are given in table I. The primary function of the return passage is to duct reenergized air from the power section through the air exchange section back to the quiescent chamber. Air velocities throughout the return passage are too low to yield much pressure recovery in the diffuser portion of the return passage. The cylindrical portion has two 90° elbows which incorporate the third and fourth sets of turning vanes.

Air exchange section.- The air exchange section serves to cool the wind-tunnel airstream and to provide scavenging of exhaust gases when engines are under investigation in the test section. All the energy expended through the main drive fans is eventually converted into heat which elevates the airstream temperature. With no cooling of the wind tunnel during operation at high power, the airstream temperature would increase rapidly to a dangerous level. In most high-speed wind tunnels, the airstream is cooled by a water-cooled heat exchanger. An important advantage of that method of cooling is that the wind tunnel may be a closed circuit charged with dry air to avoid condensation. The Langley 16-foot transonic tunnel was designed primarily for investigation of propulsion system effects on airframe aerodynamic characteristics. Investigations of this type frequently entail the operation in the test section of real engines emitting hot and toxic exhaust gases which must be scavenged continuously from the wind-tunnel airstream. The process of cooling by air exchange consists of exhausting a part of the wind-tunnel airstream which has become heated and by replacing the heated air with cool ambient air. The air exchange section which performs this function is shown in figures 2 and 3. A

7

photograph from inside the return passage looking downstream (fig. 5) shows in the foreground the air exchange exhaust openings which duct the heated boundary-layer air out of the wind-tunnel tube and into the exchange tower. Farther downstream may be seen the inner surfaces of the intake louvers, and in the far background are the third set of turning vanes. The air exchange section basically is a constriction in the return passage with exhaust and intake openings located, respectively, upstream and downstream of the constricted cross section. Both exhaust and intake openings are essentially annular, each having 36 segments equipped with adjustable louvers. The interconnected intake louvers are manually adjustable and are generally left in an open position. The interconnected exhaust louvers are mechanically actuated, and heated air exhaust is subject to quick adjustment during a test for partial control of airstream stagnation temperature. Air exchange can be varied between 5 and 20 percent of the tunnel mass flow. When test section air removal is applied, the air exchange intake mass flow exceeds the exhaust by the amount being removed from the test section plenum. The air exchange section is housed in a rectangular tower with baffles which duct the heated exhaust out of the top of the tower while cool air is taken in at the sides near the top. Dust is removed from the intake air by filters. In both intake and exhaust, acoustic baffles are used to attenuate tne noise which issues from these openings.

Antiturbulence screens.- Two antiturbulence screens, each composed of a single layer of square mesh woven wire, are installed one in the air exchange section and the other in the quiescent chamber (fig. 3). The screens have the following dimensions and characteristics:

	Quiescent chamber		Air exchange section	
Axial station	0.70 m	(2.3 ft)	227.75 m	(747.2 ft)
Screen diameter	17.68 m	(58 ft)	17.07 m	(56 ft)
Wire diameter	1.37 mm	(0.054 in.)	2.03 mm	(0.080 in.)
Wire center-line spacing . .	4.24 mm	(0.167 in.)	11.28 mm	(0.444 in.)
Screen solidity	0.56		0.325	
Pressure loss, $\Delta p/q$ . . .	2.5		0.650	

In addition to reducing turbulence, the screen in the air exchange section also increases the effectiveness of the air exchange by creating a slight pressure drop between exhaust and intake.

Test Section

General description.- Overall views of tne test section incorporating the axial center-line survey tube are shown in figure 6(a), a view from the quiescent chamber, and in figure 6(b), a view from the diffuser. The test section and diffuser entrance, which are

the portions of the wind tunnel having variable geometry, extend from station 32.61 m (107 ft) to station 46.94 m (154 ft) as indicated in figure 7. The cross section at station 32.61 m (107 ft) is a closed regular octagon having an area of 18.50 m^2 (199.15 ft^2). Other sections are also octagonal but are open at the corners, and cross-sectional area varies with test section wall divergence. The feature which gives the tunnel transonic capability is the venting of the test section to the plenum. In this tunnel, the vents are eight longitudinal slots located at the intersections of the wall flats. The plenum is a sealed tank 9.75 m (32 ft) in diameter which encloses the test section and diffuser entrance.

Test section wall.- The test section wall is made up of eight longitudinal flats symmetrically disposed about the tunnel center line. For convenience, the flats are numbered in clockwise order for a viewer looking upstream, number 1 being on the lower left as shown in figure 7. The surface of each flat is a continuous steel plate from station 32.61 m (107 ft) to station 46.94 m (154 ft), the width being 195.38 cm (76.92 in.) at the upstream station and less at other stations by the amount of the slot width. Each flat is rigidly supported by a main truss and strongback between stations 34.75 m (114 ft) and 42.06 m (138 ft) and by a second truss and strongback between stations 42.67 m (140 ft) and 46.94 m (154 ft). (See figs. 8 and 9(a).) The trusses are attached to the tunnel structure through flexure plates at stations 34.14 m (112 ft) and 46.94 ' '54 ft) and are jointly supported at station 42.06 m (138 ft) through an actuate   a provides radial motion with respect to the tunnel center line. The long steel   which form the walls are attached rigidly to the tunnel structure between stations 3.   ' in (107 ft) and 33.53 m (110 ft). These plates have flexural regions centered at stations 34.14 m (112 ft) and 42.37 m (139 ft) and a sliding joint at station 46.94 (154 ft), where there is a sealed transverse gap which varies with wall divergence. The region where the tunnel walls are flat therefore extends from station 34.75 m (114 ft) to station 42.06 m (138 ft). The eight wall divergence actuators are interconnected and are driven by a single electric motor. At zero wall divergence, the test section walls form an octagonal cylinder between stations 32.61 m (107 ft) and 42.06 m (138 ft), bending occurs between stations 42.06 m (138 ft) and 42.67 m (140 ft), and the upstream portion of the diffuser starts at an angle of 2.75^o to the tunnel center line. When the test section walls are diverged, bending takes place between stations 33.53 m (110 ft) and 34.75 m (114 ft) and divergence is measured as the angle between the tunnel center line and the rigid portion of the wall from station 34.75 m (114 ft) to station 42.06 m (138 ft). As divergence increases, the wall bending between stations 42.06 m (138 ft) and 42.67 m (140 ft) decreases and the divergence angle of the diffuser entrance decreases. Actuation is provided for a maximum angular divergence of 0°45'.

Slots.- The test section slots, located at the intersections of the wall flats, are eight longitudinal openings generally parallel to the tunnel center line which provide vents

between the test section airstream and the plenum which surrounds the test section. The slot width or opening is nominally zero between stations 32.61 m (107 ft) and 32.77 m (107.5 ft). Each slot proper starts at station 32.77 m (107.5 ft) and extends to station 46.94 m (154 ft) but is closed by the diffuser entrance vanes between stations 43.10 m (141.4 ft) and 46.94 m (154 ft). Some structural details of the wall flats and slots are shown by the sectional views of figures 7 and 8 and by figure 9(a). Longitudinally, the major portion of the skin of each wal. .iat is made of a single steel plate extending from station 32.61 m (107 ft) to station 46.94 m (154 ft); in cross section, however, the construction is composite. Each edge of a flat is trimmed with a strip which carries a skirt 60.96 cm (24 in.) wide normal to the plane of the flat. In cross section, the skirts adjacent to a slot form a channel with walls mutually inclined at 45° completely open to the plenum. At the test section wall, the edges of these skirts form a basic rectangular slot having a half-width of 13.23 cm (5.207 in.). The actual slot shape is determined by the contour of the slot-edge strip which is effectively an extension of the flat in width as shown in figure 8. The slot half-widths (table II) are measured in the plane of the flat surface from and normal to the intersection of two adjacent flats when the wall divergence angle is zero.

Diffuser entrance vanes.- The purpose of the diffuser entrance vanes and lips is to reintroduce into the tunnel airstream the low energy axial flow existing in the plenum adjacent to and at the downstream end of the slots. The diffuser entrance vanes and lips, which are integral and are adjustable as a unit, form a part of the tunnel wall serving to close the openings between the plenum and airstream in the region where the downstream end of the slots would otherwise extend into the diffuser. The slot width increases abruptly just ahead of the diffuser, near station 42.67 m (140 ft), so that in plan view the leading edge of the diffuser entrance lip at station 43.10 m (141.4 ft) is 40.64 cm (16 in.) wide. The vane width increases linearly with distance downstream to a value of 53.34 cm (21 in.) at station 46.94 m (154 ft). In longitudinal section, the vanes are flat between stations 43.59 m (143 ft) and 46.94 m (154 ft), and the lips between stations 43.10 m (141.4 ft) and 43.59 m (143 ft) are deflected 20° away from the tunnel center line to form scoops extending into the plenum. The diffuser entrance with vanes and lips installed is shown in figures 9(a) and 9(b). The vanes are hinged at station 46.88 m (153.8 ft) to permit, in a radial plane, angular motion with respect to the tunnel center line, and each vane is individually supported by an adjustable strut connecting the underside of the vane to the plenum wall near station 43.89 m (144 ft). When the flats are diverged, the approximately parallel walls of the channel in which the diffuser entrance vanes are installed separate laterally and thereby create a channel of greater width. The sealing of the vane edges is maintained by spring loaded blocks which take up the change in width as the flats are diverged. Vane setting is specified as depth of the entrance lip leading edge into the

10

plenum, measured from and normal to the plane of the flat surface at station 43.10 m (141.4 ft). (See fig. 9(b).)

Model support strut.- Although various methods have been used for mounting models in the test section, each depending on the nature of the investigation, the type of mounting most commonly used in this wind tunnel is a sting which is cantilevered from a strut, as shown in figure 10(a). A sketch showing the critical dimensions for locating a model in the test section is presented in figure 10(b). The part of the support strut exposed to the airstream is a cast steel circular-arc segment surmounted by a short straight swept strut carrying at its upper end the strut head which is a cylindrical body 2.13 m (7.0 ft) long and 35.56 cm (14 in.) in diameter, terminated downstream by a tail cone. At zero angle of attack, the strut head is coaxial with the tunnel center line. The upstream end of the strut head falls at tunnel station 43.26 m (141.94 ft). Forward of this station is a sting butt and interchangeable knuckle extending to station 42.34 m (138.90 ft). The knuckle is a coupling that attaches the model sting to the sting butt. The sting from knuckle to model can be supplied from a wide assortment of standard stings or can be fabricated to suit specific model requirements. The support strut penetrates the tunnel floor (flat 8) in the diffuser entrance region through an unsealed opening and is attached to a carriage which moves on a circular-arc track located in the plenum. The support system moves in a vertical plane containing the tunnel center line and is centered on this axis at station 40.84 m (134 ft). A model station, therefore, located at that station on the tunnel center line will remain at that point as angle of attack is varied. The model support system is actuated through an angle-of-attack range of 20^0, from -5^0 to $+15^0$ with a straight knuckle. The angle-of-attack range can be shifted by the use of interchangeable knuckles incorporating positive or negative bends of 2^0, 5^0, 10^0, 15^0, 20^0, 30^0, and 45^0. These knuckles installed with the bend in a lateral plane also provide fixed angles of side-slip. Alternatively, models can be installed with the wings in the vertical plane so that the strut pitch mechanism can provide variable angles of sideslip and the bent knuckles can provide fixed angles of attack. The roll mechanism in the strut head is manually variable at fixed angles of 90^0 increments.

Windows and access hatches.- Two windows (1.83 m (6 ft) long and 0.91 m (3 ft) high), centered at station 40.84 m (134 ft), are located in wall flats 2 and 6. (See fig. 7.) In line with these windows are others of equal size in the walls of the plenum. The windows are used primarily for model observation. They have been put to limited use for schlieren observation and more extensively for shadowgraph observation. For this latter application, the window in wall flat 2 is replaced by a steel plate which, with a large portion of the adjacent test section wall, is finished in a flat white. Small circular windows in the ceiling (flat 4) at stations 41.45 m (136 ft) and 41.76 m (137 ft) are used for visual and motion-picture observation of flow on a model defined by tufts, oil, or dyes.

The model installation hatch for this wind tunnel was made unusually large to permit free use of the hoist required for handling heavy models. Approximately the upper three-eighths of the plenum with the upper three flats (flats 3, 4, and 5) can be raised as a unit and stowed overhead to permit free movement of a 13 608-kg (15 ton) traveling hoist over the entire control room and test section area. The open hatch is thus 4.72 m (15.5 ft) wide and 15.85 m (52 ft) long, extending from stations 32.31 m (106 ft) to 48.16 m (158 ft). One reason for the length upstream was to avoid transverse cuts in the test section wall in the region of supersonic flow. A view of the test section with the upper hatch open is shown in figure 11. Quick access walk-through hatches are located as follows: one in the floor of the tunnel wall downstream of the plenum at station 49.68 m (163 ft) leading to the test section, and one on each side of the plenum leading to the region surrounding the test section.

Test Section Air Removal System

Arrangement and function.- Figures 1, 3, and 12 show the general arrangement of the test section air removal equipment with respect to the wind tunnel proper. Basically, this is a large motor-driven axial-flow compressor which removes low energy air (up to 4.5 percent of test section mass flow) from the plenum surrounding the test section and discharges this air to the atmosphere.

Test section air removal is beneficial primarily for the attainment of low supersonic speeds in a transonic wind tunnel. As indicated in reference 3, properly sized longitudinal slots in a test section wall and the plenum around the test section serve to reduce or eliminate solid blockage of a model and thereby permit testing of the model at sonic speed without choking the airstream at the station of model maximum cross-sectional area. By application of sufficient tunnel drive power and by creation at the diffuser entrance of a sufficiently low static pressure related to the local supersonic flow on the curved wall between test section and diffuser, it was found that low supersonic speeds could be established in the test section. The low static pressure in the vicinity of the diffuser entrance is transmitted through the slots at their downstream end into the plenum and establishes in that region a low static pressure corresponding to a supersonic speed. Because air in the plenum is relatively stagnant, the low pressure in the plenum is exerted directly through the slots and test section boundary layer to the test section airstream along the full length of the slots. The result is an expansion of a portion of the test section airstream through the slots into the plenum and, when airstream velocity is sonic at the upstream end of the test section, supersonic speeds are established throughout the length of the test section. The air which flows from the test section into the plenum loses most of its kinetic energy in the process. With no test section air removal, this low energy air is reintroduced into the tunnel airstream at the diffuser entrance and causes further energy loss by reducing the effectiveness of the diffuser. In this case the

12

tunnel main drive is required to overcome the energy losses in the test section due to slot mixing and terminal shock as well as increased diffuser losses and the friction and turbulence losses in the remainder of the wind tunnel. Thus, without test section air removal the maximum supersonic speed attainable in a slotted or vented test section is limited by the power of the tunnel main drive. In applying test section air removal, the compressor is sized to pump stagnant air from the plenum and to exhaust it to the atmosphere. The pressure difference and compressor mass flow are determined by the test section Mach number and air state. The compressor pumping redirects the slot mixing losses and some of the tunnel skin-friction loss because boundary-layer air is removed. The tunnel main drive then, aided by this quasi-boundary-layer control, is required to overcome only the normal friction and turbulence losses of the wind tunnel and the test section terminal shock. Thus, as shown in a subsequent section, to achieve a specified low supersonic speed in a slotted wind-tunnel test section, less total power is required when applied partly in the main drive and partly in a test section air removal system than when all the power is applied through the main drive.

Compressor.- The air removal compressor is a nine-stage axial-flow compressor rated as follows:

Total pressure ratio	3.33	(3.33)
Inlet volume flow	451 m^3/sec	(956 000 ft^3/min)
Rotational speed	2290 rpm	(2290 rpm)
Inlet pressure	3.24 N/cm^2	(4.7 psia)
Inlet temperature	49° C	(120° F)
Power	26 100 kW	(35 000 hp)
Mass flow	170 kg/sec	(11.65 slugs/sec)
Throat area	3.4 m^2	(36.6 ft^2)

The compressor installation is shown in figure 13(a) and the open compressor is shown in figure 13(b). The normal operating range in this application is between 80 and 100 percent of rated speed. The pressure ratio and efficiency as functions of corrected mass flow are presented in figure 14 for this range of operation. The performance data presented in figure 14 are from measurements made during acceptance tests.

Motor.- The compressor is driven by a wound rotor induction motor through a speedup gear. The drive and pinion gears have 328 and 79 teeth, respectively; this gives a ratio of compressor to motor speed of approximately 4.15. The motor rating is 26 855 kW (36 000 hp) at 552 rpm. Speed control is obtained by a slip regulator incorporating a brine tank rheostat.

Valves and controls.- The compressor inlet consists of a dual-passage manifold with protective screens and bell mouth (fig. 12). The manifold air passages consist of a

13

central 3.66-m-diameter (12 ft) pipe leading from the 4.88-m (16-ft) tunnel surrounded by the 5.49-m-diameter (18 ft) wall of the manifold which forms an annular passage as indicated in figure 12. The annular passage carries air brought by a long 1.83-m-diameter (6 ft) pipe from the Langley high-speed 7- by 10-foot tunnel which in the past used this equipment for test section air removal in common with the 16-foot transonic tunnel, but not simultaneously. The annular passage also receives and distributes to the compressor inlet the air taken in through the surge control valve. The dual-passage manifold was arranged as indicated to minimize the generation of turbulence when flows from separate sources mix ahead of the compressor inlet.

The surge control valve, located on top of the compressor inlet manifold, is a 1.219-m-diameter (4 ft) hydraulically actuated butterfly valve. Because surge pressure ratio varies with rotational speed, the electronic component of the control accepts signals from a compressor drive tachometer and from a pressure transducer in the inlet manifold, combines these signals, and through a servo maintains the surge control valve position. The valve is modulated at compressor rotational speeds from 80 to 100 percent of rated speed to maintain a safe margin between maximum operating and surge pressure ratios. At a pressure ratio closer to surge and at speeds below 80 percent of rated speed, an overriding or surge limit control causes the valve to move to the full open position. During operation of the wind tunnel at near maximum air speed, the surge control valve remains closed. An additional 1.219-m-diameter (4 ft) relief valve, remotely operated, is provided for emergency control.

The flow of air from the test section to the compressor is controlled by a 3.048-m-diameter (10 ft) hydraulically actuated butterfly valve located in the air removal duct just outside the test section plenum as indicated in figure 12. This valve can be controlled either automatically to maintain preselected values of compressor pressure ratio as a function of rotational speed, or compressor inlet suction pressure can be set manually to any value less than that established by the surge control.

Compressor cooling is not required under normal operating conditions. The compressor is rated for inlet air at 49° C (120° F), and the blading is capable of safe operation with even higher inlet temperatures. However, a water injection cooling system for the compressor is provided which acts automatically when the inlet air temperature reaches 49° C (120° F), and the rate of water injection is regulated to maintain that temperature. The water spray nozzles are located in the air removal duct a short distance downstream from the 3.048-m-diameter (10 ft) main flow control valve, as indicated in figure 12. This method of cooling the compressor, by direct evaporation of water in the compressor airflow, is less efficient than cooling by heat exchanger but is effective and economical in that only intermittent use is required.

14

Instrumentation

<u>Wind-tunnel air state sensors</u>.- The plenum-static-pressure orifices located in the plenum wall behind flats 2, 6, and 8, at station 33.68 m (110.5 ft), are completely open to the plenum interior but are protected from air gusts by adjacent tunnel structure. Airstream stagnation pressure is sensed by four shielded total-pressure probes carried by a cruciform support (fig. 15). The probes, located at axial station 1.31 m (4.30 ft), are 0.61 m (2.0 ft) downstream of the antiturbulence screen and 0.46 m (1.5 ft) from the tunnel center line. Airstream stagnation temperature was measured with electrical-resistance temperature probes located on the fourth set of turning vanes at four points near the tunnel center line. At the time of these wind-tunnel calibrations, 1961 to 1965, the dewpoint was measured outside the wind tunnel, near the air exchange tower, with a lithium chloride type instrument and was recorded manually. Dewpoint currently is measured with a condensation mirror-type dewpoint indicator using continuously sampled air from the wind tunnel and is recorded on magnetic tape for each data point.

<u>Center-line static pressure</u>.- The principal test section instrumentation consisted of the center-line survey tube shown in figures 6, 7, and 9(a). This tube is 10.16 cm (4 in.) in diameter and extends from station 22.71 m (74.5 ft) in the entrance cone to station 43.13 m (141.5 ft) at the downstream end of the test section where it is fastened into the special strut head shown in figures 9(a) and 16. The upstream end of the center-line survey tube is supported by eight cables anchored to the tunnel shell, which exert on the tube b⁻ h tension and bending. Deflection of the tube under its own weight resulted in an angle between the tube axis and the tunnel center line which nowhere exceeded 1°. In the vicinity of the supporting cables, airstream Mach number never exceeds about 0.35. The survey tube carried 54 static-pressure orifices 0.508 mm (0.020 in.) in diameter spaced 22.86 cm (9.0 in.) apart. The orifices lie on the tube surface 90° from the vertical plane containing the tube axis in order to minimize the effects of tube curvature in that plane on the tube surface pressures.

<u>Wall static pressure</u>.- Static-pressure orifices were provided also on the test section wall flat 1, as shown in figure 7. The orifices lie in an axial plane displaced above and 15.24 cm (6 in.) from a plane containing the tunnel center line and the center line of flat 1. The orifices were 0.508 mm (0.020 in.) in diameter with centers spaced 15.24 cm (6 in.) apart axially from tunnel station 29.11 m (95.5 ft) to station 46.79 m (153.5 ft). This row of static orifices was extended into the diffuser, with axial spacings of 0.61 m (2 ft), 1.83 m (6 ft), and 3.66 m (12 ft), to station 97.54 m (320 ft). The axial locations of the orifices on both the center-line survey tube and on wall flat 1 within the test section are given in table III.

<u>Data acquisition</u>.- For the calibrations of 1961 and 1963, pressures were measured with mercury manometers, recorded photographically, and read manually on a photoreader

which entered the data into punch cards. In the calibration of 1965, pressures were measured with remotely actuated scanning valves in conjunction with electrical pressure transducers and were recorded on magnetic tape. Temperatures of the tunnel airstream flow and of the flow through the air removal compressor were sensed by thermocouples and were recorded on self-balancing potentiometers and on magnetic tape.

TEST SECTION DEVELOPMENT AND CALIBRATION PROCEDURE

Test section walls have primary control of the flow conditions provided for the test model. Because of this well recognized fact, considerable study and effort were applied to the development of the walls which are presently installed in the Langley 16-foot transonic tunnel. A historical explanation is presented to show the reader how the 16-foot slotted-wall test section was developed. After the final slot shape was chosen, the test section flow conditions were examined with respect to the effects of test section wall divergence angle, tunnel drive power, moisture content in the tunnel airstream, model blockage, shock reflection, and several other smaller related effects. Before launching directly into a wall-slot development program, it was believed important to perform some initial exploratory tests to establish operating procedures and to obtain data using earlier designed slot shapes. The following description begins with the discussion of some early work (1950) and the exploratory tests (1961).

Slot Shape Studies

When the 16-foot tunnel was repowered and converted from a high-speed wind tunnel to a transonic wind tunnel in 1950, the objective of slot shape development at that time was to minimize test section wall interference related to model solid blockage at near sonic speeds. Studies by Wright and Ward (ref. 3) indicated that for an eight-slot octagonal test section, an open porosity of about 12 percent of the test section periphery would be near optimum. The theory of Goethert (ref. 12) indicates that for $M < 1.0$, the slot width should be about one-half that indicated by Wright and Ward. For the test section modification of 1950, slots providing a 13.5-percent open periphery (slot shape 18) were developed by using a cut and try method to obtain uniform flow in the region of model tests. This original slot development work is reported in reference 5. The geometry of slot shape 18 is also defined herein in table II. This original slot shape continued in use until the wind tunnel was provided with the test section air removal system in 1961. Before installation of the test section air removal system, the maximum test section Mach number with uniform flow was 1.08. When test section air removal was made available, the maximum Mach number was found to have been increased to about 1.3; however, it was observed that slot shape 18 did not provide a uniform flow in the test section at the higher supersonic speeds. As a consequence, a new objective was established to devise

16

a slot shape which would yield the highest feasible test section Mach number with the largest possible testing region over the complete Mach number range.

Criteria for Flow Uniformity

The general criteria of acceptability applied to Mach number distribution in evaluating slot shapes were that the average Mach number gradient be less than about ±0.003 per meter (±0.001 per ft) and that the standard and maximum deviations of Mach number from a straight-line fit by the method of least squares be less than ±0.005 and ±0.010, respectively, within an approximate length of 1.8 m (6 ft).

Exploratory Investigations

Before proceeding with an experimental study of the effects of slot shape on test section Mach number distribution and on tunnel power, exploratory investigations were required to determine the factors essential to the wind-tunnel operating procedure with test section air removal. At this stage of the work, there was no test section calibration; consequently, visual data Mach number was determined directly from airstream stagnation pressure and test section wall static pressure at station 40.84 m (134 ft) without regard to Mach number gradient in the test section.

Power balance between drive motors.- To determine the extent to which test section air removal affected the power balance between the main drive motors, an initial test with the test section empty, except for the support strut with a conical nose fairing (fig. 16), was made at near top power of the two main drive motors and with the compressor at top speed. Power of these two drive motors was measured first with the plenum valve closed and then full open. The 4.5-percent reduction in mass flow of air through the drive fans caused by removal of air from the plenum surrounding the test section had no noticeable effect on the power balance between the two main drive motors. This finding eliminated power imbalance as a potential operating problem. For further investigations, the center-line survey tube (figs. 6, 7, and 9(a)) was installed in the test section which still incorporated slot shape 18.

Diffuser entrance vane setting.- Two tests which differed only in position of the diffuser entrance vanes (fig. 9) showed that this variable had relatively small influence on maximum speed at constant power (fig. 17). A vane lip depth of 27.94 cm (11.0 in.) was arbitrarily chosen subsequently as a permanent setting.

Diffuser entrance leakage.- Between stations 43.10 m and 46.94 m (141.4 ft and 154 ft), the juncture between the edges of the diffuser entrance wall flats and the adjacent tunnel structure was a sliding fit. Some leakage of air from the diffuser into the plenum surrounding the test section was possible. Results obtained with and without sealing of these joints (fig. 18) showed that at the higher speeds with the air removal system in use,

17

the leakage was immaterial. At lower speeds without test section air removal, sealing was slightly beneficial.

Test section wall divergence.- Remotely controlled test section wall divergence had been incorporated in the design of 1950 as a means to control the effect of boundary-layer growth on longitudinal distribution of Mach number. In general, the variation of test section wall divergence was not required as an operating procedure prior to the use of test section air removal when the maximum practical Mach number was 1.08. In a final exploratory test, the main drive motors were operated at maximum power, with the compressor at top speed, and the plenum valve set full open. With no further adjustment of these controls, the test section walls were diverged in angular increments of about $0°5'$. Results are shown in figure 19. An increase in wall divergence angle from $0°5'$ to $0°26'$ increased the Mach number from 1.28 to about 1.33 (visual data) without regard to Mach number distribution. The slight decrease in power with increasing Mach number is possibly related to an improvement in diffuser efficiency with increased wall divergence angle. Inasmuch as Mach number gradients in the test section varied with wall divergence angle, this test showed that test section wall divergence angular setting would be a critical parameter in operation of the wind tunnel.

Effects of Slot Modifications

Slot shapes 18 to 23.- After completion of the exploratory tests, the experimental study of the effect of slot shape on maximum speed and power and on test section Mach number distribution was begun with slot shape 18. All the slot shapes treated in this investigation are presented in figure 20, and their coordinates are listed in table II. The variation of slot half-width increment with test section wall divergence angle is shown in figure 21. The effects of the slot shape changes on Mach number distribution in the test section are shown in figures 22 to 31. For slot shape 18 at speeds not requiring test section air removal, the Mach number distributions are similar to those of reference 5, although not at identical values of Mach number. At the higher speeds, test section air removal was applied fully and tunnel air speed was varied by controlling rotational speed and power of the main drive fans. At supersonic speeds, the usable length of testing region provided by slot shape 18 (fig. 22) was regarded as too short, with excessive drop-off in Mach number at the downstream end of the testing region. Slot shape 19 was obtained by an arbitrary approximate doubling of the open area of slot shape 18 over the upstream one-third of its length. Although the modification had a beneficial effect on the flow ahead of the testing region (fig. 23), the flow in the testing region proper was not improved. Shape 20 was obtained by reducing the slot width over the downstream one-third of the slot length and this shape did yield an increase in Mach number at the downstream end of the testing region (fig. 24). The results obtained with slot shapes 18 to 23 (figs. 22 to 27) indicate that (1) at near maximum tunnel air speed, an increase in width of

18

the upstream one-third of the slots increased air speed upstream of the testing region but had an adverse effect on uniformity of flow at the downstream end, (2) a general increase in slot width (shape 22) adversely affected flow in the test section, and, conversely, (3) a reduction in slot width over the downstream one-third of the slot length (shapes 20, 21, and 23) improved flow uniformity at the downstream end of the test section. At maximum tunnel air speed, the Mach number distributions produced by slot shapes 18 to 23 were not regarded as acceptable either in length of testing region or in uniformity of flow.

Slot shapes 24 to 26.- Results of the foregoing investigations of trial slot shapes seemed to indicate that uniform flow would be achieved only through a reduction in slot width. For slot shape 24, the width was reduced to approximately 7.62 cm (3 in.) over most of the slot length. The Mach number distributions at maximum and at lower air speeds obtained with slot shape 24 (fig. 28) were regarded as acceptable for test section lengths both of 1.83 m (6 ft) and of 2.29 m (7.5 ft). An increase in width of the upstream end of the slot which resulted in slot shape 25 again was found to have an adverse effect on uniformity of flow in the test section (fig. 29). Accordingly, a trial reduction in width of the starting section of slot 24 produced slot shape 26. The test section flow obtained with slot shape 26 (fig. 30) was regarded as the most uniform thus far achieved. In comparison with the earlier slots of greater width, the narrow shapes 24, 25, and 26 seemed to greatly reduce the operating noise and turbulence of the wind tunnel. Slot shapes 18 through 26 were investigated with no sealing of the diffuser entrance joints; however, for the final calibration of slot shape 26, and as a permanent fixture of the test section, the sliding joint at the downstream ends of the flats (station 46.94 m (154 ft)) was provided with a thin metal strip labyrinth seal. The wind tunnel incorporating slot shape 26 was operated over a wide range of test section wall divergence angles at each of several nominal values of Mach number. For each value of Mach number, test section wall divergence angle was selected to yield zero axial gradient of static pressure. Axial distributions of Mach number for slot shape 26 are presented in figure 30, and from these data was established the wind-tunnel calibration of 1961 which continued in use until 1963.

Slot shapes 27 to 29.- Slot shapes 27, 28, and 29 are shown at the top of figure 20, and coordinates for these shapes are given in table II. These shapes are the same as slot shape 26 except in a short region downstream from station 40.23 m (132 ft) where shape 26 incorporates slightly reduced width and shapes 27, 28, and 29 have uniform width. In slot shape 27, the active narrow portion of the slot was extended downstream slightly into the diffuser with a view toward improving diffuser efficiency and, thereby, increasing maximum speed. Because shape 27 presented a mechanical problem where it traversed the flexure in the test section wall at station 42.37 m (139 ft) and because no increase in maximum speed was realized, shape 27 was converted to the simpler shape 28. Separate Mach number distributions for slot shapes 27 and 28 are not presented because neither is significantly different from that for shape 29 (fig. 31). The wind-tunnel calibration of 1963

19

included an abbreviated verification of the performance of slot shape 26, an investigation of slot shape 27, and a complete calibration of the wind tunnel incorporating slot shape 28. Slot 28 was fabricated with wooden edge strips fastened to the remnants of the steel edge strips of miscellaneous obsolete slot shapes. Although regarded as temporary, slot shape 28 continued in use until the wind tunnel was calibrated in 1965 with slot shape 29. The coordinates of slot shapes 28 and 29 are identical (see table II); however, the slot edge strips for shape 29 are almost entirely of steel and the new designation "29" was given primarily for physical differentiation of these slot installations. Under all operating conditions, the most uniform flow in the test section was achieved with slot shape 29 which is defined over the upstream one-third of the slot length by an approximately triangular starting section that faired into a relatively narrow slot having a constant width (3.9 percent open periphery) over the downstream two-thirds of its length.

Calibration With Slot Shape 29

Operating variables.- Experience acquired in operation of the wind tunnel with test section air removal prior to 1965 had established the techniques for obtaining any pre-selected value of Mach number up to 1.30. Speed of the main drive fans, compressor speed, plenum valve and surge control valve positions, and approximate values of test section wall divergence angle were known. This experience had shown also that although moisture content of the airstream did not have a large effect on aerodynamic data (ref. 13), it did have some effect on the axial gradient of static pressure in the test section. Although the gradient does not affect the mean value of Mach number in the test section, a static-pressure gradient can exert horizontal buoyancy on a model and may thereby cause an error in drag measurement. In the wind-tunnel calibration of 1965, resort was made to empirical determination of the effect of air humidity on static-pressure gradient in the test section and on selection of the proper angle of wall divergence to eliminate the gradient.

Presentation of data.- Two sets of calibration data are presented for slot shape 29. Data designated as "low dewpoint" were obtained when air dewpoint was less than 4^0 C (40^0 F), and for the "high dewpoint" data the corresponding dewpoint was greater than 18^0 C (64^0 F). The data for these calibrations are identified by run number and point number for cross-reference between figures and tables. Distributions of Mach number along the tunnel center line are shown in figure 31, and the values of Mach number for both the center line and test section wall are given in table III. There is generally very good agreement between the center-line and wall Mach number distributions except in the vicinity of station 42.37 m (139 ft) where the curvature of the wall between test section and diffuser causes local Mach number on the wall to exceed that at the center line. The wind-tunnel operating conditions for each data point are given in table IV, and a discussion of table IV including a description of each item of the table is given in appendix A. Item 23

20

of table IV requires also the use of information given in appendix B. Results of a least-squares analysis of Mach number distributions on the center line for two lengths of test section are presented in table V.

Calibration test and procedure.- Since 1950 all calibration tests of the 16-foot transonic tunnel test section have had test number 100. Designation of test number, run number, and point number identifies a unique set of data. A typical calibration "run" includes all testing performed between start and stop of the wind-tunnel drive motors. A single run may include many values of Mach number and appropriate variation of operating parameters at each Mach number. A "test point" provides data for a unique value of each of the several operating parameters. When the wind tunnel is brought to a predetermined speed, that speed is held nominally constant while data are recorded at each of several preselected values of test section wall divergence angle. For each test point all pertinent data, outside air state, wind-tunnel operating conditions, test section pressures and temperatures, and wind-tunnel air state and humidity are recorded simultaneously. Generally for a test section calibration, critical runs are repeated to verify repeatability of measurements.

Data reduction and analysis.- Static pressures measured on the test section wall and center-line survey tube are expressed as Mach number, as follows:

$$M = \sqrt{\frac{2}{\gamma - 1}\left[\left(\frac{p_t}{p}\right)^{\frac{\gamma-1}{\gamma}} - 1\right]}$$

(1)

For air, $\gamma = 1.4$ and

$$M = \sqrt{5\left[\left(\frac{p_t}{p}\right)^{2/7} - 1\right]}$$

Initial study of the results may be made with a graphic presentation of center-line Mach number distributions given in figure 31 for slot shape 29. The data reduction also includes the fit of a straight line by the method of least squares to values of Mach number in the test section. Two lengths of test section are treated:

Short (1.8 m (6 ft) long) test section: Stations 39.93 m (131 ft) to 41.76 m (137 ft)

Long (2.3 m (7.5 ft) long) test section: Stations 39.70 m (130.25 ft) to 41.99 m (137.75 ft)

Typical results of this least-squares analysis are listed in table V. In this table, the test section Mach number is the value of M at tunnel station 40.84 m (134 ft) (corresponding to the midpoint of the test section) of a least-squares straight-line fit to the Mach number data over the chosen length of test section; the slope dM/dx defines the Mach number gradient; the standard deviation of Mach number from the straight line of best fit is a measure of average discrepancy; and the maximum deviation represents the worst departure from the line of best fit of a single value of Mach number on the center line within the selected length of test section. A least value of Mach number gradient was generally the criterion used to select the test points listed in tables III, IV, V, and VI for establishing the wind-tunnel calibration. Test points obtained over a wide variation in wall divergence angle at each Mach number were screened to select those falling closest to zero gradient in Mach number. This procedure also established the wall-divergence-angle settings for subsequent wind-tunnel operation.

Wind-tunnel calibration.- As mentioned in the section entitled "Wind-tunnel air state sensors," the wind-tunnel reference measurements are airstream stagnation (total) pressure and plenum static pressure. The value of Mach number computed from these reference pressures is designated "Plenum Mach number." The basic calibration is a correlation of test section airstream Mach number with the plenum Mach number. The calibration may also be regarded as a comparison of test section airstream average static pressure with the reference static pressure measured in the plenum. The values of test section airstream Mach number selected for the calibration and the corresponding values of plenum Mach number are compiled in table VI and presented graphically in figure 32. This single calibration defines test section airstream Mach number with no more deviation than ±0.001, for both the long and short lengths of test section and for high and low dewpoints. The absolute error of the calibration, however, is believed to be no worse than $\Delta M = \pm 0.004$. (See table V.)

Selection of test section wall divergence angle.- In addition to ability to operate at a predetermined value of Mach number, it is desired also to reduce the axial gradient of static pressure in the test section to a minimal value. A typical procedure is outlined as follows: During the calibration test under low dewpoint conditions, $M = 1.3$ was achieved with test section wall divergence angles of $0^\circ 25'$, $0^\circ 27'$, and $0^\circ 29'$. The distributions of Mach number in the test section for these three test points are shown in figure 33 with their respective values of Mach number gradient evaluated by the least-squares analysis. This variation of Mach number gradient with test section wall divergence angle for $M = 1.3$ is shown in figure 34. The curve indicates that an average pressure gradient of zero would be achieved under the specified operating conditions with a wall divergence angle of $0^\circ 28'$. The closest angle at which actual data existed was $0^\circ 27'$, and that data point therefore was selected for the calibration. Similar data for lower values of test section airstream Mach number are also presented in figure 34. Although the data for

22

M = 1.02 and 1.15 appear to be anomalous, the values are believed to be correct; in any case, no large values of gradient were encountered at these speeds. The data of figure 34 and similar results have been compiled in table VII, which presents a correlation of test section wall divergence angle, airstream dewpoint, and Mach number for use in operation of the wind tunnel. Table VII also contains interpolated values obtained from plots similar to figure 35. In figure 35 the variation of test section wall divergence angle with dewpoint required to achieve zero axial gradient of static pressure at Mach number 1.15 does not follow the systematic trend of the data for the higher values of Mach number. Although the data for M = 1.15 in figure 35 also appear to be anomalous, as was mentioned in the discussion of figure 34, the data are believed to be correct. The authors are aware that the trend of the data for M = 1.15 is different from that for the higher Mach numbers and offer no technical explanation for this lack of consistency with the other data. It is apparent from figure 34 that, in general, between M = 1.00 and 1.15 no large values of static-pressure gradient were encountered at any value of test section wall divergence angle investigated. Therefore, except for the low supersonic Mach number range up to M = 1.15, an increase in test section wall divergence angle caused a positive increment in the test section static-pressure gradient, a phenomenon which offers a means to achieve zero gradient. At near maximum tunnel speed, an increase in moisture content of the airstream results in a negative increment of static-pressure gradient in the test section; the test section static-pressure gradient can be eliminated, however, by adjusting test section wall divergence angle by an amount indicated as optimum by wind-tunnel calibration.

Strut-head blockage.- An inspection of the Mach number distributions on the test section center line (fig. 31) shows generally that at supersonic speeds the distributions are uniform almost to station 42.67 m (140 ft), but that at high subsonic speeds the indi-
..dual values of Mach number decrease progressively downstream of station 41.76 m (137 ft). To investigate this phenomenon, a "dummy" strut head (fig. 36) was fastened around the center-line survey tube; this addition effectively extended the strut-head shape upstream by 0.457 m (1.5 ft) or by two spacings of the pressure orifices. Some of the calibration runs were then repeated with this modification to the strut head. Mach number distributions obtained with the strut-head extension are compared in figure 37 with those obtained during the regular calibration. At M = 1.01 and M = 1.06, positive pressure at the leading edge of the strut-head shape appears to be transmitted upstream through the boundary layer on the tube for a distance of slightly more than one orifice spacing or approximately 1 strut-head diameter. At these low supersonic speeds, the comparisons may be confused by expansions generated at the curvature of the test section wall (station 42.37 m (139 ft)) and radiated to the center line. At subsonic speeds, upstream extension of the strut-head shape resulted in a corresponding translation of the Mach number distributions by an almost equal amount. It appears that in the regular

23

calibration at subsonic speeds, the Mach number distributions at the downstream end of the test section indeed are depressed by interference from the strut head. This interference does not extend upstream of station 41.76 m (137 ft) but is always considered in choosing the axial position of a model in the test section.

Diffuser wall pressures.- A few data pertaining to flow in the wind tunnel downstream of the test section are presented in figures 38 and 39, in the form of Mach number distributions. Mach number is computed in the same manner as for the test section with airstream total pressure assumed to be the same as that measured in the quiescent chamber. Loss of total pressure in the diffuser is caused by skin friction and air turbulence at all speeds and, at supersonic speeds, by shock losses at the downstream end of the test section. The values of local Mach number shown are nearly true values just downstream of the test section but are not true values in the downstream half of the diffuser because stream total pressure in this region is much less than the assumed value. The data presented in figure 38 were obtained during calibration of slot shape 26. Local Mach numbers obtained from diffuser wall pressures measured during the calibration of slot shape 29 are presented in figure 39(a) for low dewpoint conditions and in figure 39(b) for high dewpoint conditions. Most of the pressure recovery in the diffuser appears to have been obtained within a length of about 4 test section diameters (20 m (64 ft)) from the downstream end of the test section. Differences in moisture content of the airstream appear not to have had a large effect on pressure recovery in the diffuser.

Airstream stagnation temperature.- Representative values of the stagnation temperature of the wind-tunnel airstream, as these vary with air speed, are presented in figure 40. Temperatures shown by the dash-line curve are taken directly from reference 5. The temperature at each air speed represents the average obtained from many runs at near stabilized conditions during the calibration of 1951 and these data are assumed to remain valid for operation without test section air removal. When the wind tunnel is operated above $M = 1.0$ with test section air removal, energy expended through the drive fans is greatly reduced from that required during operation without test section air removal, except at top speed, and temperature rise of the airstream is correspondingly reduced. The solid curve in figure 40 presents calculated values of stagnation temperature with test section air removal, using values of Mach number, tunnel and secondary mass flows, and drive fan shaft power from table IV and assuming an air exchange rate of 18 percent with a reference outside air temperature chosen to yield a match of the 1951 calibration data at $M = 1.0$. The values of tunnel stagnation temperature (item 27 in table IV) are not stabilized but were measured generally when the airstream was heating or cooling rapidly and therefore do not agree with the values presented in figure 40. Comparisons of power required for operation, when needed, are to be made at identical temperatures and pressures. One purpose of figure 40 is to provide an "average," or arbitrary standard, temperature at each Mach number to which power data may be corrected.

24

Power requirements.- A fairly thorough breakdown of the actual power required for operation of the wind tunnel during the calibration tests is listed in table IV. Attention is given here to the "aerodynamic" power requirement represented by the flow sustenance power (item 20 in table IV) which is shaft power to the main drive fans and to the air removal compressor. The estimated values of flow sustenance power, derived from measured values minus estimated losses, have been corrected to standard atmospheric pressure and to airstream average stagnation temperature, defined in figure 40, by use of the following equation:

$$P_{corr} = \frac{p_{a,o}}{p_t} \sqrt{\frac{T_{t,A}}{T_t}} \, P_{meas} \tag{2}$$

The corrected values of flow sustenance power are presented in figure 41(a) for operation with both low and high dewpoint air. At subsonic speeds, the power measurements for these different conditions are in excellent agreement. The dash-line curve in this figure, taken directly from reference 5, represents power measurements made in 1951 with slot shape 18 which had about three times the width of slot shape 29. The power reduction of approximately 10 percent achieved with slot shape 29 is attributed to reduced air mixing in the slots and to the consequently improved diffuser performance.

At the supersonic speeds which require test section air removal ($M = 1.10$ to $M = 1.31$), operation with moist air requires 3 to 5 percent more power than operation with the relatively dry air. The breakdown of power components in table IV shows that the power increase required for operation with moist air is expended through the main drive fans and not through the compressor. It is conjectured that in operation with moist air, condensation may occur between the quiescent chamber and the drive fans with a consequent loss of total pressure which must be restored by the fans; this pressure loss is never sensed by the wind-tunnel stagnation-pressure probes and is therefore not accounted for in the correction applied by use of equation (2).

At speeds where the surge control valve is partially open, the compressor mass flow $\dot{m}_c$ (item 24 in table IV) remains at a nearly maximum value even though the secondary mass flow $\dot{m}_s$ being pumped from the plenum (item 23 in table IV) may be much less. At supersonic speeds somewhat below maximum, a large portion of the compressor power is being wasted in pumping bypass air ($\dot{m}_c - \dot{m}_s$). From $M = 1.10$ to $M = 1.26$ the power required to pump the surge control bypass air has been estimated and subtracted from the power data of figure 41(a). The resulting values of power presented in figure 41(b) include shaft power to the main drive fans and compressor shaft power required to pump only the secondary flow from the plenum. At maximum speed the surge

25

control (bypass) valve is closed and the power measurements require no adjustment. The data of figure 41(b) then represent the estimated power requirement for operation of a wind tunnel with test section air removal having a system which would not require the pumping of bypass air. The rate of power increase with increasing Mach number is considerably less when test section air removal is being used (M = 1.10 to M = 1.31) than for operation solely with the main drive (M = 1.00 to M = 1.08). The significant indication of the data of figure 41(b) is that a transonic wind tunnel incorporating an efficient system for test section air removal can be operated at low supersonic speeds with less power than would be required if all power were expended only through the main drive fans.

Test section temperature distribution.- With the present system for cooling the wind tunnel by continuous air exchange in which the cool air is introduced in an annulus adjacent to the wall of the cylindrical return passage, a radial gradient of temperature in the test section airstream is almost inherent. After having passed through the drive fans, the airstream in the return passage is of uniform temperature. On the downstream (inlet) side of the air exchange, the step difference in temperature between the cool incoming air and the recirculated airstream is equal to the difference between stagnation and outside air temperatures. By the time that the airstream has traversed the third and fourth sets of turning vanes, an antiturbulence screen, the quiescent chamber, and the entrance cone, the region of radial gradient of temperature extends inwardly from the test section wall for about one-half of the test section radius. Radial distributions of stagnation temperature in the test section for several values of Mach number are shown in figure 42. The temperature of the airstream core is very uniform and is identical with stagnation temperature indicated by the probes located in the quiescent chamber. The difference between test section core and wall temperatures is about 0.90 of the difference between stagnation and outside air temperatures.

The gradient of temperature in the test section airstream is not a desirable feature but, in general, has no adverse effect on most investigations. The temperature gradient has no effect on Mach number distribution but does result in a velocity gradient directly related to the temperature gradient. Most models are much smaller than the airstream hot core and are therefore not affected. Except in special cases, the temperature gradient effectively eliminates consideration of the investigation of wall-mounted models.

On a trial basis for a short time, the test section temperature gradient was eliminated by mixing of the tunnel airstream and inlet air. Of the 36 inlet vanes in the air exchange, 30 were closed fully and six were extended at 45° into the airstream. The foregoing alteration resulted in uniform temperature both in the quiescent chamber and in the test section, but the related increase in airstream turbulence had a very adverse effect on measurement of aerodynamic forces on models, and tunnel operating noise was greatly increased. The air exchange was restored to the configuration shown in figure 5.

Air moisture condensation.- During tests made with high dewpoints, condensation of water vapor in the test section airstream occurs in varying degrees. The tendency toward the formation of fog in the test section airstream increases with absolute humidity and with increasing air speed, and this moisture condensation decreases as air stagnation temperature is raised. Because of the radial gradient of temperature, condensation occurs first in the annular layer of air adjacent to the test section wall as shown in figure 43(a), which is a view of the test section from the downstream end of the diffuser. At supersonic speeds when air moisture content is very high, condensation will occur throughout the entire test section as illustrated in figure 43(b). Under such conditions, the condensation cannot be completely eliminated by increasing the airstream stagnation temperature. Limits to airstream stagnation temperature have been set at 82° C (180° F) for about 30 min and at 88° C (190° F) for 10 min.

The extent to which moisture condensation in the test section airstream may invalidate aerodynamic data is controversial. For the 16-foot transonic tunnel, the effects of air moisture content on the wind-tunnel test section static-pressure gradient are accounted for in the calibration procedure through test section wall divergence. There remains, however, the effects of local condensation adjacent to model curved surfaces. The investigation reported in reference 13 shows very little difference in data obtained with the same model tested first in moist air and subsequently in relatively dry air. Another facet of this problem related to moisture effects is the validity of the procedure of applying wind-tunnel data obtained in desiccated air to aircraft performance estimation when the aircraft must operate in air having a natural moisture content frequently sufficient to cause visible condensation locally on curved surfaces of the aircraft.

Airstream Reynolds number.- The variation with Mach number of Reynolds number per unit length is presented in figure 44 for the corresponding range of operating air stagnation temperatures. The information is presented in SI Units in figure 44(a) and in U.S. Customary Units in figure 44(b). The variation of static pressure, dynamic pressure, and equivalent pressure altitude with Mach number in the test section is presented in SI Units in figure 45(a) and in U.S. Customary Units in figure 45(b).

Airstream turbulence.- During the wind-tunnel calibration of 1950 − 1951, with slot shape 18 (ref. 5) and on several occasions prior to use of test section air removal and before an antiturbulence screen was installed in the quiescent chamber, attempts were made to measure airstream turbulence. The wire elements of hot-wire anemometers broke at Mach numbers above 0.60. Fluctuating flow angle was measured with a three-degree cone pitch and yaw meter, but interpretation of the data was uncertain. If isotropic turbulence can be assumed, those early results indicated that the stream angle fluctuation expressed in radians ranged from about 0.003 to 0.008. (See fig. 6 of ref. 14.)

No comparable measurements of fluctuating flow have been made since operation with test section air removal was started with slot shape 29. However, subsequent to the installation of the antiturbulence screen and slot shape 29, measurements have been made of the length of run of laminar flow on a highly polished 10^0 core, and some of the results are reported in reference 15. These measurements in the Langley 16-foot transonic tunnel at Mach numbers up to 1.30 were made by the same investigators using the same techniques and equipment as for the other investigations reported in reference 15. The analysis of the flow transition data presented in reference 15 indicates that longer runs of laminar flow were obtained in the Langley 16-foot transonic tunnel than in the other wind tunnels investigated. A long run of laminar flow is interpreted to indicate a low level of airstream turbulence.

Boundary-reflected-disturbance length.- The experimental studies made in the 16-foot transonic tunnel by Couch and by Brooks (refs. 16 and 17) with slots (shape 29) which have a width of only 3.9 percent open periphery indicate that no serious wall interference occurred at subsonic Mach numbers up to M = 0.985.

At low supersonic Mach numbers, boundary-reflected disturbances tend to limit the useful test section length. Surface static-pressure measurements on several cone-cylinder or ogive-cylinder bodies of revolution were used to determine the location of the reflected bow shock which determines the extent of the interference-free region. These results, taken from reference 18 and including some unpublished data, are presented in figure 46. The disturbance length is seen to depend on the strength of the bow shock as affected by the body nose angle and change in nose shape from conical to ogive. At Mach numbers greater than 1.15, aircraft models of reasonable length (1.8 m (70.87 in.)) are generally free of boundary-reflected disturbances.

OBSERVATIONS AND CONCLUSIONS

The Langley 16-foot transonic tunnel is a single-return atmospheric wind tunnel, having a slotted transonic test section, and operates at stagnation temperatures up to about 82^0 C (180^0 F). Temperature control with airstream scavenging is obtained by the use of an air exchange system. A test section air removal system is available which can pump a preselected amount of flow (up to 4.5 percent of test section flow) from the plenum which surrounds the test section. Specially shaped longitudinal slots in the test section wall are used to develop a uniform flow and also to prevent test section blockage at transonic speeds.

Detailed wind-tunnel calibrations made under a wide range of flow conditions and geometric changes have led to the following conclusions:

1. The relatively open (13.5 percent porosity) slot shape (shape 18), which was optimum for near sonic speeds without test section air removal, did not yield uniform distributions of static pressure in the test section at the higher Mach numbers obtained with test section air removal.

2. At near maximum air speed, an increase in width of the upstream one-third of the slots increased air speed upstream of the testing region but had an adverse effect on uniformity of flow at the downst eam end. A general increase in slot width degraded the uniformity of flow in the test section; conversely, a reduction in slot width over the downstream one-third of the slot length improved flow uniformity at the downstream end.

3. Under all operating conditions the most uniform flow in the test section was achieved with a slot shape (shape 29) defined over the upstream one-third of the slot length by an approximately triangular starting section that faired into a relatively narrow slot having a constant width (3.9 percent open periphery) over the downstream two-thirds of its length.

4. A single calibration defines test section Mach number with no more deviation than ±0.001, for both the long and short lengths of test section and for high and low dewpoints. The absolute error of the calibration Mach number, however, is believed to be no worse than ±0.004.

5. Except for the low supersonic Mach number range up to Mach 1.15, an increase in test section wall divergence angle caused a positive increment in the test section static-pressure gradient, a phenomenon which offers a means to achieve zero gradient.

6. At near maximum air speed, an increase in moisture content of the airstream results in a negative increment of static-pressure gradient in the test section; the test section static-pressure gradient can be eliminated, however, by adjusting test section wall divergence angle by an amount indicated as optimum by wind-tunnel calibration.

7. At low supersonic speeds (Mach 1.01 and Mach 1.06), positive pressure at the leading edge of the strut-head shape appears to be transmitted upstream through the boundary layer on the survey tube for a distance of approximately 1 strut-head diameter. At subsonic speeds, upstream extension of the strut-head shape resulted in a corresponding translation of the Mach number distributions by an almost equal amount.

8. Most of the pressure recovery in the diffuser appears to have been obtained within a length of about 4 test section diameters from the downstream end of the test section. Differences in moisture content of the airstream appear not to have had a large effect on pressure recovery in the diffuser.

9. Replacing slot shape 18 with shape 29, a reduction of slot open periphery from 13.5 percent to 3.9 percent, resulted in a reduction of power required to operate the wind tunnel at subsonic speeds of approximately 10 percent.

10. At the supersonic speeds which require test section air removal (Mach 1.10 to Mach 1.31), operation of the wind tunnel with moist air (dewpoint, 18° C (64° F)) requires 3 to 5 percent more power than with relatively dry air (dewpoint, 4° C (40° F)).

11. A transonic wind tunnel incorporating an efficient system for test section air removal can be operated at low supersonic speeds with less power than would be required if all power were expended only through the main drive fans.

Langley Research Center,
    National Aeronautics and Space Administration,
        Hampton, Va., May 14, 1974.

APPENDIX A

CALIBRATION AUXILIARY DATA

For tunnel operation at speeds which require the use of test section air removal, achievement of a specified test section Mach number with near zero axial gradient must be accomplished by setting the test section wall at a specified divergence angle which is a function of the airstream dewpoint. However, the foregoing conditions of air speed and Mach number gradient can be achieved within limits with various combinations of main drive power, test section wall divergence angle, compressor speed, and plenum valve setting. An attempt to reduce main drive power excessively at supersonic speeds by use of increased plenum suction can result in unstable flow with movement of the test section terminal shock upstream into the testing region. Table IV presents for each test point of the calibration the settings of the wind-tunnel operation controls, the physical conditions of the test, and several calculated quantities. The purpose of this appendix is to indicate the sources of the information presented in table IV.

Items 1, 2, and 3:   Identification of data for correlation with the Mach number distributions of figures 31 and 32, and the tabulated calibration data of tables III, V, and VI.

Item 4:   Dewpoint of tunnel airstream from instrument reading.

Item 5:   Test section wall divergence angle from control setting indicator (counter).

Item 6:   Plenum valve position (3.048-m-diam. (10 ft) valve) from control setting indicator (potentiometer).

Item 7:   Surge control valve position (1.219-m-diam. (4 ft) valve) from valve position indicator (potentiometer).

Item 8:   Air-removal-system compressor motor speed from tachometer.

Item 9:   Air-removal-system compressor power from instrument reading in MW of overall system power. Includes motor shaft power, motor losses, and liquid rheostat losses; does not include power for cooling tower, water pumps, and oil pumps.

Item 10:   Air-removal-system compressor shaft power — Estimated with use of figure 7 of reference 9 for a motor having secondary resistance control, maximum rated power of 26.855 MW (36 000 hp), and a synchronous speed of 600 rpm. Item 10 = Item 9 - c × Maximum rated power where c is a function of the ratio of motor operating

31

speed to synchronous speed. At 475 rpm, $c = 0.172$; at 552 rpm, $c = 0.130$.

Item 11:   Air-removal-system power — For this calibration, the same as item 9.

Items 12 and 16:   Main drive fan rotational speed from tachometer.

Items 13 and 17:   Electrical power to main drive motor from panel meter reading.

Items 14 and 18:   Shaft power P_{Sh} to main drive fan — Electrical power to main drive motor minus estimated rotational and copper losses.

$$P_{Sh} = 3.27 \text{ (Rotational speed in rpm) (Power in MW)}$$
$$- \left[0.269 \text{ (Rotational speed in rpm)} \right.$$
$$\left. + 0.0000428 \text{ (Rotational speed in rpm)}^{2.5365} \right]$$

Items 15 and 19:   Main drive unit system power — Sum of shaft power, rotational losses, and losses for a modified Kramer system having a maximum shaft power of 25.364 MW (34 000 hp) and a synchronous speed of 400 rpm. The modified Kramer system losses have been estimated from information given in figure 7 of reference 9 and are presented in figure 47.

Item 20:   Flow sustenance power — Sum of shaft power delivered to the air removal compressor and to each main drive fan. Wind-tunnel energy ratio is the ratio of kinetic energy per second traversing the test section to the flow sustenance power (item 20) expressed in the same units.

Item 21:   Total system power — Sum of electrical power supplied to the main drive systems and to the air removal compressor drive system. Item 21 represents the overall energy rate required for operation of the wind tunnel. The ratio of item 20 to item 21 in a sense represents the electrical system efficiency.

Item 22:   Wind-tunnel airstream mass flow — Calculated for isentropic flow of air, with a flow coefficient of unity assumed. Generalized equation:

$$\dot{m} = \sqrt{\frac{7}{R}} \frac{A_{107} p_{107}}{\sqrt{T_t}} \sqrt{\left(\frac{p_t}{p_{107}}\right)^{2/7} \left[\left(\frac{p_t}{p_{107}}\right)^{2/7} - 1\right]} \tag{A1}$$

APPENDIX A

When units are in SI, that is, A in m^2, p in N/m^2, and T_t in K,

$$\dot{m} = 2.89 \frac{p_{107}}{\sqrt{T_t}} \sqrt{\left(\frac{p_t}{p_{107}}\right)^{2/7} \left[\left(\frac{p_t}{p_{107}}\right)^{2/7} - 1\right]} \frac{kg}{sec}$$

When units are in U.S. Customary, that is, A in ft^2, p in lb/ft^2, and T_t in $^{\circ}R$,

$$\dot{m} = 12.72 \frac{p_{107}}{\sqrt{T_t}} \sqrt{\left(\frac{p_t}{p_{107}}\right)^{2/7} \left[\left(\frac{p_t}{p_{107}}\right)^{2/7} - 1\right]} \frac{slugs}{sec}$$

Item 23:   Mass flow of air removed from plenum surrounding the test section $\dot{m}_s$. $\dot{m}_s = \dot{m}_c - \dot{m}_v$ where $\dot{m}_v$ is the calculated mass flow of air through the surge control valve (fig. 48 and appendix B).

Item 24:   Compressor mass flow $\dot{m}_c$ is mass flow at compressor throat calculated from measured total and static pressures and throat area.

Item 25:   Air exchange louver setting from louver position indicator. Always full open for the data of table IV, but a significant variable when wind-tunnel stagnation temperature must be controlled. Wind-tunnel calibration data obtained with louver settings from 17 percent open to 100 percent open showed no deviation from the single-curve wind-tunnel calibration of figure 32.

Item 26:   Outside air temperature from thermocouple used with recording potentiometer.

Item 27:   Tunnel stagnation temperature — Average of readings from four stagnation thermocouple probes in quiescent chamber near tunnel center line indicated on a recording potentiometer.

Item 28:   Tunnel stagnation pressure — Average of readings from four pitot-pressure probes in quiescent chamber near tunnel center line, measured with a automatic mercury manometer with a backup measurement from an electrical pressure transducer; both recorded on the tunnel data readout.

Item 29:   Atmospheric pressure — Recorded signal from an automatic mercury manometer with a backup measurement from a barometer.

33

APPENDIX A

Item 30:   Test section plenum pressure – Recorded signal from electrical
            pressure transducer with a backup measurement from an auto-
            matic mercury manometer; both recorded on the tunnel data
            readout.

APPENDIX B

FLOW THROUGH SURGE CONTROL VALVE

During operation of the wind tunnel at speeds that require test section air removal, the surge control valve may be fully closed or, if partially open, operates with choked flow. The mass flow through the surge control valve $\dot{m}_v$ is computed basically as flow through a choked orifice of variable area, with atmospheric total pressure at the inlet reduced by a small loss through the inlet screen and pipe elbows.

With the plenum valve closed, mass flow through the surge control valve was computed from measurements of pressure and temperature at the compressor inlet. For atmospheric pressure of 10.13 N/cm^2 (2116 lb/ft^2) and temperature of 15° C (59° F), the surge-control-valve maximum mass flow $\dot{m}_{v,max}$ corrected to the foregoing standard conditions is 187.97 kg/sec (12.88 slugs/sec).

With mass flow, temperature, pressure, and inlet dimensions known, dynamic pressure at the surge-control-valve tee inlet was computed and used to determine loss of total pressure across the inlet screen (for which $\Delta p/q = 1.14$). Dynamic pressure within the inlet pipe (tee) was similarly used to determine pressure loss in the bends ($\Delta p/q = 0.25$) just upstream of the valve. At maximum mass flow, the net loss of total pressure ahead of the surge control valve was estimated as

$$\Delta p_t = 0.022 p_t = a p_t$$

The foregoing loss was assumed to be maximum at maximum mass flow and to vary as the square of the relative mass flow; that is,

$$\Delta p_t = 0.022 \mu^2 p_t = a \mu^2 p_t$$

where $\mu = \dot{m}_v / \dot{m}_{v,max}$. The total pressure which determines mass flow through the valve is

$$p_t = (1 - a\mu^2) p_a \tag{B1}$$

If A_p is the cross-sectional area inside the valve pipe (body), A_v is the area of choked flow between the edge of the valve disk and the valve pipe inside wall, and θ is the angle between a plane normal to the valve pipe center line and the plane of the disk (valve closed at $\theta = 0^O$, full open at $\theta = 90^O$), then the area of sonic surface between valve disk and pipe wall can be expressed as

APPENDIX B

$$A_v = A_p(1 - \cos \theta) \tag{B2}$$

Because the valve disk is lenticular with a thickness-to-diameter ratio of 0.156 and is supported by a relatively large spindle, the effective flow area reaches a maximum at $\theta \approx 79^\circ$ and remains essentially constant for values of θ between 79° and 90°. The measured and computed areas for the surge control valve are

$$A_p = 1.167 \text{ m}^2 \quad (12.56 \text{ ft}^2)$$

$$A_{v,max} = 0.935 \text{ m}^2 \quad (10.06 \text{ ft}^2)$$

The flow area through the valve then relative to the maximum flow area is $A_v/A_{v,max}$. From equation (B2),

$$\frac{A_v}{A_{v,max}} = \frac{A_p}{A_{v,max}} (1 - \cos \theta) \tag{B3}$$

The relative mass flow μ is proportional to the relative flow areas and to the total pressure relative to atmospheric pressure. Combining equations (B1) and (B3) yields

$$\mu = \frac{A_v}{A_{v,max}} \frac{p_t}{p_a}$$

$$\mu = \frac{A_p}{A_{v,max}} (1 - \cos \theta)(1 - a\mu^2)$$

Let

$$\left(\frac{A_p}{A_{v,max}}\right)(1 - \cos \theta) = b$$

then

$$\mu = b(1 - a\mu^2) \tag{B4}$$

for which the solution is

$$\mu = \frac{1}{2ab} \left(\sqrt{4ab^2 + 1} - 1 \right) \tag{B5}$$

Because of the geometry of the valve, the solution is valid only for $0^\circ < \theta \leq 79^\circ$. Note that the relative mass flow μ may not exceed unity. The product $\mu \dot{m}_{v,max}$, which is the mass flow $\dot{m}_v$ through the surge control valve corrected to standard conditions, is presented in figure 48 as a function of valve position.

REFERENCES

1. Corson, Blake W., Jr.; and Maynard, Julian D.: The Langley 2,000-Horsepower Propeller Dynamometer and Tests at High Speed of an NACA 10-(3)(08)-03 Two-Blade Propeller. NACA TN 2859, 1952. (Supersedes NACA RM L7L29.)

2. Runckel, Jack F.; and Hieser, Gerald: Pressure-Rise and Leakage-Loss Characteristics of a Rotating Cowling. NACA RM L50D07, 1950.

3. Wright, Ray H.; and Ward, Vernon G.: NACA Transonic Wind-Tunnel Test Sections. NACA Rep. 1231, 1955. (Supersedes NACA RM L8J06.)

4. Ward, Vernon G.; Whitcomb, Charles F.; and Pearson, Merwin D.: An NACA Transonic Test Section With Tapered Slots Tested at Mach Numbers to 1.26. NACA RM L50B14, 1950.

5. Ward, Vernon G.; Whitcomb, Charles F.; and Pearson, Merwin D.: Air-Flow and Power Characteristics of the Langley 16-Foot Transonic Tunnel With Slotted Test Section. NACA RM L52E01, 1952.

6. Maynard, Julian D.; Swihart, John M.; and Norton, Harry T., Jr.: Effect of Blade-Section Camber on Aerodynamic Characteristics of Full-Scale Supersonic-Type Propellers at Mach Numbers to 1.04. NACA RM L56E10, 1956.

7. Runckel, Jack F.; and Swihart, John M.: A Hydrogen Peroxide Hot-Jet Simulator for Wind-Tunnel Tests of Turbojet-Exit Models. NASA MEMO 1-10-59L, 1959.

8. Little, B. H., Jr.; and Cubbage, James M., Jr.: Effects of Combining Auxiliary Bleed With Ejector Pumping on the Power Requirements and Test-Section Flow of an 8-Inch by 8-Inch Slotted Tunnel. NACA RM L55E25, 1955.

9. Lindbeck, S. L.; and Kilgore, L. A.: Big Winds for Model Planes. Westinghouse Eng., vol. 8, no. 2, Mar. 1948, pp. 57-62.

10. Corson, Blake W., Jr.: The Aerodynamics of a Wind-Tunnel Fan. NACA TN 820, 1941.

11. Mair, W. A.: The Design of Fans and Guide Vanes for High-Speed Wind Tunnels. R. & M. No. 2435, British A.R.C., 1951.

12. Goethert, Bernhard H.: Transonic Wind Tunnel Testing. AGARDograph No. 49, Pergamon Press, 1961.

13. Norton, Harry T., Jr.; Runckel, Jack F.; and Pendergraft, Odis C., Jr.: Transonic Performance of Two Convergent-Divergent Ejector Nozzles Designed for Corrected Secondary Flows of 3 and 9.4 Percent. NASA TM X-909, 1964.

14. Igoe, William B.: Wind-Tunnel Buffeting Measurements on Two Wing—End-Plate Airplane Model Configurations. NASA TM X-1454, 196?.

15. Dougherty, N. S., Jr.; and Steinle, Frank W., Jr.: Transition Reynolds Number Comparisons in Several Major Transonic Tunnels. AIAA Paper No. 74-627, July 1974.

16. Couch, Lana M.: Transcnic Wall Interference Effects on Bodies of Revolution. AIAA Paper No. 72-1008, Sept. 1972.

17. Couch, Lana M.; and Brooks, Cuyler W., Jr.: Effect of Blockage Ratio on Drag and Pressure Distributions for Bodies of Revolution at Transonic Speeds. NASA TN D-7331, 1973.

18. Capone, Francis J.; and Coates, Edward M., Jr.: Determination of Boundary-Reflected-Disturbance Lengths in the Langley 16-Foot Transonic Tunnel. NASA TN D-4153, 1967.

TABLE I.- MAJOR DIMENSIONS OF LANGLEY 16-FOOT TRANSONIC TUNNEL

Component	Axial station		Equivalent circular diameter, $\sqrt{4A/\pi}$		Shape
	Meters	Feet	Meters	Feet	
Quiescent chamber begins	0.00	0.0	17.68	58.0	Circular
Antiturbulence screen	0.70	2.3	17.68	58.0	Circular
Quiescent chamber ends	12.19	40.0	17.68	58.0	Circular
Converging fillet begins	12.19	40.0	17.68	58.0	Circular
Converging transition begins	13.72	45.0	16.86	55.3	Circular
Converging octagon begins.	21.34	70.0	8.25	27.1	Octagonal
Entrance liner begins	29.11	95.5	4.91	16.1	Octagonal
Entrance cone ends	32.61	107.0	4.85	15.9	Octagonal
Test section begins	32.61	107.0	4.85	15.9	Octagonal
Test section ends[1]	42.06	138.0	4.85	15.9	Octagonal
Diffuser entrance begins[1]	42.06	138.0	4.85	15.9	Octagonal
Diffuser entrance ends.	46.94	154.0	5.27	17.3	Polygon having 16 sides
Diverging transition begins	46.94	154.0	5.27	17.3	Polygon having 16 sides
Diverging transition ends	54.56	179.0	6.25	20.5	Circular
Conical diffuser begins	54.56	179.0	6.25	20.5	3° half-angle
Diffuser continues	87.14	285.9	9.66	31.7	1.64° half-angle
Diffuser ends.	99.40	326.1	10.36	34.0	Circular
Power section begins	99.40	326.1	10.36	34.0	Circular
First set turning vanes on ¢[2]	106.41	349.1	10.36	34.0	Ellipse $\sqrt{2}$:1
Drive fan 1[3]	117.84	386.6	10.36	34.0	Circular
Drive fan 2[3]	120.88	396.6	10.36	34.0	Circular
Second set turning vanes on ¢[2,3]	132.31	434.1	10.36	34.0	Ellipse $\sqrt{2}$:1
Power section ends	139.32	457.1	10.36	34.0	Circular
Return passage begins	139.32	457.1	10.36	34.0	1.67° half-angle
Return passage continues	152.49	500.3	11.19	36.7	3.0° half-angle
Return passage ends	214.27	703.0	17.68	58.0	Circular
Lips of air exit vanes[4].	214.27	703.0	16.46	54.0	Polygon having 36 sides
Antiturbulence screen	227.75	747.2	17.07	56.0	Polygon having 36 sides
Lips of air inlet vanes[4]	235.61	773.0	16.46	54.0	Polygon having 36 sides
Cylindrical return begins	235.61	773.0	17.68	58.0	Circular
Third set turning vanes on ¢[2]	248.17	814.2	17.68	58.0	Ellipse $\sqrt{2}$:1
Fourth set turning vanes on ¢[2]	274.08	899.2	17.68	58.0	Ellipse $\sqrt{2}$:1
Cylindrical return ends	283.46	930.0 (0.0)	17.68	58.0	Circular

[1]Test section wall divergence angle, 0°.

[2]Minor axis.

[3]Includes nacelle cross-sectional area.

[4]Air exchange full open.

TABLE II.- HALF-WIDTH DIMENSIONS FOR TEST SECTION
LONGITUDINAL SLOT SHAPES 18 TO 29

(a) SI Units

Tunnel station, m	Slot half-widths in centimeters for —											
	Slot shape 18	Slot shape 19	Slot shape 20	Slot shape 21	Slot shape 22	Slot shape 23	Slot shape 24	Slot shape 25	Slot shape 26	Slot shape 27	Slot shape 28	Slot shape 29
32.766	0	0	0	0	0	0	0	0	0	0	0	0
32.918	.381	.792	.792	.607	.607	.607	.607	.792	.394	.394	.394	.394
33.071	.711	1.506	1.506	1.128	1.128	1.128	1 128	1.506	.737	.737	.737	.737
33.223	.973	2.144	2.144	1.575	1.575	1.575	1.575	2.144	1.067	1.067	1.067	1.067
33.376	1.207	2.708	2.708	1.986	1.986	1.986	1.986	2.708	1.384	1.384	1.384	1.384
33.528	1.397	3.238	3.238	2.355	2.355	2.355	2.355	3.238	1.702	1.702	1.702	1.702
33.680	1.562	3.675	3.675	2.657	2.657	2.657	2.657	3.675	1.981	1.981	1.981	1.981
33.833	1.709	4.039	4.039	2.880	2.880	2.880	2.880	4.039	2.261	2.261	2.261	2.261
33.985	1.829	4.331	4.331	3.066	3.066	3.066	3.066	4.331	2.515	2.515	2.515	2.515
34.138	1.930	4.516	4.516	3.198	3.198	3.198	3.213	4.516	2.781	2.781	2.781	2.781
34.290	2.032	4.572	4.572	3.299	3.299	3.299	3.365	4.572	2.959	2.959	2.959	2.959
34.442	2.108	4.542	4.542	3.371	3.371	3.371	3.492	4.542	3.162	3.162	3.162	3.162
34.595	2.184	4.465	4.465	3.424	3.424	3.424	3.614	4.465	3.353	3.353	3.353	3.353
34.747	2.245	4.313	4.313	3.454	3.454	3.454	3.708	4.313	3.505	3.505	3.505	3.505
34.900	2.311	4.082	4.082	3.454	3.454	3.454	3.772	4.082	3.658	3.658	3.658	3.658
35.052	2.350	3.767	3.767	3.452	4.452	3.452	3.810	3.810	3.759	3.759	3.759	3.759
35.204	2.393	3.416	3.416	3.406	3.777	3.777			3.810	3.810	3.810	3.810
35.357	2.438	3.086	3.086	3.327	4.105	4.105						
35.509	2.477	2.802	2.802	3.238	4.430	4.430						
35.662	2.515	2.598	2.598	3.152	4.757	4.757						
35.814	2.555	2.555	2.555	3.071	5.083	5.083						
35.966	2.598	2.598	2.598	3.000	5.408	5.408						
36.119	2.637	2.637	2.637	2.939	5.735	5.735						
36.271	2.680	2.680	2.680	2.891	6.060	6.060						
36.424	2.723	2.723	2.723	2.857	6.388	6.388						
36.576	2.794	2.794	2.794	2.845	6.713	6.713						
36.728	3.023	3.023	3.023	2.850	7.038	7.038						
36.881	3.353	3.353	3.353	2.903	7.366	7.366						
37.033	3.762	3.762	3.762	3.086	7.691	7.691						
37.186	4.293	4.293	4.293	3.386	8.019	8.019						
37.338	4.877	4.877	4.877	3.843	8.344	8.344						
37.490	5.524	5.524	5.524	4.519								
37.643	6.223	6.223	6.223	5.433								
37.795	6.934	6.934	6.934	6.457								
37.948	7.620	7.620	7.620	7.460								
38.100	8.344	8.344	8.344	8.318								
38.252	8.974	8.974	8.974	8.974	8.974	8.974						
38.405	9.627	9.627	9.627	9.627	9.627	9.627						
38.557	10.287	10.287	10.287	10.287	10.287	10.287						
38.710	10.904	10.904	10.904	10.904	10.904	10.904						

TABLE II.- HALF-WIDTH DIMENSIONS FOR TEST SECTION

LONGITUDINAL SLOT SHAPES 18 TO 29 – Continued

(a) SI Units – Concluded

Tunnel station, m	Slot half-widths in centimeters for –											
	Slot shape 18	Slot shape 19	Slot shape 20	Slot shape 21	Slot shape 22	Slot shape 23	Slot shape 24	Slot shape 25	Slot shape 26	Slot shape 27	Slot shape 28	Slot shape 29
38.862	11.468	11.468	11.468	11.468	11.468	11.468	3.810	3.810	3.810	3.810	3.810	3.810
39.014	11.968	11.958	11.882	11.882	11.958	11.882						
39.167	12.395	12.395	11.557	11.557	12.395	11.557						
39.319	12.763	12.763	10.731	10.731	12.763	10.731						
39.472	13.081	13.081	9.423	9.423	13.081	9.423						
39.624	13.226	13.226	7.739	7.739	13.226	7.739						
39.776			6.241	6.241		6.241						
39.929			4.895	4.895		4.895						
40.081			3.777	3.777		3.777	↓	↓	↓			
40.234			3.193	3.193		3.193	3.193	3.193	3.193			
40.386												
40.538												
40.691												
40.843												
40.996												
41.148			↓	↓		↓	↓	↓	↓			
41.300			3.828	3.828		3.828	3.828	3.828	3.828			
41.453			5.250	5.250		5.250	5.250	5.250	5.250		↓	↓
41.478			----	----		----	----	----	----		4.056	4.056
41.504			----	----		----	----	----	----		4.387	4.387
41.529			----	----		----	----	----	----		4.717	4.717
41.555			----	----		----	----	----	----		5.072	5.072
41.580			----	----		----	----	----	----		5.530	5.530
41.605			7.079	7.079		7.079	7.079	7.079	7.079		6.368	6.368
41.631			----	----		----	----	----	----		6.673	6.673
41.656			----	----		----	----	----	----		7.181	7.181
41.682			----	----		----	----	----	----		7.714	7.714
41.707			----	----		----	----	----	----		8.197	8.197
41.732			----	----		----	----	----	----		8.654	8.654
41.758			9.060	0.060		9.060	9.060	9.060	9.060		9.060	9.060
41.910			11.295	11.295		11.295	11.295	11.295	11.295		11.321	11.321
42.062	↓	↓	13.226	13.226	↓	13.226	13.226	13.226	13.226	↓	13.226	13.226
42.215	13.261	13.261	13.261	13.261	13.261	13.261	13.261	13.261	13.261	3.846	13.261	13.261
42.367	13.373	13.373	13.373	13.373	13.373	13.373	13.373	13.373	13.373	3.957	13.373	13.373
42.520	13.556	13.556	13.556	13.556	13.556	13.556	13.556	13.556	13.556	4.140	13.556	13.556
42.672	13.815	13.815	13.815	13.815	13.815	13.815	13.815	13.815	13.815	10.259	13.815	13.815
42.754	13.985	13.985	13.985	13.985	13.985	13.985	13.985	13.985	13.985	13.985	13.985	13.985

TABLE II.- HALF-WIDTH DIMENSIONS FOR TEST SECTION

LONGITUDINAL SLOT SHAPES 18 TO 29 – Continued

(b) U.S. Customary Units

Tunnel station, ft	Slot half-widths in inches for –											
	Slot shape 18	Slot shape 19	Slot shape 20	Slot shape 21	Slot shape 22	Slot shape 23	Slot shape 24	Slot shape 25	Slot shape 26	Slot shape 27	Slot shape 28	Slot shape 29
107.5	0	0	0	0	0	0	0	0	0	0	0	0
108	.150	.312	.312	.239	.239	.239	.239	.312	.155	.155	.155	.155
108.5	.280	.593	.593	.444	.444	.444	.444	.593	.290	.290	.290	.290
109	.383	.844	.844	.620	.620	.620	.620	.844	.420	.420	.420	.420
109.5	.475	1.066	1.066	.782	.782	.782	.782	1.066	.545	.545	.545	.545
110	.550	1.275	1.275	.927	.927	.927	.927	1.275	.670	.670	.670	.670
110.5	.615	1.447	1.447	1.046	1.046	1.046	1.046	1.447	.780	.780	.780	.780
111	.673	1.590	1.590	1.134	1.134	1.134	1.134	1.590	.890	.890	.890	.890
111.5	.720	1.705	1.705	1.207	1.207	1.207	1.207	1.705	.990	.990	.990	.990
112	.760	1.778	1.778	1.259	1.259	1.259	1.265	1.778	1.095	1.095	1.095	1.095
112.5	.800	1.800	1.800	1.299	1.299	1.299	1.325	1.800	1.165	1.165	1.165	1.165
113	.830	1.788	1.788	1.327	1.327	1.327	1.375	1.788	1.245	1.245	1.245	1.245
113.5	.860	1.758	1.758	1.348	1.348	1.348	1.423	1.758	1.320	1.320	1.320	1.320
114	.884	1.698	1.698	1.360	1.360	1.360	1.460	1.698	1.380	1.380	1.380	1.380
114.5	.910	1.607	1.607	1.360	1.360	1.360	1.485	1.607	1.440	1.440	1.440	1.440
115	.925	1.483	1.483	1.359	1.359	1.359	1.500	1.500	1.480	1.480	1.480	1.480
115.5	.942	1.345	1.345	1.341	1.487	1.487			1.500	1.500	1.500	1.500
116	.960	1.215	1.215	1.310	1.616	1.616						
116.5	.975	1.103	1.103	1.275	1.744	1.744						
117	.990	1.023	1.023	1.241	1.873	1.873						
117.5	1.006	1.006	1.006	1.209	2.001	2.001						
118	1.023	1.023	1.023	1.181	2.129	2.129						
118.5	1.038	1.038	1.038	1.157	2.258	2.258						
119	1.055	1.055	1.055	1.138	2.386	2.386						
119.5	1.072	1.072	1.072	1.125	2.515	2.515						
120	1.100	1.100	1.100	1.120	2.643	2.643						
120.5	1.190	1.190	1.190	1.122	2.771	2.771						
121	1.320	1.320	1.320	1.143	2.900	2.900						
121.5	1.481	1.481	1.481	1.215	3.028	3.028						
122	1.690	1.690	1.690	1.333	3.157	3.157						
122.5	1.920	1.920	1.920	1.513	3.285	3.285						
123	2.175	2.175	2.175	1.779								
123.5	2.450	2.450	2.450	2.139								
124	2.730	2.730	2.730	2.542								
124.5	3.000	3.000	3.000	2.937								
125	3.285	3.285	3.285	3.275								
125.5	3.533	3.533	3.533	3.533	3.533	3.533						
126	3.790	3.790	3.790	3.790	3.790	3.790						
126.5	4.050	4.050	4.050	4.050	4.050	4.050						
127	4.293	4.293	4.293	4.293	4.293	4.293						

TABLE II.- HALF-WIDTH DIMENSIONS FOR TEST SECTION

LONGITUDINAL SLOT SHAPES 18 TO 29 – Concluded

(b) U.S. Customary Units – Concluded

Tunnel station, ft	Slot half-widths in inches for –											
	Slot shape 18	Slot shape 19	Slot shape 20	Slot shape 21	Slot shape 22	Slot shape 23	Slot shape 24	Slot shape 25	Slot shape 26	Slot shape 27	Slot shape 28	Slot shape 29
127.5	4.515	4.515	4.515	4.515	4.515	4.515	1.500	1.500	1.500	1.500	1.500	1.500
128	4.708	4.708	4.678	4.678	4.708	4.678						
128.5	4.880	4.880	4.550	4.550	4.880	4.550						
129	5.025	5.025	4.225	4.225	5.025	4.225						
129.5	5.150	5.150	3.710	3.710	5.150	3.710						
130	5.207	5.207	3.047	3.047	5.207	3.047						
130.5			2.457	2.457		2.457						
131			1.927	1.927		1.927						
131.5			1.487	1.487		1.487						
132			1.257	1.257		1.257	1.257	1.257	1.257			
132.5												
133												
133.5												
134												
134.5												
135												
135.5			1.507	1.507		1.507	1.507	1.507	1.507			
136			2.067	2.067		2.067	2.067	2.067	2.067			
136.083			-----	-----		-----	-----	-----	-----		1.597	1.597
136.167			-----	-----		-----	-----	-----	-----		1.727	1.727
136.250			-----	-----		-----	-----	-----	-----		1.857	1.857
136.333			-----	-----		-----	-----	-----	-----		1.997	1.997
136.417			-----	-----		-----	-----	-----	-----		2.177	2.177
136.500			2.787	2.787		2.787	2.787	2.787	2.787		2.507	2.507
136.583			-----	-----		-----	-----	-----	-----		2.627	2.627
136.667			-----	-----		-----	-----	-----	-----		2.827	2.827
136.750			-----	-----		-----	-----	-----	-----		3.037	3.037
136.833			-----	-----		-----	-----	-----	-----		3.227	3.227
136.917			-----	-----		-----	-----	-----	-----		3.407	3.407
137			3.567	3.567		3.567	3.567	3.567	3.567		3.567	3.567
137.5			4.447	4.447		4.447	4.447	4.447	4.447		4.457	4.457
138			5.207	5.207		5.207	5.207	5.207	5.207		5.207	5.207
138.5	5.221	5.221	5.221	5.221	5.221	5.221	5.221	5.221	5.221	1.514	5.221	5.221
139	5.265	5.265	5.265	5.265	5.265	5.265	5.265	5.265	5.265	1.558	5.265	5.265
139.5	5.337	5.337	5.337	5.337	5.337	5.337	5.337	5.337	5.337	1.630	5.337	5.337
140	5.439	5.439	5.439	5.439	5.439	5.439	5.439	5.439	5.439	4.039	5.439	5.439
140.27	5.506	5.506	5.506	5.506	5.506	5.506	5.506	5.506	5.506	5.506	5.506	5.506

TABLE III.- TEST SECTION MACH NUMBER DISTRIBUTION – SLOT SHAPE 29

(a) Center-line Mach number distribution at low dewpoint

Tunnel station		Calibration run																		
		320	320	320	320	320	320	320	320	320	320	318	320	320	320	320	320	320	320
		Data point																	
		0.199	0.401	0.604	0.701	0.802	0.854	0.902	0.951	0.983	1.004	1.023	1.048	1.080	1.105	1.156	1.208	1.263	1.311
Meters	Feet	83	85	82	56	79	76	39	35	32	23	27	24	26	55	53	48	47	43
		Mach number																	
30.556	100.25	0.198	0.395	0.592	0.683	0.773	0.818	0.853	0.879	0.890	0.893	0.894	0.896	0.896	0.897	0.897	0.896	0.895	0.895
30.785	101.00	.197	.396	.594	.685	.777	.823	.861	.889	.901	.905	.906	.907	.908	.908	.908	.907	.906	.906
31.013	101.75	.198	.397	.595	.688	.781	.828	.867	.898	.913	.914	.916	.919	.919	.920	.920	.919	.918	.919
31.242	102.5	.199	.397	.597	.692	.784	.833	.875	.907	.921	.928	.929	.931	.932	.932	.933	.932	.931	.931
31.471	103.25	.199	.399	.599	.697	.788	.837	.880	.915	.932	.936	.914	.943	.944	.943	.945	.943	.943	.944
31.699	104.00	.199	.401	.604	.699	.800	.852	.898	.941	.959	.966	.970	.973	.972	.974	.976	.975	.972	.972
31.928	104.75	.199	.402	.604	.698	.794	.847	.891	.931	.951	.957	.961	.965	.966	.966	.967	.967	.967	.966
32.156	105.50	.199	.402	.606	.701	.795	.849	.892	.934	.958	.965	.971	.973	.973	.975	.974	.975	.974	.972
32.385	106.25	.198	.401	.603	.698	.799	.852	.897	.939	.965	.974	.979	.983	.984	.986	.985	.985	.983	.983
32.614	107.00	.198	.399	.600	.694	.795	.847	.894	.936	.963	.973	.980	.985	.986	.987	.988	.989	.987	.987
32.812	107.75	.198	.402	.604	.700	.791	.842	.890	.934	.958	.970	.980	.984	.989	.989	.990	.991	.992	.991
33.071	108.50	.199	.402	.605	.700	.798	.848	.900	.944	.969	.984	.993	1.000	1.005	1.004	1.009	1.008	1.009	1.008
33.299	109.25	.200	.402	.607	.700	.801	.851	.902	.947	.973	.991	1.003	1.010	1.016	1.019	1.023	1.023	1.024	1.024
33.528	110.00	.200	.402	.605	.700	.800	.855	.903	.949	.977	1.000	1.009	1.020	1.025	1.031	1.035	1.038	1.038	1.038
33.757	110.75	.198	.402	.603	.701	.802	.853	.902	.950	.979	1.006	1.017	1.028	1.035	1.031	1.044	1.048	1.048	1.050
33.985	111.50	.199	.402	.605	.703	.801	.854	.903	.953	.982	1.013	1.025	1.038	1.048	1.053	1.059	1.064	1.066	1.067
34.214	112.25	.200	.402	.605	.702	.803	.857	.900	.952	.981	1.014	1.029	1.043	1.056	1.063	1.074	1.078	1.081	1.092
34.442	113.00	.200	.403	.606	.703	.802	.856	.903	.954	.982	1.015	1.036	1.050	1.068	1.073	1.089	1.093	1.101	1.105
34.671	113.75	.200	.402	.606	.701	.804	.853	.901	.954	.979	1.008	1.033	1.052	1.070	1.081	1.103	1.107	1.115	1.122
34.900	114.50	.199	.403	.606	.702	.803	.854	.898	.955	.979	1.002	1.033	1.053	1.075	1.069	1.115	1.118	1.134	1.143
35.128	115.25	.200	.402	.606	.704	.803	.855	.899	.954	.976	1.005	1.028	1.052	1.075	1.088	1.122	1.127	1.144	1.155
35.357	116.00	.201	.402	.607	.705	.802	.858	.900	.952	.976	1.008	1.025	1.052	1.078	1.092	1.130	1.136	1.153	1.165
35.585	116.75	.201	.402	.606	.703	.803	.855	.903	.951	.975	.999	1.018	1.056	1.081	1.095	1.138	1.144	1.176	1.176
35.814	117.50	.200	.402	.607	.702	.803	.855	.901	.953	.980	1.002	1.019	1.055	1.090	1.107	1.146	1.153	1.190	1.192
36.043	118.25	.199	.402	.605	.698	.802	.852	.902	.953	.983	1.002	1.021	1.049	1.088	1.114	1.158	1.165	1.205	1.205
36.271	119.00	.199	.402	.605	.701	.801	.854	.899	.955	.990	1.005	1.026	1.048	1.087	1.114	1.167	1.176	1.210	1.225
36.500	119.75	.200	.403	.605	.702	.800	.859	.906	.953	.986	1.002	1.024	1.044	1.082	1.111	1.167	1.179	1.218	1.231
36.728	120.50	.200	.402	.606	.701	.800	.854	.907	.954	.969	1.006	1.027	1.049	1.082	1.112	1.173	1.186	1.220	1.241
36.957	121.25	.201	.402	.606	.703	.801	.857	.905	.953	.988	1.007	1.021	1.048	1.079	1.111	1.174	1.187	1.224	1.245
37.186	122.00	.200	.402	.605	.701	.805	.856	.906	.955	.988	.903	1.020	1.045	1.084	1.109	1.174	1.190	1.233	1.250
37.414	122.75	.201	.403	.606	.701	.802	.857	.906	.956	.987	1.009	1.021	1.048	1.086	1.112	1.176	1.196	1.239	1.260
37.643	123.50	.201	.403	.606	.703	.799	.856	.903	.954	.986	1.009	1.020	1.051	1.077	1.113	1.177	1.200	1.237	1.269
37.871	124.25	.200	.402	.606	.701	.800	.856	.904	.951	.985	1.007	1.013	1.050	1.078	1.111	1.176	1.199	1.246	1.267
38.100	125.00	.200	.403	.6r6	.702	.798	.858	.905	.952	.991	1.009	1.028	1.053	1.073	1.109	1.180	1.201	1.254	1.274
38.329	125.75	.199	.404	.603	.699	.803	.850	.900	.946	.984	1.002	1.021	1.044	1.078	1.105	1.182	1.211	1.245	1.286
38.557	126.50	.199	.404	.606	.704	.806	.860	.906	.954	.990	1.009	1.033	1.059	1.072	1.097	1.172	1.204	1.263	1.280
38.786	127.25	.200	.401	.609	.706	.802	.855	.908	.958	.984	1.011	1.056	1.056	1.086	1.108	1.183	1.217	1.270	1.295
39.014	128.00	.200	.402	.606	.702	.803	.857	.902	.953	.986	1.005	1.048	1.048	1.085	1.109	1.176	1.222	1.264	1.306
39.243	128.75	.199	.404	.607	.701	.804	.854	.904	.954	.979	1.006	1.050	1.050	1.079	1.104	1.168	1.215	1.270	1.305
39.472	129.50	.199	.402	.603	.702	.798	.855	.898	.948	.984	1.000	1.043	1.043	1.074	1.107	1.165	1.214	1.263	1.308
39.700	130.25	.199	.403	.605	.699	.802	.851	.902	.953	.979	1.005	1.043	1.049	1.071	1.048	1.155	1.204	1.264	1.303
39.929	131.00	.199	.401	.606	.702	.802	.854	.902	.952	.983	1.005	1.049	1.043	1.080	1.105	1.056	1.209	1.263	1.314
40.157	131.75	.199	.402	.604	.702	.800	.855	.899	.952	.984	1.000	1.047	1.047	1.082	1.103	1.155	1.207	1.265	1.313
40.386	132.50	.199	.400	.606	.700	.804	.852	.904	.949	.980	1.005	1.043	1.043	1.078	1.097	1.161	1.202	1.257	1.306
40.615	133.25	.199	.401	.605	.703	.802	.854	.901	.953	.985	1.003	1.051	1.051	1.081	1.105	1.155	1.208	1.261	1.309
40.843	134.00	.199	.402	.604	.701	.801	.856	.903	.951	.981	1.004	1.047	1.047	1.078	1.107	1.159	1.208	1.259	1.307
41.072	134.75	.199	.401	.603	.701	.799	.855	.903	.952	.983	1.004	1.048	1.048	1.081	1.109	1.155	1.210	1.266	1.309
41.300	135.50	.198	.400	.602	.700	.794	.853	.901	.951	.984	1.003	1.047	1.047	1.083	1.107	1.154	1.211	1.268	1.318
41.529	136.25	.198	.399	.598	.699	.794	.852	.900	.950	.982	1.004	1.051	1.051	1.081	1.106	1.155	1.206	1.262	1.312
41.758	137.00	.197	.397	.602	.694	.799	.845	.893	.942	.981	1.002	1.046	1.048	1.081	1.103	1.154	1.198	1.251	1.306
41.986	137.75	.196	.394	.598	.689	.787	.838	.883	.930	.973	.982	1.049	1.049	1.075	1.100	1.160	1.194	1.246	1.298
42.215	138.50	.195	.392	.594	.683	.779	.828	.870	.912	.957	.950	1.054	1.049	1.074	1.103	1.156	1.191	1.243	1.294
42.443	139.25	.195	.392	.590	.683	.779	.828	.870	.912	.933	.950	1.054	1.054	1.074	1.103	1.160	1.191	1.243	1.296
42.672	140.00	.192	.386	.580	.671	.763	.808	.846	.880	.897	.909	1.065	1.065	1.087	1.118	1.166	1.195	1.243	1.296

TABLE III - TEST SECTION MACH NUMBER DISTRIBUTION - SLOT SHAPE 29 - Continued

(b) Wall Mach number distribution at low datapoint

Tunnel Station		Calibration run																		
		320	320	320	320	320	320	320	320	320	320	320	320	318	320	320	320	320	320	310
									Datapoint											
		88	85	82	56	79	76	39	36	32	23	27	24	26	55	53	48	47	43
									Mach number											
Meters	Feet	0.199	0.401	0.604	0.701	0.802	0.854	0.902	0.951	0.983	1.004	1.023	1.048	1.080	1.105	1.156	1.208	1.263	1.311
32.766	107.5	0.201	0.402	0.604	0.700	0.798	0.850	0.897	0.941	0.968	0.978	0.986	0.994	0.998	0.999	1.002	1.002	1.002	1.002
32.918	108.0	.199	.402	.605	.701	.799	.852	.900	.944	.972	.983	.992	1.000	1.005	1.007	1.010	1.011	1.010	1.012
33.071	108.5	.200	.403	.604	.701	.800	.852	.900	.945	.975	.985	.994	1.004	1.011	1.012	1.017	1.020	1.019	1.022
33.223	109.0	.201	.403	.605	.703	.801	.854	.903	.949	.978	.993	1.001	1.011	1.017	1.020	1.026	1.027	1.029	1.030
33.376	109.5	.199	.403	.607	.704	.804	.857	.905	.953	.985	1.000	1.009	1.020	1.028	1.032	1.037	1.038	1.041	1.044
33.528	110.0	.200	.403	.609	.704	.806	.859	.907	.958	.991	1.008	1.019	1.030	1.038	1.042	1.051	1.054	1.055	1.056
33.680	110.5	.199	.402	.609	.696	.805	.860	.909	.958	.993	1.012	1.022	1.035	1.045	1.048	1.059	1.062	1.067	1.069
33.833	111.0	.199	.402	.602	.702	.794	.851	.896	.945	.983	1.004	1.015	1.027	1.037	1.059	1.073	1.062	1.062	1.065
33.985	111.5	.199	.402	.607	.701	.802	.856	.905	.953	.992	1.010	1.027	1.041	1.053	1.061	1.073	1.076	1.082	1.088
34.138	112.0	.201	.406	.605	.708	.800	.854	.902	.951	.989	1.010	1.026	1.041	1.053	1.080	1.077	1.084	1.090	1.096
34.290	112.5	.198	.402	.611	.701	.810	.862	.914	.963	.996	1.015	1.036	1.055	1.072	1.067	1.099	1.104	1.116	1.112
34.442	113.0	.199	.402	.604	.699	.798	.850	.903	.951	.981	1.021	1.041	1.041	1.058	1.080	1.989	1.092	1.105	1.123
34.595	113.5	.200	.403	.607	.702	.802	.855	.908	.956	.984	1.005	1.026	1.049	1.068	1.067	1.104	1.108	1.116	1.130
34.747	114.0	.200	.402	.607	.702	.802	.855	.904	.952	.981	1.008	1.029	1.048	1.065	1.078	1.106	1.112	1.122	1.135
34.900	114.5	.200	.403	.605	.703	.802	.857	.905	.953	.981	1.005	1.030	1.050	1.069	1.079	1.110	1.116	1.126	1.143
35.028	114.9	.199	.403	.605	.701	.805	.857	.903	.954	.983	1.007	1.031	1.056	1.076	1.081	1.120	1.127	1.132	1.155
35.204	115.5	.200	.404	.608	.706	.807	.861	.908	.958	.981	1.012	1.032	1.055	1.077	1.090	1.126	1.132	1.144	1.161
35.357	116.0	.200	.403	.605	.706	.807	.859	.906	.958	.984	1.011	1.028	1.060	1.086	1.093	1.136	1.143	1.149	1.177
35.509	116.5	.200	.404	.608	.704	.804	.855	.901	.954	.982	1.006	1.022	1.059	1.086	1.101	1.141	1.147	1.164	1.184
35.662	117.0	.200	.403	.605	.705	.805	.853	.899	.955	.977	1.005	1.023	1.055	1.085	1.102	1.146	1.153	1.172	1.186
35.814	117.5	.199	.402	.606	.702	.802	.854	.899	.950	.974	1.002	1.022	1.054	1.083	1.105	1.148	1.157	1.177	1.195
35.966	118.0	.199	.404	.609	.708	.808	.860	.906	.958	.977	1.002	1.020	1.057	1.092	1.102	1.165	1.173	1.181	1.197
36.119	118.5	.200	.403	.609	.701	.807	.861	.907	.958	.985	1.010	1.030	1.054	1.092	1.114	1.163	1.178	1.196	1.213
36.271	119.0	.200	.402	.608	.707	.806	.860	.907	.954	.982	1.009	1.033	1.053	1.092	1.118	1.169	1.180	1.203	1.222
36.424	119.5	.200	.405	.610	.706	.807	.861	.909	.959	.990	1.010	1.031	1.056	1.090	1.120	1.173	1.186	1.212	1.229
36.576	120.0	.200	.403	.608	.706	.806	.860	.907	.959	.993	1.010	1.033	1.054	1.091	1.122	1.175	1.194	1.215	1.239
36.728	120.5	.201	.403	.608	.706	.805	.861	.912	.960	.995	1.012	1.033	1.056	1.088	1.120	1.181	1.198	1.220	1.243
36.881	121.0	.200	.404	.609	.708	.807	.860	.910	.959	.988	1.007	1.025	1.052	1.082	1.115	1.180	1.197	1.227	1.252
37.033	121.5	.201	.402	.606	.700	.803	.858	.907	.956	.987	1.004	1.021	1.048	1.080	1.110	1.176	1.192	1.226	1.254
37.186	122.0	.201	.405	.605	.703	.801	.854	.903	.952	.986	1.004	1.021	1.058	1.090	1.119	1.173	1.197	1.235	1.255
37.338	122.5	.201	.404	.607	.707	.808	.863	.911	.962	.995	1.013	1.031	1.058	1.090	1.120	1.187	1.206	1.244	1.271
37.490	123.0	.201	.406	.610	.706	.807	.864	.912	.961	.995	1.013	1.028	1.060	1.089	1.119	1.186	1.210	1.251	1.278
37.643	123.5	.200	.405	.609	.705	.806	.860	.911	.958	.997	1.016	1.032	1.057	1.090	1.120	1.197	1.213	1.256	1.284
37.795	124.0	.200	.404	.609	.705	.805	.859	.909	.957	.994	1.013	1.028	1.057	1.088	1.117	1.184	1.211	1.253	1.286
37.948	124.5	.200	.401	.603	.698	.796	.849	.901	.949	.991	1.010	1.030	1.056	1.087	1.115	1.182	1.212	1.258	1.289
38.100	125.0	.199	.402	.605	.705	.800	.853	.902	.952	.978	1.000	1.018	1.044	1.073	1.103	1.166	1.198	1.244	1.292
38.252	125.5	.199	.403	.607	.708	.804	.853	.905	.945	.982	1.003	1.026	1.049	1.079	1.105	1.174	1.205	1.252	1.276
38.405	126.0	.200	.404	.608	.703	.807	.858	.907	.956	.986	1.003	1.021	1.055	1.073	1.112	1.167	1.201	1.249	1.281
38.557	126.5	.199	.403	.607	.707	.807	.860	.908	.959	.987	1.012	1.030	1.059	1.081	1.116	1.176	1.216	1.258	1.294
38.710	127.0	.200	.404	.608	.706	.806	.860	.907	.958	.985	1.011	1.030	1.056	1.086	1.115	1.178	1.215	1.265	1.301
38.862	127.5	.200	.403	.610	.707	.806	.859	.906	.960	.984	1.011	1.031	1.053	1.085	1.112	1.174	1.216	1.264	1.302
39.014	128.0	.199	.404	.605	.702	.803	.858	.904	.957	.985	1.012	1.029	1.054	1.084	1.112	1.178	1.217	1.265	1.305
39.167	128.5	.200	.405	.609	.706	.809	.860	.906	.958	.982	1.010	1.024	1.053	1.086	1.114	1.161	1.209	1.271	1.308
39.319	129.0	.199	.401	.603	.706	.801	.854	.904	.951	.975	1.003	1.021	1.046	1.075	1.109	1.156	1.204	1.288	1.310
39.472	129.5	.200	.402	.606	.705	.806	.859	.899	.957	.985	1.011	1.035	1.054	1.084	1.110	1.163	1.207	1.269	1.313
39.624	130.0	.200	.403	.605	.707	.808	.862	.900	.955	.982	1.007	1.032	1.053	1.079	1.108	1.164	1.204	1.263	1.308
39.776	130.5	.199	.404	.609	.706	.807	.866	.910	.962	.990	1.013	1.037	1.051	1.076	1.103	1.173	1.201	1.259	1.317
39.929	131.0	.200	.401	.606	.702	.801	.854	.903	.957	.982	1.010	1.028	1.050	1.084	1.110	1.145	1.201	1.244	1.307
40.081	131.5	.199	.402	.603	.706	.806	.858	.906	.961	.990	1.011	1.032	1.054	1.069	1.115	1.163	1.207	1.249	1.303
40.234	132.0	.200	.403	.607	.705	.808	.862	.904	.955	.996	1.014	1.035	1.051	1.076	1.112	1.170	1.248	1.256	1.315
40.386	132.5	.200	.404	.608	.707	.807	.856	.910	.952	.981	1.007	1.017	1.041	1.084	1.104	1.209	1.267	1.290	1.321
40.538	133.0	.201	.405	.610	.706	.806	.854	.907	.958	.989	1.013	1.035	1.075	1.151	1.198	1.226	1.248	1.290	1.332
40.691	133.5	.201	.402	.611	.711	.813	.866	.911	.961	.990	1.012	1.051	1.123	1.175	1.181	1.255	1.267	1.257	1.304
40.843	134.0	.200	.405	.608	.703	.800	.857	.902	.945	.981	1.005	1.096	1.144	1.164	—	—	—	—	—
41.148	135.0	.200	.402	.696	.704	.818	.867	.922	.960	.995	1.033	1.091	1.130	—	—	—	—	—	—
41.453	136.0	.202	.405	.813	.705	.800	.854	.929	.970	1.005	1.012	—	—	—	—	—	—	—	—
41.758	137.0	.204	.412	.617	.718	.818	.873	.912	.980	.981	1.021	—	—	—	—	—	—	—	—
42.215	138.5	.202	.411	.623	.723	.823	.871	.918	.966	1.005	1.010	—	—	—	—	—	—	—	—
42.367	139.0	.202	.406	.613	.710	.811	.859	.903	.945	.993	.985	—	—	—	—	—	—	—	—
42.672	140.0	.199	.404	.609	.706	.803	.851	.889	.929	.953	.964	—	—	—	—	—	—	—	—

TABLE III. TEST SECTION MACH NUMBER DISTRIBUTION – SLOT SHAPE 20 – Continued

(c) Center-line Mach number distribution at high dewpoint

Calibration run / Data point / Mach number

Tunnel station Meters	Feet	314	314	314	314	314	314	314	314	314	314	317	314	314	314	314	317	317	317	317
Data point		1	2	3	4	5	13	14	15	16	17	19	18	6	7	8	26	30	34	38
Mach number		1.310	1.260	1.207	1.159	1.102	1.064	1.052	1.021	1.004	0.985	0.954	0.953	0.904	0.854	0.803	0.704	0.604	0.400	0.199
30.556	100.25	0.892	0.894	0.894	0.895	0.895	0.896	0.895	0.894	0.892	0.889	0.878	0.879	0.853	0.816	0.774	0.687	0.593	0.395	0.196
30.785	101.00	.901	.904	.905	.906	.905	.907	.906	.906	.904	.901	.888	.888	.862	.823	.778	.687	.593	.397	.196
31.013	101.75	.915	.917	.919	.918	.919	.921	.919	.918	.915	.912	.896	.898	.869	.827	.781	.690	.594	.397	.197
31.242	102.50	.926	.928	.929	.918	.930	.931	.930	.930	.927	.921	.906	.907	.874	.832	.786	.693	.595	.398	.197
31.471	103.25	.938	.940	.942	.941	.943	.943	.942	.940	.938	.930	.914	.915	.881	.836	.791	.695	.597	.398	.197
31.699	104.00	.967	.968	.971	.970	.971	.972	.971	.966	.964	.957	.957	.938	.898	.849	.803	.703	.604	.400	.199
31.928	104.75	.960	.961	.963	.965	.963	.964	.962	.959	.957	.950	.939	.931	.892	.845	.798	.699	.603	.400	.198
32.156	105.50	.968	.969	.972	.966	.971	.972	.970	.966	.964	.954	.934	.936	.897	.848	.799	.700	.603	.400	.199
32.385	106.25	.977	.979	.983	.983	.982	.982	.980	.978	.972	.962	.942	.942	.901	.851	.801	.703	.605	.402	.200
32.614	107.00	.982	.983	.983	.985	.985	.984	.982	.979	.972	.963	.938	.941	.896	.847	.797	.701	.601	.401	.198
32.842	107.75	.986	.986	.988	.988	.987	.986	.984	.979	.972	.961	.935	.936	.892	.842	.795	.699	.597	.399	.198
33.071	108.50	1.005	1.005	1.007	1.006	1.004	1.002	.999	.992	.984	.973	.944	.947	.900	.848	.802	.704	.603	.401	.198
33.299	109.25	1.020	1.020	1.021	1.020	1.016	1.012	1.009	1.000	.992	.977	.948	.949	.902	.852	.804	.705	.603	.403	.200
33.528	110.00	1.033	1.034	1.035	1.033	1.027	1.021	1.018	1.008	1.000	.981	.951	.952	.904	.853	.804	.703	.604	.401	.200
33.757	110.75	1.046	1.046	1.045	1.043	1.037	1.031	1.026	1.016	1.005	.984	.951	.954	.902	.855	.804	.705	.603	.401	.199
33.985	111.50	1.062	1.062	1.061	1.057	1.050	1.042	1.037	1.024	1.013	.986	.954	.954	.904	.855	.805	.703	.603	.400	.199
34.214	112.25	1.081	1.078	1.075	1.071	1.061	1.050	1.043	1.027	1.013	.987	.954	.953	.903	.854	.803	.702	.604	.401	.198
34.442	113.00	1.104	1.099	1.093	1.087	1.073	1.059	1.050	1.031	1.012	.989	.956	.953	.907	.855	.804	.704	.605	.402	.199
34.671	113.75	1.121	1.115	1.109	1.098	1.079	1.062	1.052	1.029	1.003	.987	.955	.952	.905	.855	.804	.705	.606	.402	.199
34.900	114.50	1.144	1.133	1.119	1.110	1.085	1.062	1.054	1.028	1.005	.988	.955	.954	.907	.856	.804	.706	.606	.402	.199
35.128	115.25	1.157	1.143	1.130	1.115	1.085	1.065	1.053	1.023	1.008	.986	.955	.954	.906	.855	.805	.706	.605	.402	.198
35.357	116.00	1.172	1.154	1.137	1.123	1.091	1.067	1.054	1.023	1.008	.985	.956	.953	.906	.855	.805	.704	.605	.401	.199
35.585	116.75	1.184	1.168	1.146	1.129	1.093	1.070	1.057	1.017	1.000	.985	.956	.954	.905	.856	.807	.703	.605	.402	.200
35.814	117.50	1.202	1.178	1.155	1.138	1.105	1.074	1.058	1.020	1.005	.986	.955	.953	.903	.854	.805	.704	.605	.401	.200
36.043	118.25	1.216	1.193	1.176	1.153	1.108	1.073	1.052	1.022	1.013	.987	.954	.954	.903	.857	.806	.706	.607	.401	.200
36.271	119.00	1.236	1.211	1.180	1.158	1.110	1.071	1.050	1.026	1.008	.987	.955	.955	.899	.854	.803	.705	.606	.401	.200
36.500	119.75	1.243	1.213	1.184	1.157	1.105	1.064	1.048	1.022	.999	.985	.953	.953	.906	.857	.802	.702	.606	.402	.200
36.728	120.50	1.250	1.223	1.190	1.161	1.108	1.070	1.050	1.022	1.002	.986	.954	.952	.908	.854	.800	.705	.603	.403	.199
36.957	121.2	1.251	1.223	1.191	1.162	1.104	1.065	1.049	1.021	1.002	.987	.955	.951	.905	.857	.798	.702	.603	.402	.194
37.186	122.00	1.258	1.228	1.194	1.163	1.106	1.068	1.047	1.020	1.005	.988	.952	.953	.905	.855	.804	.703	.605	.402	.199
37.414	122.75	1.266	1.234	1.201	1.164	1.108	1.070	1.049	1.025	1.002	.986	.956	.953	.906	.856	.798	.704	.602	.402	.200
37.643	123.50	1.274	1.240	1.207	1.166	1.111	1.065	1.051	1.025	1.009	.985	.954	.949	.907	.851	.804	.703	.605	.402	.199
37.871	124.25	1.274	1.237	1.202	1.167	1.104	1.062	1.050	1.020	1.005	.985	.954	.953	.907	.855	.806	.706	.606	.401	.199
38.100	125.00	1.280	1.243	1.205	1.172	1.110	1.061	1.049	1.020	1.005	.986	.959	.953	.906	.855	.804	.704	.605	.402	.199
38.329	125.75	1.294	1.253	1.211	1.175	1.104	1.065	1.054	1.025	1.008	.984	.957	.957	.911	.857	.797	.701	.601	.401	.199
38.557	126.50	1.288	1.247	1.212	1.167	1.095	1.060	1.045	1.020	1.000	.979	.953	.951	.904	.852	.802	.708	.603	.403	.200
38.786	127.25	1.303	1.264	1.214	1.178	1.109	1.070	1.059	1.029	1.010	.992	.958	.958	.907	.859	.808	.709	.608	.402	.199
39.014	128.00	1.310	1.270	1.225	1.173	1.105	1.067	1.060	1.027	1.010	.992	.960	.959	.909	.857	.806	.707	.608	.402	.200
39.243	128.75	1.310	1.264	1.218	1.164	1.105	1.065	1.054	1.021	1.005	.986	.955	.955	.904	.854	.804	.705	.606	.402	.199
39.472	129.50	1.314	1.270	1.216	1.165	1.096	1.068	1.060	1.023	1.007	.988	.957	.953	.900	.851	.800	.707	.602	.402	.199
39.700	130.25	1.307	1.260	1.206	1.156	1.096	1.061	1.056	1.021	.999	.981	.950	.949	.906	.854	.806	.702	.605	.401	.199
39.929	131.00	1.317	1.262	1.209	1.158	1.100	1.066	1.053	1.014	1.005	.985	.954	.953	.900	.851	.800	.705	.602	.400	.199
40.157	131.75	1.315	1.261	1.203	1.161	1.095	1.065	1.048	1.020	1.000	.982	.951	.950	.905	.855	.804	.705	.605	.401	.198
40.386	132.50	1.306	1.253	1.208	1.156	1.099	1.060	1.052	1.019	1.005	.986	.956	.954	.901	.852	.801	.703	.603	.400	.198
40.615	133.25	1.307	1.258	1.206	1.166	1.103	1.067	1.048	1.023	1.003	.987	.956	.954	.906	.856	.805	.706	.605	.402	.199
40.843	134.00	1.305	1.257	1.206	1.156	1.103	1.065	1.055	1.020	1.003	.984	.952	.952	.904	.854	.803	.704	.604	.401	.198
41.072	134.75	1.306	1.262	1.206	1.156	1.103	1.065	1.051	1.019	1.003	.984	.952	.952	.904	.854	.803	.702	.604	.400	.198
41.300	135.50	1.316	1.263	1.208	1.162	1.106	1.064	1.052	1.020	1.005	.986	.953	.954	.908	.855	.803	.705	.604	.400	.198
41.529	136.25	1.305	1.260	1.205	1.156	1.103	1.064	1.055	1.022	1.006	.984	.954	.953	.904	.853	.800	.702	.601	.399	.198
41.758	137.00	1.303	1.248	1.197	1.153	1.098	1.062	1.051	1.021	1.005	.976	.946	.945	.897	.846	.794	.697	.597	.394	.197
41.986	137.75	1.295	1.244	1.193	1.155	1.099	1.064	1.053	1.024	1.007	.960	.935	.933	.888	.839	.787	.692	.593	.394	.196
42.215	138.50	1.289	1.240	1.189	1.154	1.102	1.068	1.057	1.033	.969	.935	.916	.915	.874	.828	.778	.685	.588	.391	.194
42.443	139.25	1.292	1.241	1.195	1.163	1.116	1.075	1.068	1.042	.916	.899	.885	.884	.850	.809	.762	.674	.579	.386	.192

47

TABLE III - TEST SECTION MACH NUMBER DISTRIBUTION — SLOT SHAPE 29 - Concluded

(d) Wall Mach number distribution at high dewpoint

Tunnel Station		Calibration run → 314/314/314/314/314/314/314/314/314/314/317/314/314/314/314/317/317/317/317
Meters	Feet	Data point: 1, 2, 3, 4, 5, 13, 14, 15, 16, 17, 19(Cosi), 18, 6, 7, 8, 26, 30, 34, 38 — Mach number: 1.310, 1.260, 1.207, 1.159, 1.102, 1.064, 1.062, 1.021, 1.004, 0.985, 0.941, 0.953, 0.904, 0.854, 0.803, 0.704, 0.604, 0.400, 0.199

Meters	Feet
32.766	107.5
32.818	108.0
33.071	108.5
33.223	109.0
33.376	109.5
33.528	110.0
33.680	110.5
33.833	111.0
33.985	111.5
34.138	112.0
34.290	112.5
34.442	113.0
34.595	113.5
34.747	114.0
34.900	114.5
35.028	114.9
35.204	115.5
35.357	116.0
35.509	116.5
35.662	117.0
35.814	117.5
35.966	118.0
36.119	118.5
36.271	119.0
36.424	119.5
36.576	120.0
36.728	120.5
36.881	121.0
37.033	121.5
37.186	122.0
37.338	122.5
37.490	123.0
37.643	123.5
37.795	124.0
37.948	124.5
38.100	125.0
38.252	125.5
38.405	126.0
38.557	126.5
38.710	127.0
38.862	127.5
39.014	128.0
39.167	128.5
39.319	129.0
39.472	129.5
39.624	130.0
39.776	130.5
39.929	131.0
40.081	131.5
40.234	132.0
40.386	132.5
40.538	133.0
40.691	133.5
40.843	134.0
40.996	134.5
41.148	135.0
41.300	135.5
41.453	136.0
41.605	136.5
41.758	137.0
41.910	137.5
42.038	138.0
42.215	138.5
42.367	139.0
42.520	139.5
42.672	140.0

TABLE IV - CALIBRATION AUXILIARY DATA

(a) Low dewpoint, SI Units

Item																			
1. Calibration run	320	320	320	320	320	320	320	320	320	320	320	320	318	320	320	320	320	320
2. Test point	88	85	82	56	79	76	39	35	32	23	27	24	26	55	53	48	47	43
3. Test section Mach number	0.199	0.401	0.604	0.701	0.802	0.854	0.902	0.951	0.983	1.004	1.023	1.048	1.080	1.105	1.156	1.206	1.263	1.311
4. Dewpoint, °C	4	4	4	3	2	4	6	10	14	15	7	0	7	3	3	10	2	2
5. Wall divergence angle, min	—	—	—	—	—	—	—	—	—	—	—	—	—	3	13	10	20	27
6. Plenum valve position, percent open	—	—	—	—	—	—	—	—	—	—	—	—	—	28	36	37	45	100
7. Surge control valve position, percent open	—	—	—	—	—	—	—	—	—	—	—	—	—	61	56	22	0	0
8. Compressor motor speed, rpm	—	—	—	—	—	—	—	—	—	—	—	—	—	175	475	552	552	552
9. Compressor power, MW	—	—	—	—	—	—	—	—	—	—	—	—	—	28.0	28.0	29.0	29.0	29.0
10. Compressor shaft power, MW	—	—	—	—	—	—	—	—	—	—	—	—	—	23.4	23.4	25.5	25.5	25.5
11. Air-removal-system power, MW	—	—	—	—	—	—	—	—	—	—	—	—	—	28.0	28.0	29.0	29.0	29.0
12. Drive fan 1 speed, rpm	94	183	255	284	305	316	320	327	333	335	338	351	371	337	342	340	341	348
13. Drive fan 1 power, MW	1.5	6.0	11.5	14.5	17.0	18.0	19.5	20.0	21.0	21.5	22.0	24.5	28.0	22.3	22.5	23.0	23.5	25.0
14. Drive fan 1 shaft power, MW	0.3	2.6	7.1	9.9	12.5	13.7	15.1	15.8	16.9	17.4	18.0	20.8	25.2	18.3	19.0	18.9	19.4	21.1
15. Drive fan 1 system power, MW	1.8	4.2	8.8	11.8	14.4	15.7	17.1	17.8	18.9	19.5	20.0	22.3	27.4	20.4	21.1	21.0	21.5	23.2
16. Drive fan 2 speed, rpm	94	183	252	279	301	313	321	324	328	332	335	348	363	335	338	337	337	343
17. Drive fan 2 power, MW	1.0	3.5	7.5	10.0	12.5	14.0	16.0	17.5	18.5	19.5	20.5	25.0	29.0	21.5	22.5	23.0	24.0	26.5
18. Drive fan 2 shaft power, MW	0.2	1.5	4.5	6.7	9.1	10.6	12.1	13.7	14.7	15.6	16.6	21.1	25.5	17.4	18.4	18.7	19.6	22.0
19. Drive fan 2 system power, MW	1.7	3.1	6.3	8.5	10.9	12.5	14.2	15.7	16.7	17.7	18.6	23.2	27.7	19.5	20.5	20.8	21.6	24.1
20. Flow sustenance power (sum of items 10, 14, 18), MW	0.5	4.1	11.6	16.6	21.6	24.3	27.3	29.5	31.6	33.0	34.6	41.9	50.7	59.1	60.8	63.1	64.5	68.6
21. Total system power (sum of items 11, 15, 19), MW	3.5	7.3	15.1	20.3	25.3	28.2	31.3	33.5	35.6	37.2	38.6	46.1	55.1	67.9	69.6	70.8	72.1	76.3
22. Tunnel mass flow (throat), kg/sec	1475.4	2742.9	3622.6	3887.2	4066.2	4103.8	4183.8	4195.9	4195.0	4189.2	4180.7	4155.4	4093.3	4161.5	4154.6	4150.4	4146.1	4141.5
23. Secondary mass flow (plenum valve), kg/sec	0	0	0	0	0	0	0	0	0	0	0	0	0	90.0	102.5	150.5	162.4	189.0
24. Compressor mass flow, kg/sec	0	0	0	0	0	0	0	0	0	0	0	0	0	193.2	192.1	165.3	162.4	183.0
25. Air exchange louver setting, percent open	100	100	100	100	100	100	100	100	100	100	100	100	100	100	100	100	100	100
26. Outside air temperature, °C	7	7	7	7	7	7	7	7	7	8	8	8	8	7	7	7	7	7
27. Tunnel stagnation temperature, °C	27	34	42	47	51	57	53	54	53	58	58	63	71	62	63	64	65	64
28. Tunnel stagnation pressure, kN/m²	102.18	102.08	101.98	101.94	101.89	101.89	101.89	101.89	101.89	101.89	101.89	101.89	101.60	101.84	101.84	101.84	101.84	101.84
29. Atmospheric pressure, kN/m²	102.18	102.18	102.18	102.27	102.27	102.27	102.27	102.27	102.27	102.27	102.27	102.27	101.75	102.27	102.27	102.27	102.27	102.27
30. Test section plenum pressure, kN/m²	99.45	91.26	79.48	73.11	66.41	62.91	59.85	56.74	54.82	53.53	52.69	50.23	48.17	45.54	43.71	41.23	38.78	36.56

TABLE IV.- CALIBRATION AUXILIARY DATA – Continued

(b) Low dewpoint. U.S. Customary Units

Parameter																	
1. Calibration run	320	320	320	320	320	320	320	320	320	320	320	318	320	320	320	320	320
2. Test point	88	85	82	79	76	39	35	32	23	77	24	26	55	53	48	47	43
3. Test section Mach number	0.199	0.401	0.604	0.701	0.802	0.854	0.902	0.951	0.983	1.004	1.023	1.048	1.105	1.156	1.208	1.263	1.311
4. Dewpoint, °F	39	39	39	37	39	38	36	35	35	38	35	33	37	37	35	36	36
5. Wall divergence angle, min	0	0	0	0	2	4	6	10	14	15	7	0	0	13	10	20	27
6. Plenum valve position, percent open	-	-	-	-	-	-	-	-	-	-	-	-	-	-	-	-	-
7. Surge control valve position, percent open	-	-	-	-	-	-	-	-	-	-	-	-	-	-	-	-	-
8. Compressor motor speed, rpm	-	-	-	-	-	-	-	-	-	-	-	-	475	475	552	552	552
9. Compressor power, MW	-	-	-	-	-	-	-	-	-	-	-	-	28.0	28.0	29.0	29.0	29.0
10. Compressor shaft power, hp	-	-	-	-	-	-	-	-	-	-	-	-	31 360	31 360	34 210	34 210	34 210
11. Air-removal-system power, hp	-	-	-	-	-	-	-	-	-	-	-	-	37 550	35 550	38 890	38 890	38 890
12. Drive fan 1 speed, rpm	94	183	255	284	305	316	320	333	335	338	351	371	337	342	340	341	348
13. Drive fan 1 power, MW	1.5	6.0	11.5	14.5	17.0	18.0	19.5	21.0	21.5	22.0	24.5	28.0	22.5	23.0	23.0	23.5	25.0
14. Drive fan 1 shaft power, hp	430	3320	9470	13 320	16 790	18 420	20 220	22 670	23 350	24 110	27 900	33 730	24 590	25 520	25 370	26 000	28 240
15. Drive fan 1 system power, hp	2320	5620	11 820	15 790	19 360	21 050	22 870	25 390	26 090	26 870	30 750	36 780	27 340	28 310	28 140	28 780	31 070
16. Drive fan 2 speed, rpm	94	183	252	279	301	312	317	328	332	335	348	363	335	338	337	337	343
17. Drive fan 2 power, MW	1.0	3.5	7.5	10.0	12.5	14.0	16.0	18.5	19.5	20.5	25.0	29.0	21.5	22.5	23.0	24.0	26.5
18. Drive fan 2 shaft power, hp	280	2020	6060	6980	12 140	14 150	16 401	19 650	20 970	22 260	28 240	34 190	23 350	24 670	25 140	25 250	28 240
19. Drive fan 2 system power, hp	2230	1120	8400	11 430	14 680	16 760	19 040	22 340	23 690	25 000	31 070	37 150	26 090	27 430	27 890	29 000	32 300
20. Flow sustenance power (sum of items 10, 14, 18), hp	710	5510	15 530	22 300	28 930	32 570	36 630	42 320	44 320	46 370	56 140	67 920	79 300	81 550	84 720	86 460	91 960
21. Total system power (sum of items 11, 15, 19), hp	4610	9740	20 220	27 220	31 040	37 810	41 910	47 730	49 780	51 870	61 820	73 930	90 980	93 290	94 920	96 670	102 260
22. Tunnel mass flow (throat), slugs/sec	101.10	187.95	248.23	266.36	278.62	281.20	286.68	287.45	287.05	286.47	285.01	280.48	285.15	284.68	284.39	284.10	283.78
23. Secondary mass flow (plenum valve), slugs/sec	0	0	0	0	0	0	0	0	0	0	0	0	6.17	7.02	10.31	11.13	12.95
24. Compressor mass flow, slugs/sec	0	0	0	0	0	0	0	0	0	0	0	0	13.24	13.16	11.33	11.13	12.95
25. Air exchange louver setting, percent open	100	100	100	100	100	100	100	100	100	100	100	100	100	100	100	100	100
26. Outside air temperature, °F	44	44	44	44	44	44	45	45	46	46	46	46	44	44	45	45	45
27. Tunnel stagnation temperature, °F	80	93	108	117	124	135	127	128	137	137	145	160	144	145	147	149	147
28. Tunnel stagnation pressure, lb/ft²	2134	2132	2130	2129	2128	2128	2128	2128	2128	2128	2128	2122	2127	2127	2127	2127	2127
29. Atmospheric pressure, lb/ft²	2134	2134	2134	2136	2136	2136	2136	2136	2136	2136	2136	2125	2136	2136	2136	2136	2136
30. Test section plenum pressure, lb/ft²	2077	1906	1660	1527	1387	1314	1250	1185	1145	1118	1068	1006	972	913	861	810	764

TABLE IV. - CALIBRATION AUXILIARY DATA – Continued

(c) High dewpoint, SI Units

1. Calibration run	317	317	317	317	311	314	314	314	317	314	314	314	314	314	314	314	314	314	314
2. Test point	38	34	30	26	8	7	6	18	19	17	16	15	11	13	5	4	3	2	1
3. Test section Mach number	0.199	0.400	0.604	0.704	0.803	0.854	0.904	0.953	0.954	0.985	1.004	1.021	1.052	1.064	1.102	1.159	1.207	1.260	1.310
4. Dewpoint, °C	19	19	19	19	18	18	18	18	19	18	18	18	18	18	18	18	18	18	18
5. Wall divergence angle, min	0	0	0	0	3	3	5	9	10	14	12	1	1	0	0	10	15	25	38
6. Plenum valve position, percent open	-	-	-	-	-	-	-	-	-	-	-	-	-	-	26	37	35	42	100
7. Surge control valve position, percent open	-	-	-	-	-	-	-	-	-	-	-	-	-	-	59	53	26	6	0
8. Compressor motor speed, rpm	-	-	-	-	-	-	-	-	-	-	-	-	-	-	475	475	552	552	552
9. Compressor power, MW	-	-	-	-	-	-	-	-	-	-	-	-	-	-	27.0	27.0	29.0	29.0	29.0
10. Compressor shaft power, MW	-	-	-	-	-	-	-	-	-	-	-	-	-	-	22.4	22.4	25.5	25.5	25.5
11. Air-removal-system power, MW	-	-	-	-	-	-	-	-	-	-	-	-	-	-	27.0	27.0	29.0	29.0	29.0
12. Drive fan 1 speed, rpm	95	185	258	288	310	321	329	335	335	335	312	346	360	370	352	354	352	355	359
13. Drive fan 1 power, MW	1.5	6.0	11.3	14.0	16.5	17.8	19.0	20.0	20.0	20.8	21.0	21.8	24.0	26.3	22.8	23.5	23.8	24.3	25.8
14. Drive fan 1 shaft power, MW	0.3	2.7	7.0	9.7	12.3	13.8	15.1	16.2	16.2	17.0	17.4	18.2	20.9	23.5	19.4	20.1	20.3	20.9	22.4
15. Drive fan 1 system power, MW	1.8	4.2	8.8	11.6	14.2	15.8	17.1	18.2	18.2	19.1	19.4	20.3	21.1	25.9	21.5	22.3	22.4	23.0	24.6
16. Drive fan 2 speed, rpm	96	184	255	284	307	316	325	331	330	336	338	342	356	366	348	351	348	350	355
17. Drive fan 2 power, MW	1.0	3.4	7.5	10.0	12.8	14.0	15.5	17.3	17.5	18.5	19.0	20.5	24.8	28.0	22.8	24.3	24.3	26.0	28.0
18. Drive fan 2 shaft power, MW	0.2	1.5	4.6	6.8	9.5	10.7	12.1	13.8	13.9	15.0	15.5	16.9	21.4	24.8	19.2	20.6	20.5	22.0	24.1
19. Drive fan 2 system power, MW	1.7	3.1	6.3	8.7	11.4	12.6	14.1	15.8	16.0	17.1	17.6	19.0	23.5	27.0	21.3	22.8	22.6	24.1	26.2
20. Flow sustenance power (sum of items 10, 14, 18), MW	0.5	4.2	11.6	16.5	21.8	24.5	27.2	30.0	30.1	32.0	32.9	35.1	42.3	48.3	61.0	63.1	66.3	68.4	72.0
21. Total system power (sum of items 11, 15, 19), MW	3.5	7.3	15.1	20.3	25.6	28.4	31.2	34.0	34.2	36.2	37.9	39.3	46.6	52.8	69.8	72.1	74.0	76.1	79.8
22. Tunnel mass flow (throat), kg/sec	1428.2	2666.6	3520.9	3789.7	3952.6	4001.6	4031.4	4059.6	4061.8	4058.7	4054.9	4044.7	4020.2	4017.0	4023.8	4019.0	4020.8	4020.5	4030.3
23. Secondary mass flow (plenum valve) kg/sec	0	0	0	0	0	0	0	0	0	0	0	0	0	0	86.8	101.0	138.1	154.3	181.1
24. Compressor mass flow, kg/sec	0	0	0	0	0	0	0	0	0	0	0	0	0	0	180.5	178.8	158.2	156.2	181.1
25. Air exchange louver setting, percent open	-	-	-	-	100	100	100	100	100	0	0	0	0	100	100	100	100	100	100
26. Outside air temperature, °C	22	22	21	21	18	18	18	18	21	18	18	18	18	18	18	18	18	18	18
27. Tunnel stagnation temperature, °C	37	43	49	55	63	66	68	68	66	68	69	74	76	75	75	75	75	75	74
28. Tunnel stagnation pressure, kN/m²	100.40	100.36	100.31	100.26	100.36	100.31	100.31	100.36	100.21	100.31	100.31	100.31	100.31	100.31	100.31	100.31	100.31	100.26	100.26
29. Atmospheric pressure, kN/m²	100.64	100.64	100.64	100.64	100.55	100.55	100.31	100.55	100.64	100.55	100.55	100.55	100.55	100.55	100.55	100.55	100.55	100.55	100.55
30. Test section plenum pressure, kN/m²	97.77	89.77	78.24	71.77	65.31	62.01	58.85	55.88	55.78	53.87	52.66	51.47	49.22	48.41	45.97	43.09	40.55	38.21	36.01

TABLE IV - CALIBRATION AUXILIARY DATA – Concluded

(b) High dewpoint, U.S. Customary Units

1. Calibration run	317	317	317	317	314	314	314	314	317	314	314	314	314	314	314	314	314	314	314
2. Test point	38	34	30	26	8	7	6	18	19	17	16	15	14	13	5	4	3	2	1
3. Test section Mach number	0.199	0.400	0.604	0.704	0.803	0.854	0.904	0.953	0.954	0.985	1.004	1.021	1.052	1.064	1.102	1.159	1.207	1.260	1.310
4. Dewpoint, °F	66	66	66	66	64	64	64	64	65	64	64	64	64	64	64	64	64	64	64
5. Wall divergence angle, min	0	0	---	0	3	3	5	9	10	14	12	6	1	0	0	10	15	25	38
6. Plenum valve position, percent open	---	---	---	---	---	---	---	---	---	---	---	---	---	---	26	37	35	42	100
7. Surge control valve position, percent open	---	---	---	---	---	---	---	---	---	---	---	---	---	---	59	53	26	6	0
8. Compressor motor speed, rpm	---	---	---	---	---	---	---	---	---	---	---	---	---	---	475	475	552	552	552
9. Compressor power, MW	---	---	---	---	---	---	---	---	---	---	---	---	---	---	27.0	27.0	29.0	29.0	29.0
10. Compressor shaft power, hp	---	---	---	---	---	---	---	---	---	---	---	---	---	---	30 020	30 020	34 210	34 210	34 210
11. Air-removal-system power, hp	---	---	---	---	---	---	---	---	---	---	---	---	---	---	36 210	36 210	38 890	38 890	38 890
12. Drive fan 1 speed, rpm	95	185	258	288	310	321	329	335	335	339	---	346	360	370	352	354	352	355	359
13. Drive fan 1 power, MW	1.5	6.0	11.3	14.0	16.5	17.8	19.0	20.0	20.0	20.8	21.0	21.8	24.0	26.3	22.8	23.5	23.0	24.3	25.8
14. Drive fan 1-shaft power, hp	440	3560	9410	13 030	16 550	18 500	20 250	21 710	21 710	22 950	23 280	24 450	28 030	31 540	26 030	26 980	27 180	27 990	30 060
15. Drive fan 1 system power, hp	2390	5660	11 770	15 520	19 100	21 160	22 950	24 450	24 450	25 610	26 060	27 260	30 960	34 610	28 890	29 860	30 040	30 880	32 980
16. Drive fan 2 speed, rpm	96	184	255	304	307	316	325	331	330	336	338	342	356	366	348	351	348	350	355
17. Drive fan 2 power, MW	1.0	3.5	7.5	10.0	12.8	14.0	15.5	17.3	17.5	18.5	19.0	20.5	24.8	28.9	22.8	24.3	24.3	26.0	28.0
18. Drive fan 2 shaft power, hp	280	2030	6130	9140	12 680	14 290	16 280	18 530	18 690	20 130	20 860	22 720	28 650	33 280	25 730	27 670	27 440	29 540	32 280
19. Drive fan 2 system power, hp	2230	4130	8480	11 610	15 260	16 900	18 950	21 240	21 400	22 870	23 350	25 500	31 550	36 270	28 360	30 520	30 270	32 380	35 170
20. Flow sustenance power (sum of items 10, 14, 18), hp	720	5590	15 540	22 170	29 230	32 790	36 530	40 240	40 400	42 980	44 080	47 170	56 680	64 860	81 780	84 670	88 830	91 740	96 550
21. Total system power (sum of items 11, 15, 19), hp	4620	9790	20 250	27 130	34 350	38 060	41 900	45 690	45 850	48 480	49 610	52 760	62 510	70 880	93 660	96 590	99 200	102 150	107 040
22. Tunnel mass flow (throat), slugs/sec	97.86	182.72	241.26	259.68	270.85	274.20	276.24	278.17	278.32	278.11	277.85	277.15	275.47	275.25	275.72	275.39	275.51	275.49	276.16
23. Secondary mass flow, slugs/sec	0	0	0	0	0	0	0	0	0	0	0	0	0	0	5.95	6.92	9.46	10.57	12.41
24. Compressor mass flow (plenum valve), percent open	---	---	---	---	---	---	---	---	---	---	---	---	---	---	12.37	12.27	10.44	10.70	12.41
25. Air exchange louver setting, percent open	---	---	---	---	100	100	100	100	100	100	100	100	100	100	100	100	100	100	100
26. Outside air temperature, °F	71	71	70	70	64	64	64	64	70	64	64	64	64	64	64	64	64	64	64
27. Tunnel stagnation temperature, °F	98	110	121	131	146	150	155	154	150	155	157	165	179	168	167	167	167	167	165
28. Tunnel stagnation pressure, lb/ft²	2097	2096	2095	2094	2096	2095	2095	2096	2093	2095	2095	2095	2095	2095	2095	2095	2095	2094	2094
29. Atmospheric pressure, lb/ft²	2102	2102	2102	2102	2100	2100	2100	2100	2102	2100	2100	2100	2100	2100	2100	2100	2100	2100	2100
30. Test section plenum pressure, lb/ft²	2642	1875	1634	1499	1364	1295	1229	1167	1165	1125	1100	1075	1028	1011	960	900	847	798	752

TABLE V. - TEST SECTION FLOW CHARACTERISTICS

Calibration run	Test point	Short test section[a]					Long test section[b]				
		Test section M	dM/dx		Standard deviation	Maximum deviation	Test section M	dM/dx		Standard deviation	Maximum deviation
			per meter	per foot				per meter	per foot		
Low dewpoint											
320	86	0.199	-0.000512	-0.000156	0.000287	-0.000456	0.199	-0.000676	-0.000206	0.000418	0.000864
320	85	.401	-.000948	-.000289	.000726	.001211	.400	-.001113	-.000339	.001104	.002091
320	82	.604	-.001604	-.000489	.000827	-.001189	.604	-.001869	-.000570	.001708	.003591
320	58	.701	-.001312	-.000400	.000856	-.001700	.700	-.001710	-.000521	.001927	.004227
320	79	.802	-.000948	-.000289	.001220	-.002228	.801	-.001312	-.000400	.002428	.005045
320	76	.854	-.000656	-.000200	.001276	.002300	.853	-.001551	-.000473	.002681	.006136
320	39	.902	-.000365	-.000111	.001407	.002722	.900	-.001193	-.000364	.002739	.006091
320	35	.951	-.000292	-.000089	.001245	.002578	.950	-.001352	-.000412	.002855	.006727
320	32	.983	-.000583	-.000178	.001533	.002822	.981	-.001511	-.000461	.002976	.006636
320	23	1.004	-.000219	-.000067	.001485	.003767	1.003	.000278	.000085	.001737	.003055
320	27	1.023	.001167	.000356	.001040	-.002267	1.022	.001233	.000376	.001646	.002955
320	24	1.048	.001094	.000333	.002189	.004389	1.047	.001193	.000364	.002374	-.004000
318	26	1.080	.000583	.000178	.001995	.004244	1.079	.001112	.000339	.003310	.006345
320	55	1.105	.003135	.000956	.002640	.006344	1.104	.002704	.000824	.002923	.005734
320	53	1.156	.000292	.000089	.002464	-.005178	1.156	-.000040	-.000012	.002307	-.005355
320	48	1.208	.001167	.000356	.002351	.005133	1.206	-.000557	-.000170	.003605	.007818
320	47	1.263	.000219	.000067	.003364	.005567	1.262	-.002267	-.000691	.004232	.008045
320	43	1.311	.000948	.000289	.003497	-.006456	1.310	.001113	.000339	.004065	-.007582
High dewpoint											
317	38	0.199	-0.000729	-0.000222	0.000248	-0.000444	0.198	-0.000795	-0.000242	0.000315	-0.000545
317	34	.400	-.000948	-.000289	.000615	-.001339	.400	-.001312	-.000400	.001132	.002500
317	30	.604	-.001531	-.000467	.000830	.001478	.603	-.001829	-.000558	.001828	.003909
317	26	.704	-.001312	-.000400	.001130	-.001811	.703	-.001710	-.000521	.002002	.004136
314	8	.803	-.001458	-.000444	.001197	.002444	.802	-.001988	-.000606	.002513	.005455
314	7	.854	-.000219	-.000067	.001092	.002211	.853	-.001113	-.000339	.002482	-.005818
314	6	.904	.000583	.000178	.001372	.003067	.903	-.000278	-.000085	.002658	.005955
314	18	.953	.000437	.000133	.001125	.002467	.952	-.000557	-.000170	.002536	.006000
317	19	.954	-.000219	-.000067	.001327	.002900	.953	-.000676	-.000206	.002701	.006136
314	17	.985	-.000365	-.000111	.001398	.002833	.984	-.001193	-.000364	.002772	.006182
314	16	1.004	.001094	.000333	.001693	.003722	1.004	.001790	.000545	.001840	.003000
314	15	1.021	.000219	.000067	.001327	-.002383	1.020	.001511	.000461	.001995	.004364
314	14	1.052	.000875	.000267	.001958	.003711	1.052	.001074	.000327	.002043	-.003609
314	13	1.064	-.000365	-.000111	.001620	.004611	1.064	.000000	.000000	.002021	.003909
314	5	1.102	.003354	.001022	.002279	.005133	1.101	.002227	.000679	.002878	.005364
314	4	1.159	-.000292	-.000089	.003427	-.007267	1.158	-.000756	-.000230	.003427	-.007918
314	3	1.207	-.001021	-.000311	.001709	.004244	1.206	-.002346	-.000715	.002763	.006136
314	2	1.260	.001385	.000422	.002935	.006144	1.259	-.001630	-.000497	.004209	.008864
314	1	1.310	-.004302	-.001311	.004228	-.008856	1.309	-.003142	-.000958	.004241	-.009073

[a]Station 39.93 m (131 ft) to station 41.76 m (137 ft).

[b]Station 39.70 m (130.25 ft) to station 41.99 m (137.75 ft).

TABLE VI.- TEST SECTION AIRSTREAM CALIBRATION DATA

	Low dewpoint					High dewpoint			
Calibration run	Data point	Plenum M	Short test section M	Long test section M	Calibration run	Data point	Plenum M	Short test section M	Long test section M
320	88	0.197	0.199	0.199	317	38	0.195	0.199	0.198
320	85	.403	.401	.400	317	34	.402	.400	.400
320	82	.608	.604	.604	317	30	.607	.604	.603
320	56	.706	.701	.700	317	26	.708	.704	.703
320	79	.806	.802	.801	314	8	.808	.803	.802
320	76	.859	.854	.853	314	7	.858	.854	.853
320	39	.906	.902	.900	314	6	.907	.904	.903
320	35	.954	.951	.950	314	18	.954	.953	.952
					317	19	.955	.954	.953
320	32	.984	.983	.981	314	17	.986	.985	.984
320	23	1.005	1.004	1.003	314	16	1.005	1.004	1.004
320	27	1.028	1.023	1.022	314	15	1.025	1.021	1.020
320	24	1.058	1.048	1.047	314	14	1.062	1.052	1.052
318	26	1.090	1.080	1.079	314	13	1.076	1.064	1.064
320	55	1.120	1.105	1.104	314	5	1.118	1.102	1.101
320	53	1.169	1.156	1.156	314	4	1.168	1.159	1.158
320	48	1.214	1.206	1.206	314	3	1.215	1.207	1.206
320	47	1.260	1.263	1.262	314	2	1.260	1.260	1.259
320	43	1.303	1.311	1.310	314	1	1.304	1.310	1.309

TABLE VII.- TEST SECTION WALL DIVERGENCE ANGLES FOR ZERO AXIAL GRADIENT OF STATIC PRESSURE IN TEST SECTION

Calibration of October 1965

(a) Without test section air removal[*]

M	δ, min		M	δ, min
0.200	0		0.925	8.2
.700	0		.950	10.4
.725	.5		.975	13.5
.750	1.0		.980	14.2
.775	1.5		1.000	13.8
.800	2.0		1.020	7.0
.825	3.0		1.025	5.4
.850	4.0		1.050	0
.875	5.0		1.075	0
.900	6.50			

[*]At subsonic speeds, the pressure gradient does not vary significantly with dewpoint.

(b) With test section air removal

Dewpoint		Wall divergence angle δ, in minutes, for —						
°C	°F	M = 1.15	M = 1.175	M = 1.20	M = 1.225	M = 1.25	M = 1.275	M = 1.30
-12.2	10	13.6	11.1	10.5	13.8	17.5	20.7	23.8
-9.4	15	13.6	11.1	10.5	13.8	17.5	20.7	23.9
-6.7	20	13.6	11.1	10.5	13.8	17.5	20.8	24.2
-3.9	25	13.6	11.1	10.5	13.8	17.5	21.2	24.8
-1.1	30	13.6	11.1	10.5	13.9	17.8	21.6	25.5
1.7	35	13.6	11.1	10.7	14.2	18.3	22.4	26.4
4.4	40	12.4	10.9	11.0	14.6	18.9	23.2	27.5
7.2	45	11.4	10.8	11.7	15.3	19.7	24.2	28.8
10.0	50	10.4	10.5	12.2	16.0	20.6	25.2	30.0
12.8	55	9.4	10.3	12.8	16.8	21.4	26.4	31.4
15.6	60	8.3	10.3	13.5	17.6	22.4	27.6	32.9
18.3	65	7.2	10.3	14.1	18.6	23.6	28.9	34.5
21.1	70	6.2	10.2	14.7	19.7	25.0	30.5	36.2
23.9	75	4.9	10.0	15.4	20.8	26.4	32.1	37.9
26.7	80	3.8	9.8	15.8	21.8	27.8	33.8	39.8
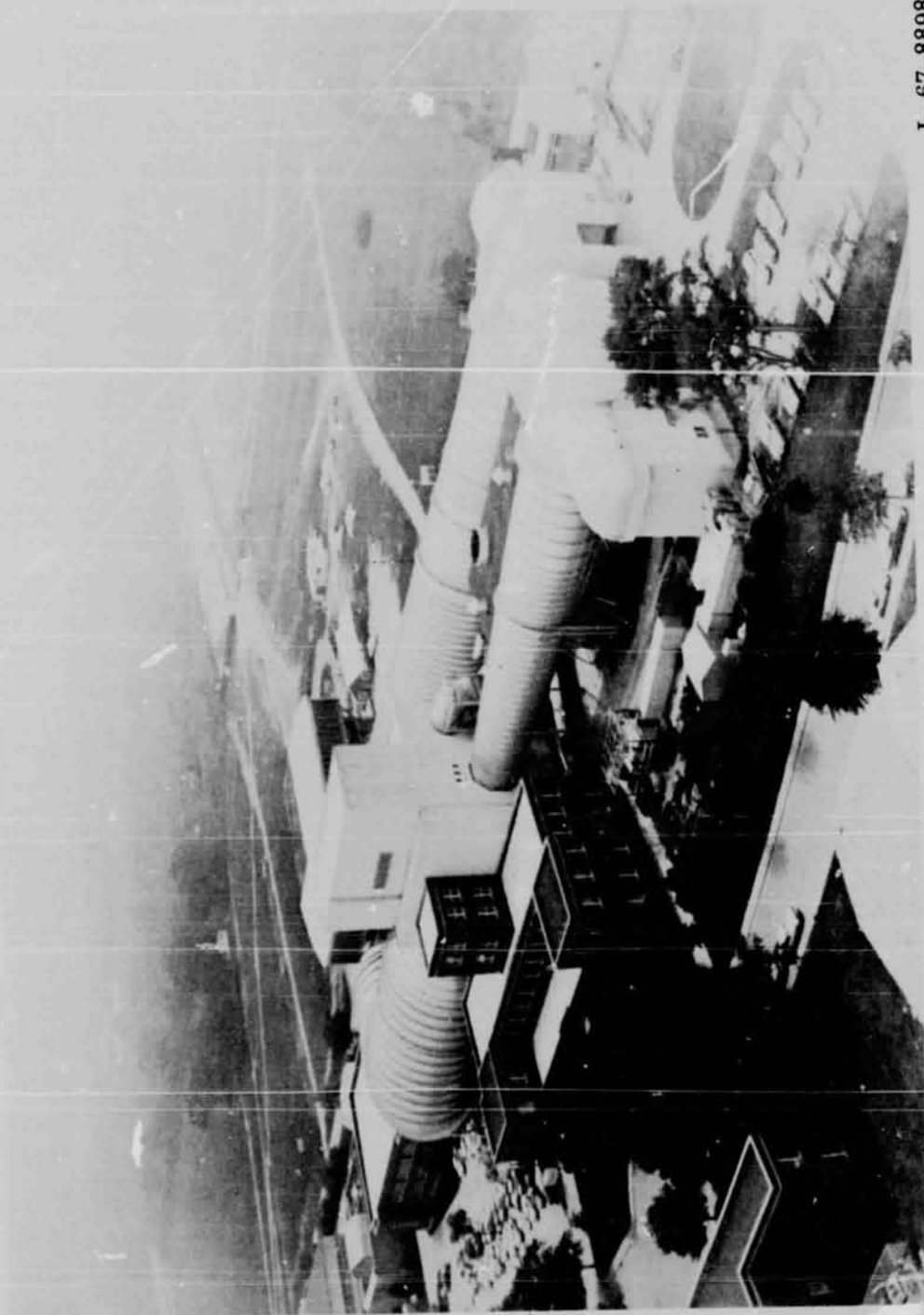
Figure 1.- The 16-foot transonic tunnel at NASA Langley Research Center.

L-67-8898
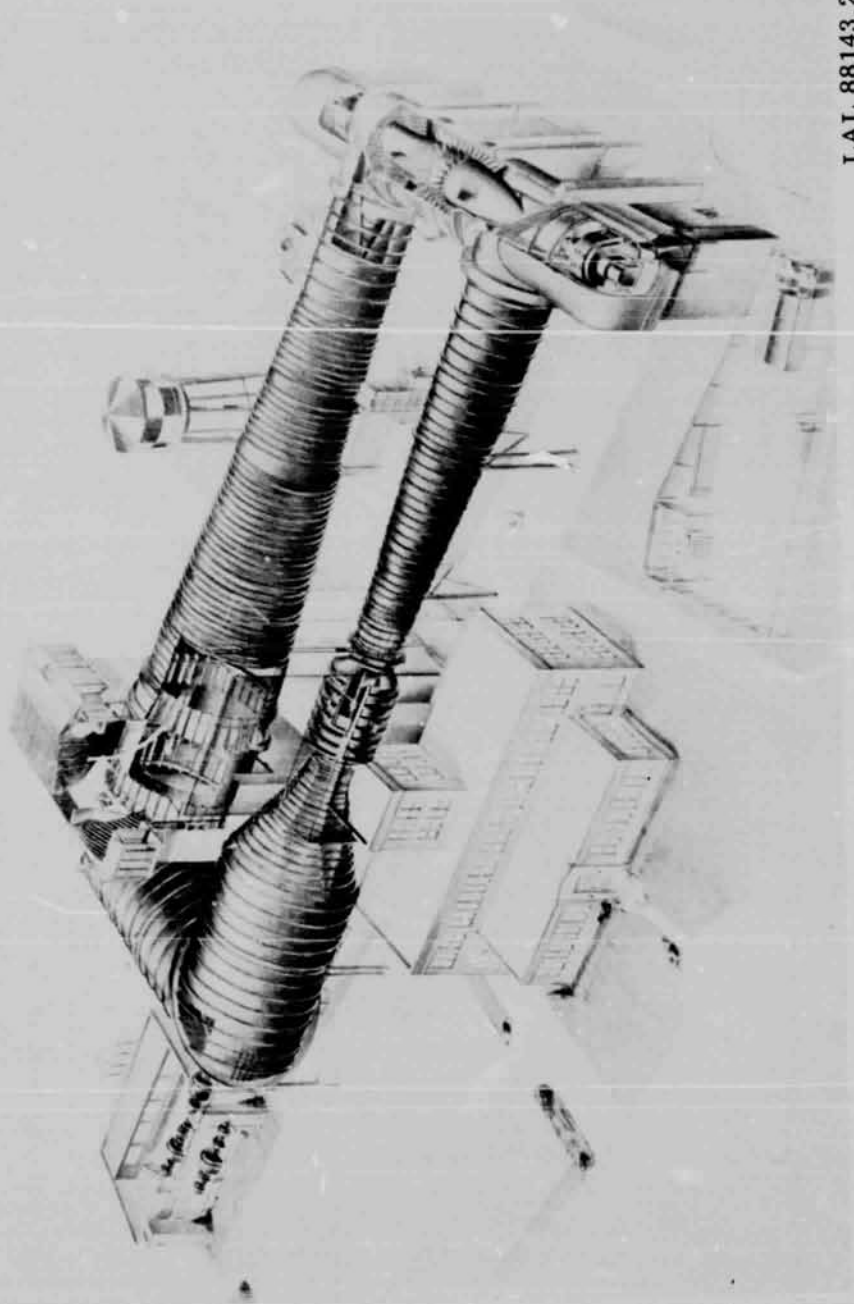
LAL 88143.2

Figure 2. - Phantom view of the Langley 16-foot transonic tunnel before addition of the air removal system.

57
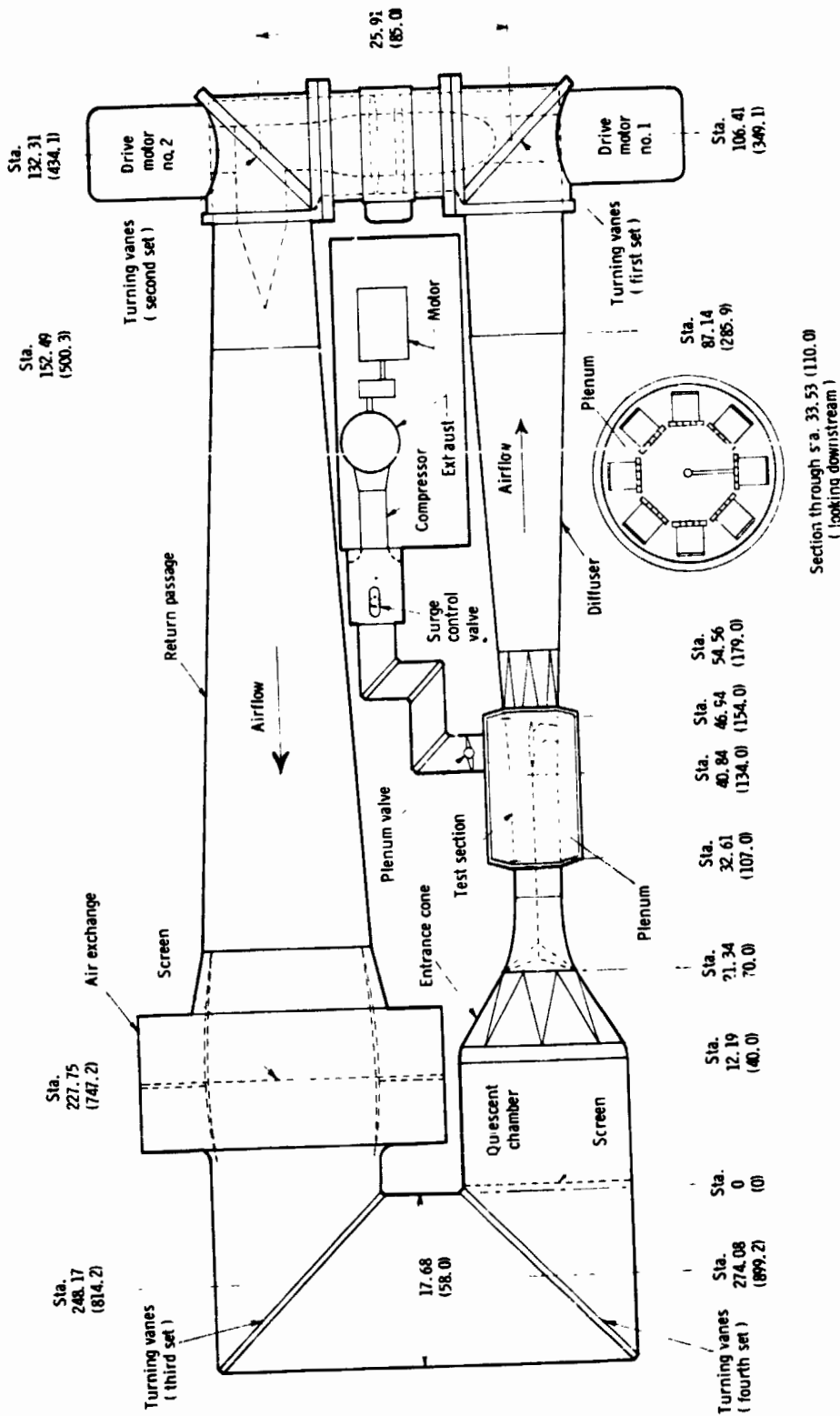
Figure 3.- Arrangement of the Langley 16-foot transonic tunnel. Dimensions are in meters (feet). (See table I for complete listing of axial stations and dimensions.)
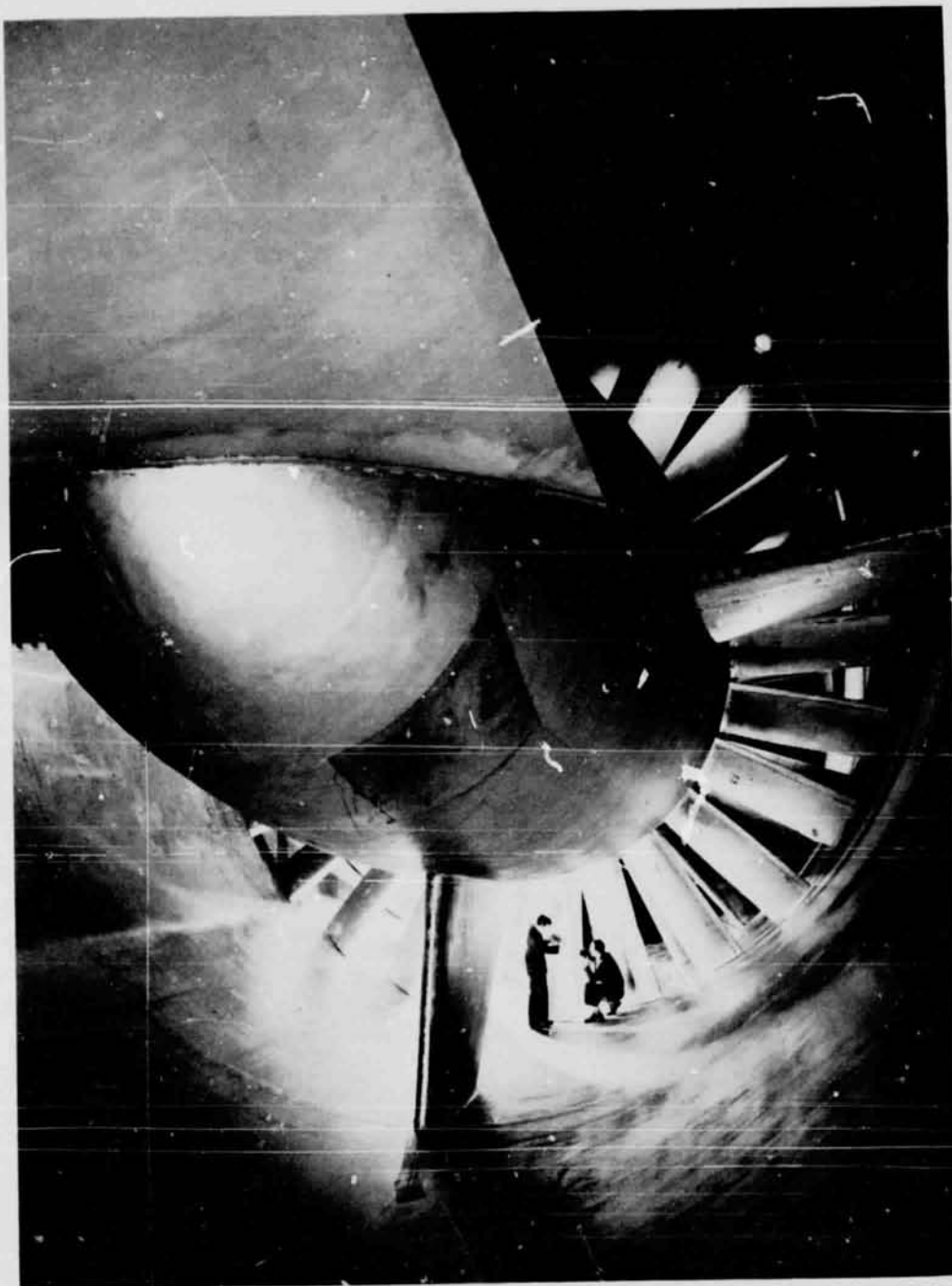
LAL 69578

Figure 4.- Main drive fans in Langley 16-foot transonic tunnel.
(View looking downstream.)
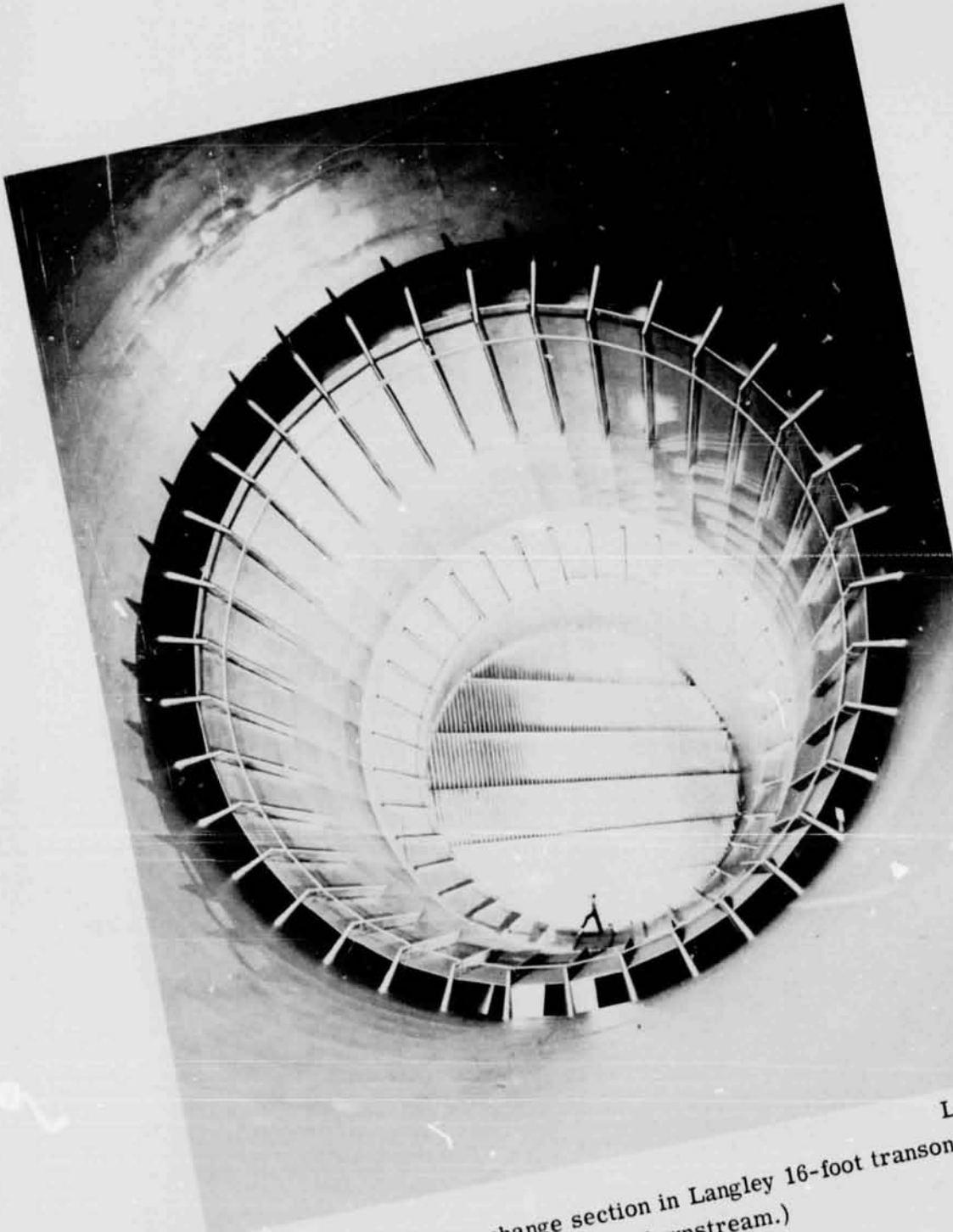
LAL 69586

Figure 5.- Cooling air exchange section in Langley 16-foot transonic tunnel.
(View looking downstream.)

LAL 69573

(b) Upstream view of axial survey tube. Slot shape 18.

LAL 69575

(a) Downstream view of axial survey tube. Slot shape 18.

Figure 6.- Survey instrumentation in the test section of the Langley 16-foot transonic tunnel.

61
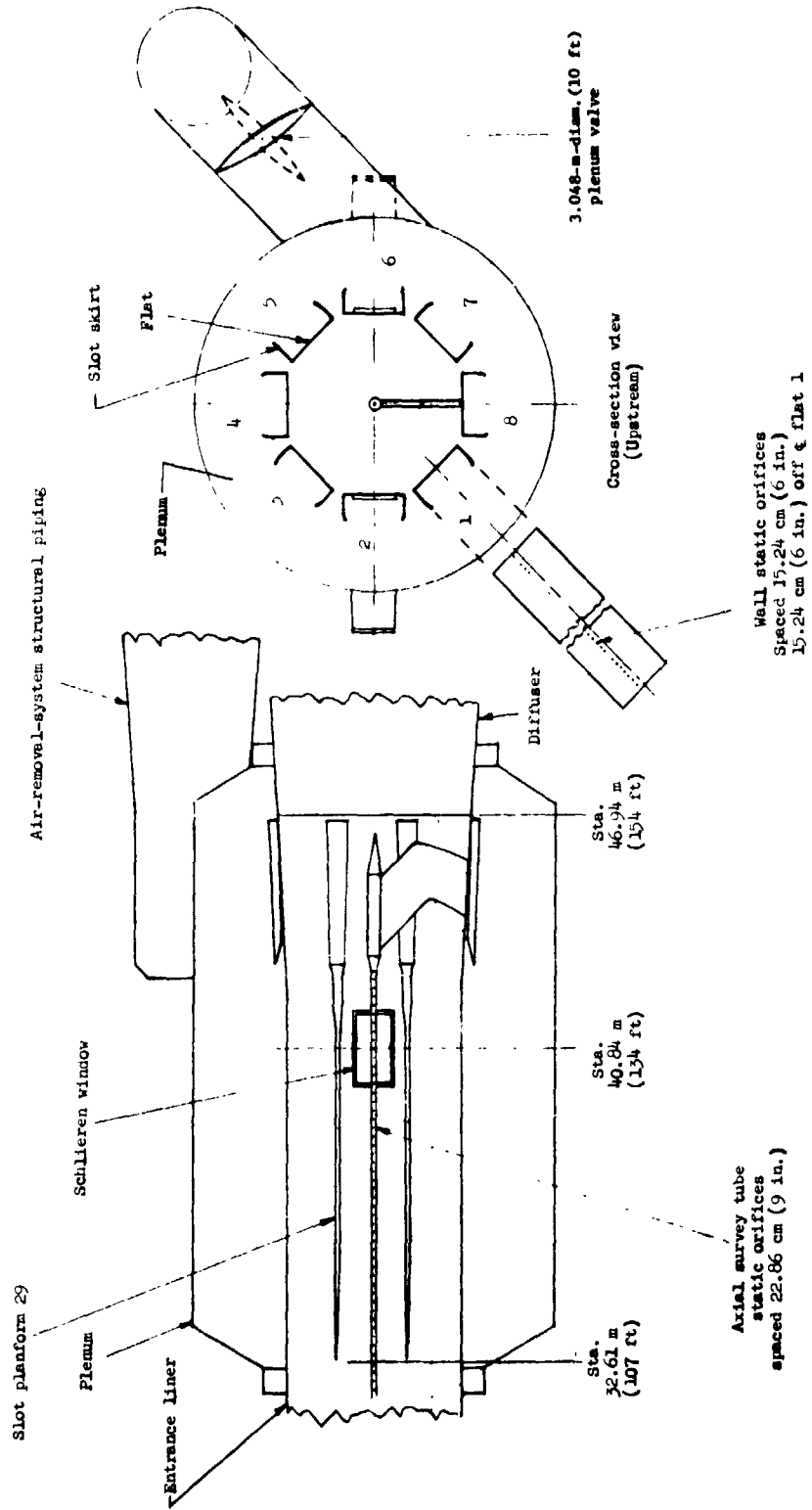
Figure 7.- Schematic arrangement of test section with calibration instrumentation.

168.91 cm (66.5 in.)

13.23 cm (5.21 in.)

60.96 cm (24 in.)

Slot half-width

Skirt

Slot edge strip

Flat

Spacer

Truss member
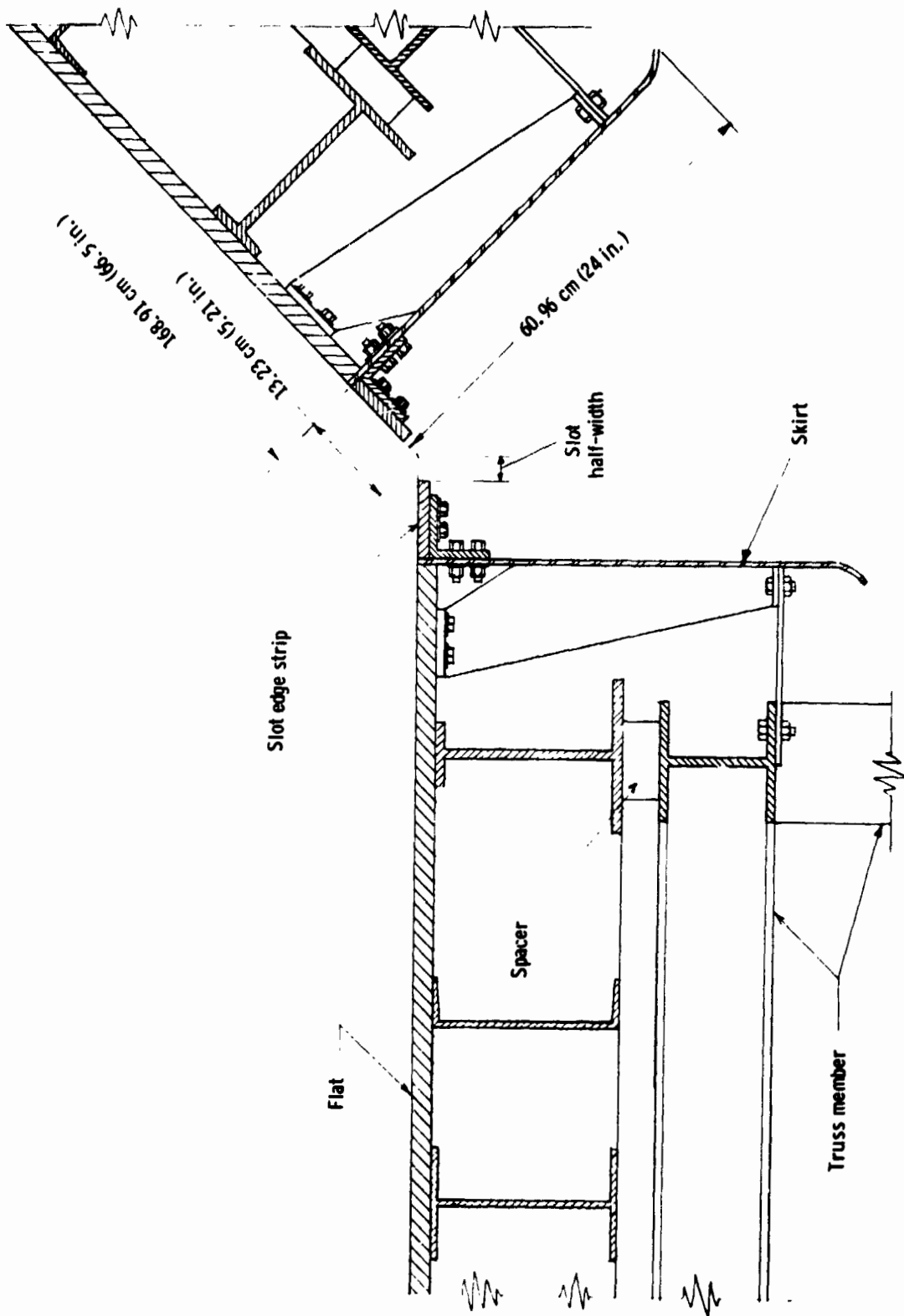
Figure 8.- Transverse section of Langley 16-foot transonic tunnel test section showing typical structural details.

63
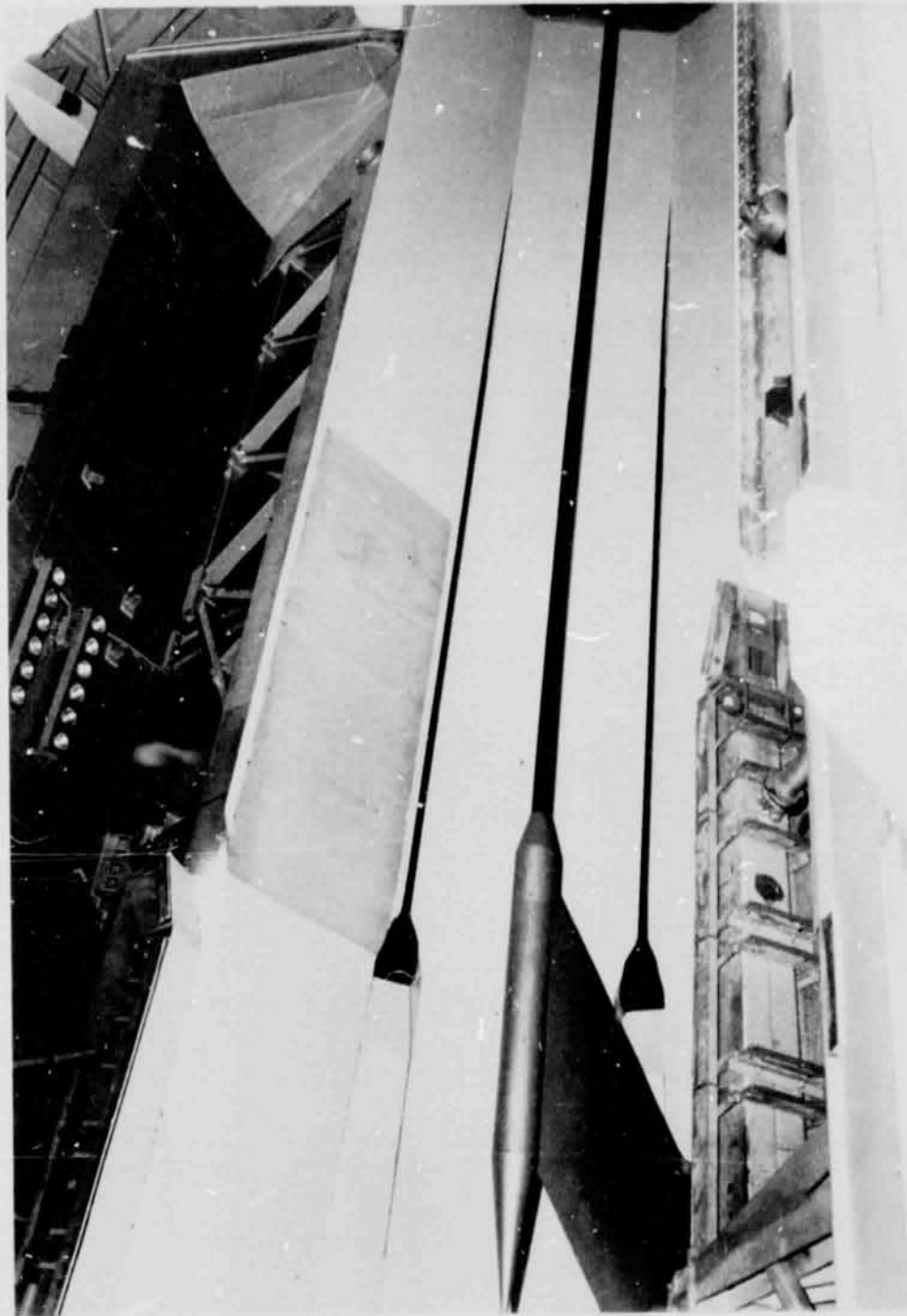
L-63-8244

(a) Survey tube and strut, diffuser entrance vanes and lips, slot shape 27.

Figure 9.- Arrangement of test section structural components.

(b) Diffuser entrance vane and lip; test section wall divergence angle, 0°0'.
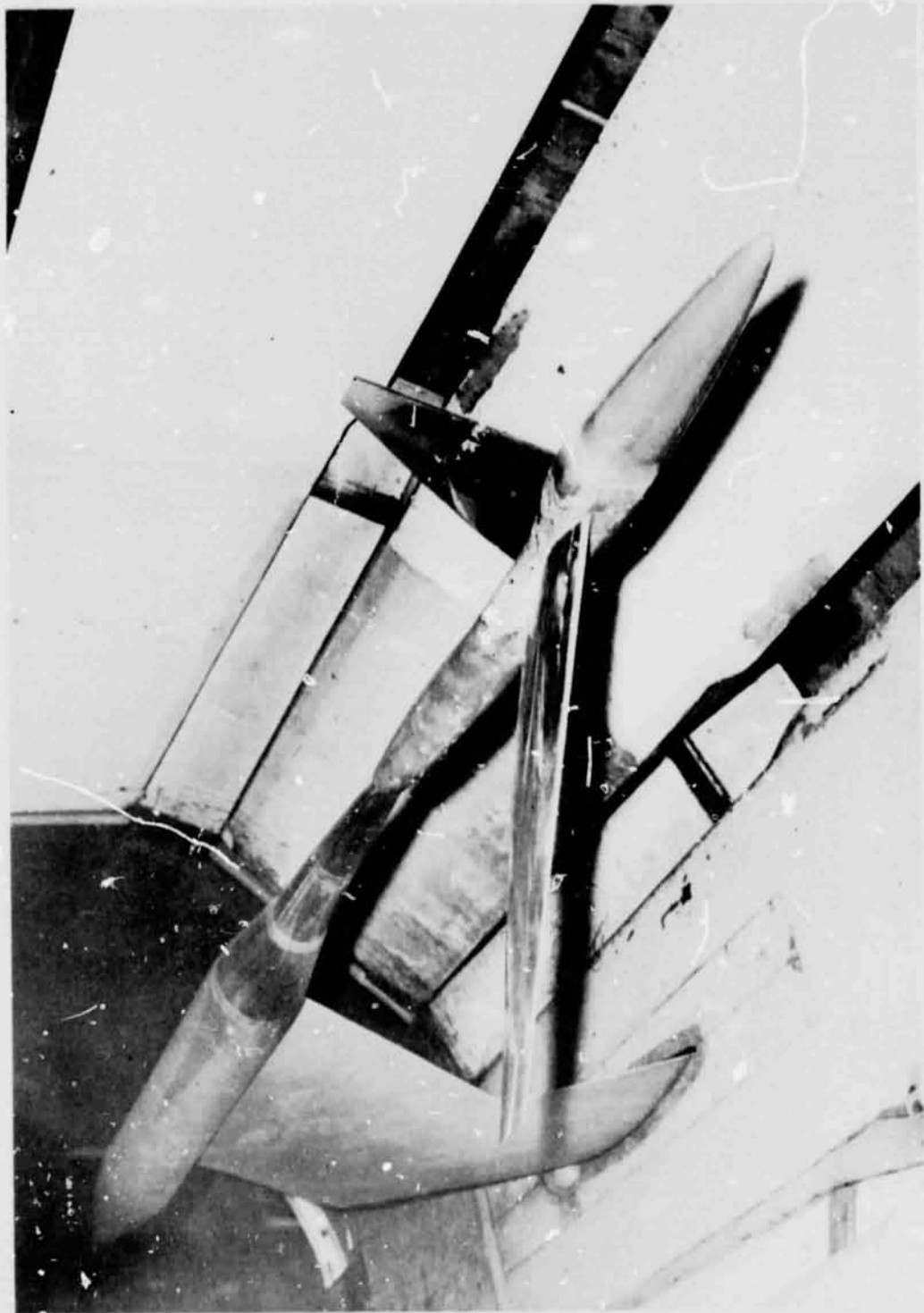
Figure 9. – Concluded.

(a) Model mounted for wind-tunnel investigation.

Figure 10.- Model support strut and sting.

66

Tunnel wall

Cylindrical body
35.56 cm (14 in.) diam.

Sting butt

85.55 cm
(33.68 in.)

182.88 cm
(72 in.)

Knuckle

241.94 cm
(95.25 in.)

Support strut

Shoes

Circular-arc track

Test section wall

Lead screw

Center of
angle-of-attack
rotation

Tunnel station
40.84 m (134 ft)

Angle-of-attack
drive motor

Plenum wall
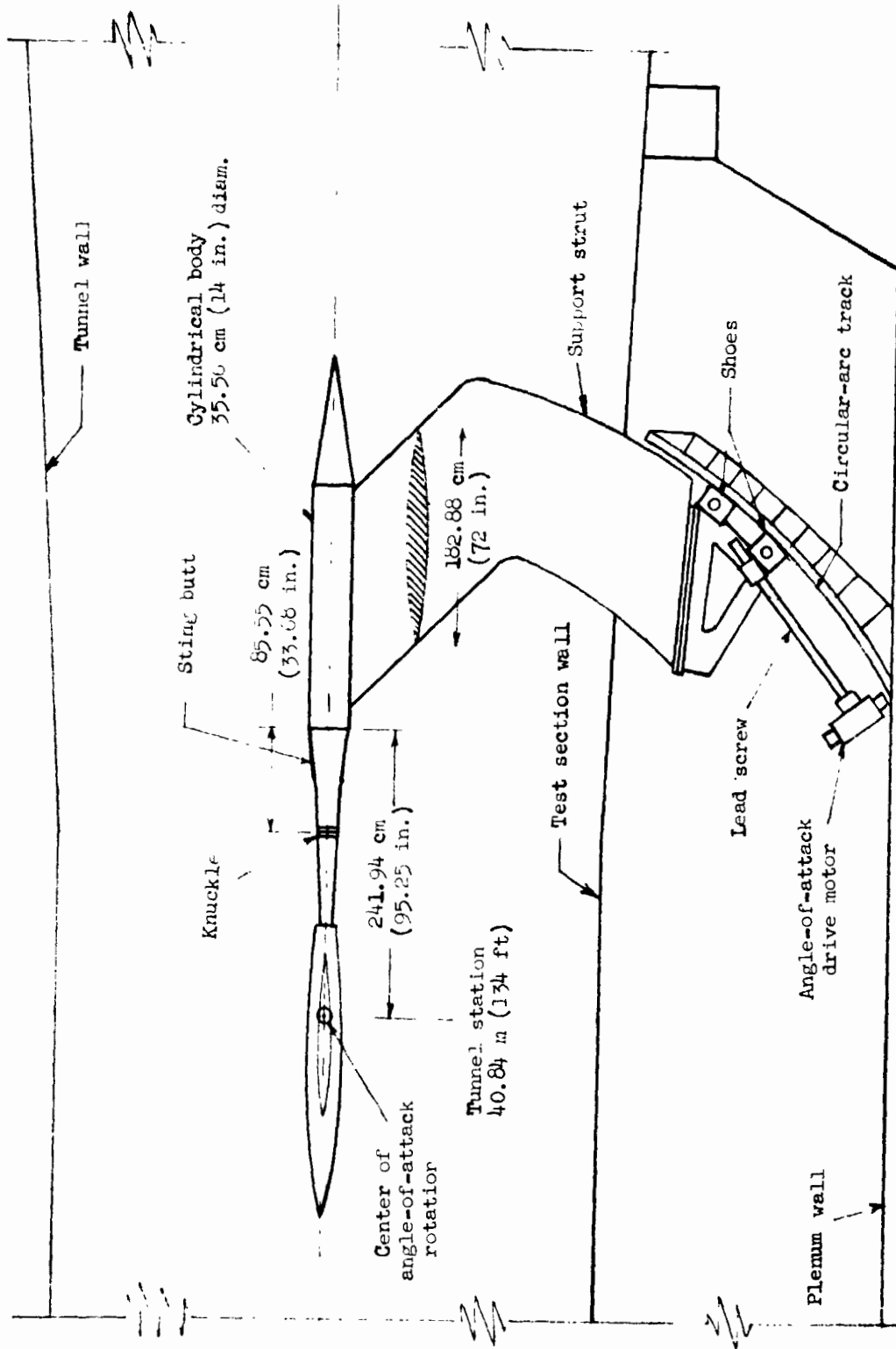
(b) Sketch of model support system in Langley 16-foot transonic tunnel.

Figure 10.- Concluded.

67
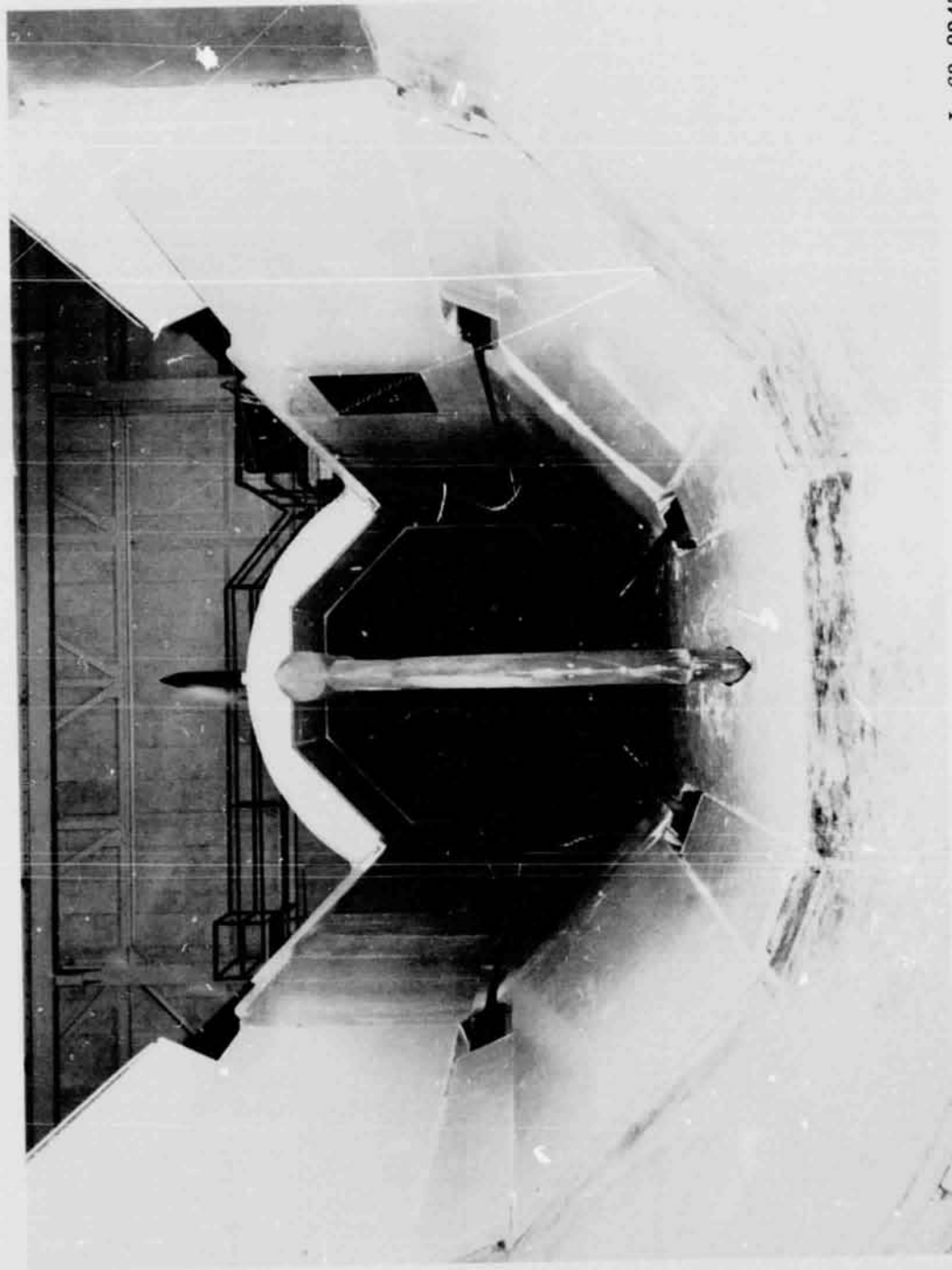
Figure 11.- View (looking upstream) of test section with upper hatch open.

L-63-8245
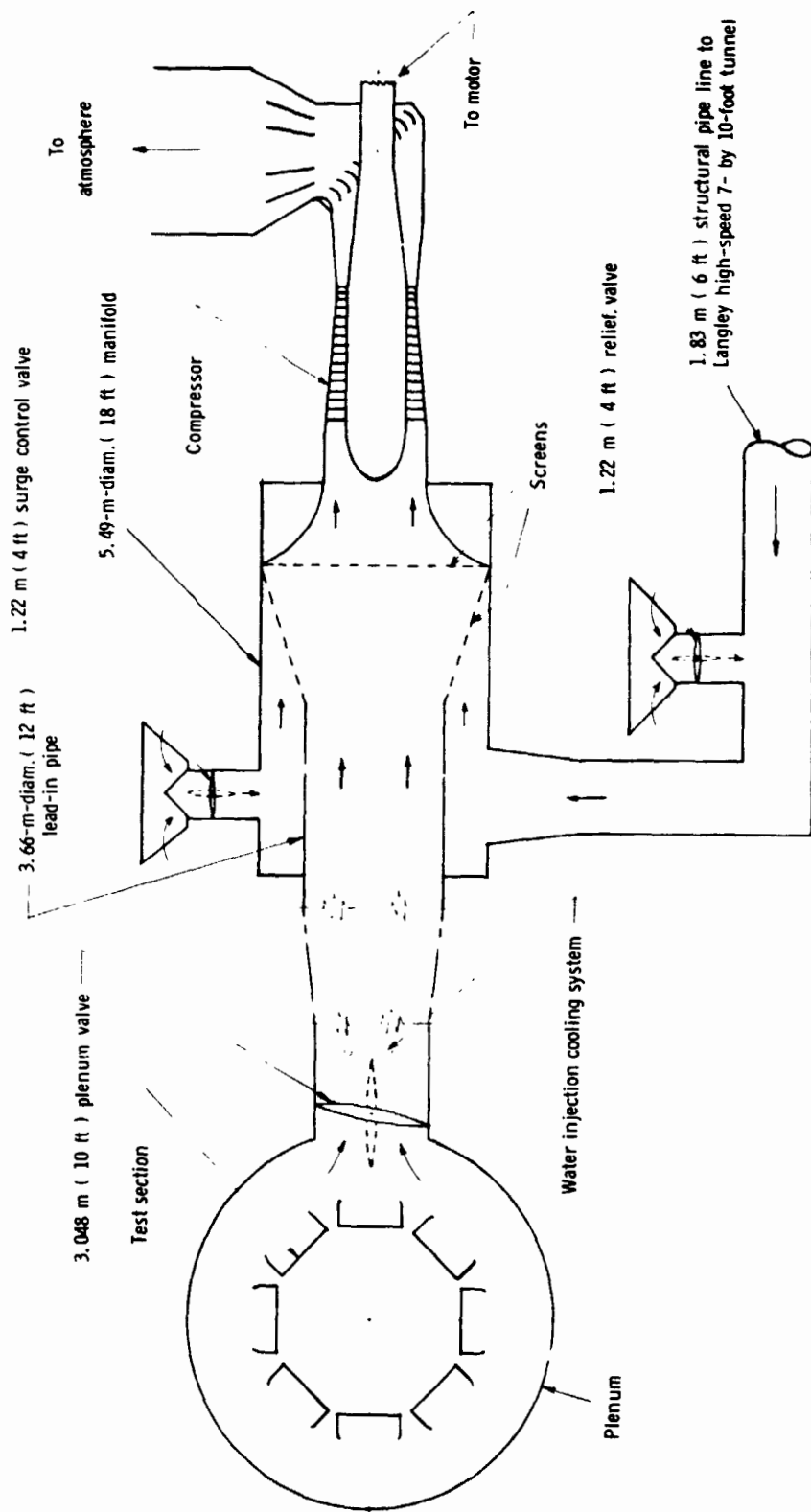
Figure 12.- Schematic arrangement of test section air removal system.

69
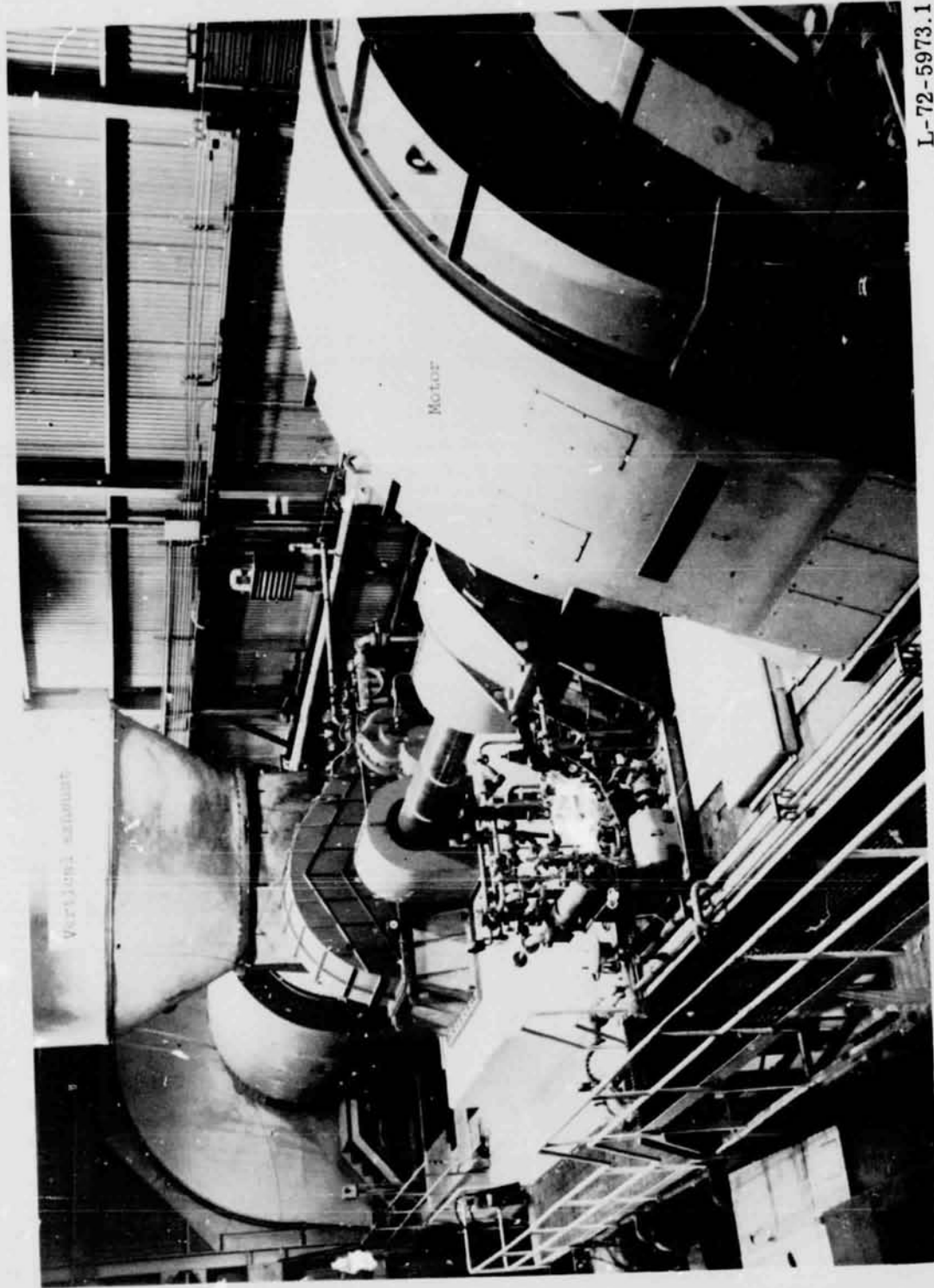
(a) Motor, drive train, compressor, and vertical exhaust.

Figure 13.- Test section air removal compressor installation.
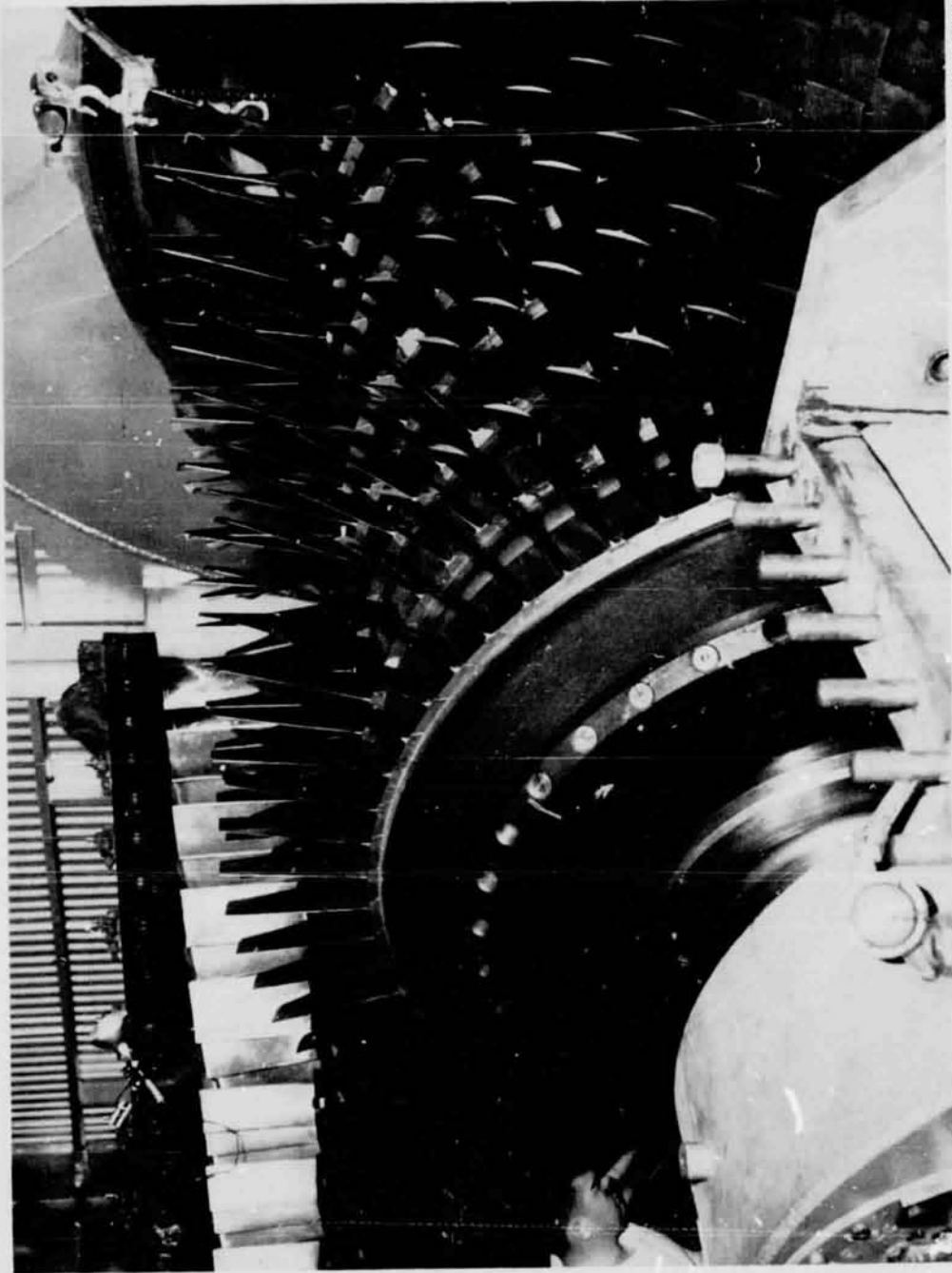
L-60-1782

(b) Compressor blading.

Figure 13.- Concluded.
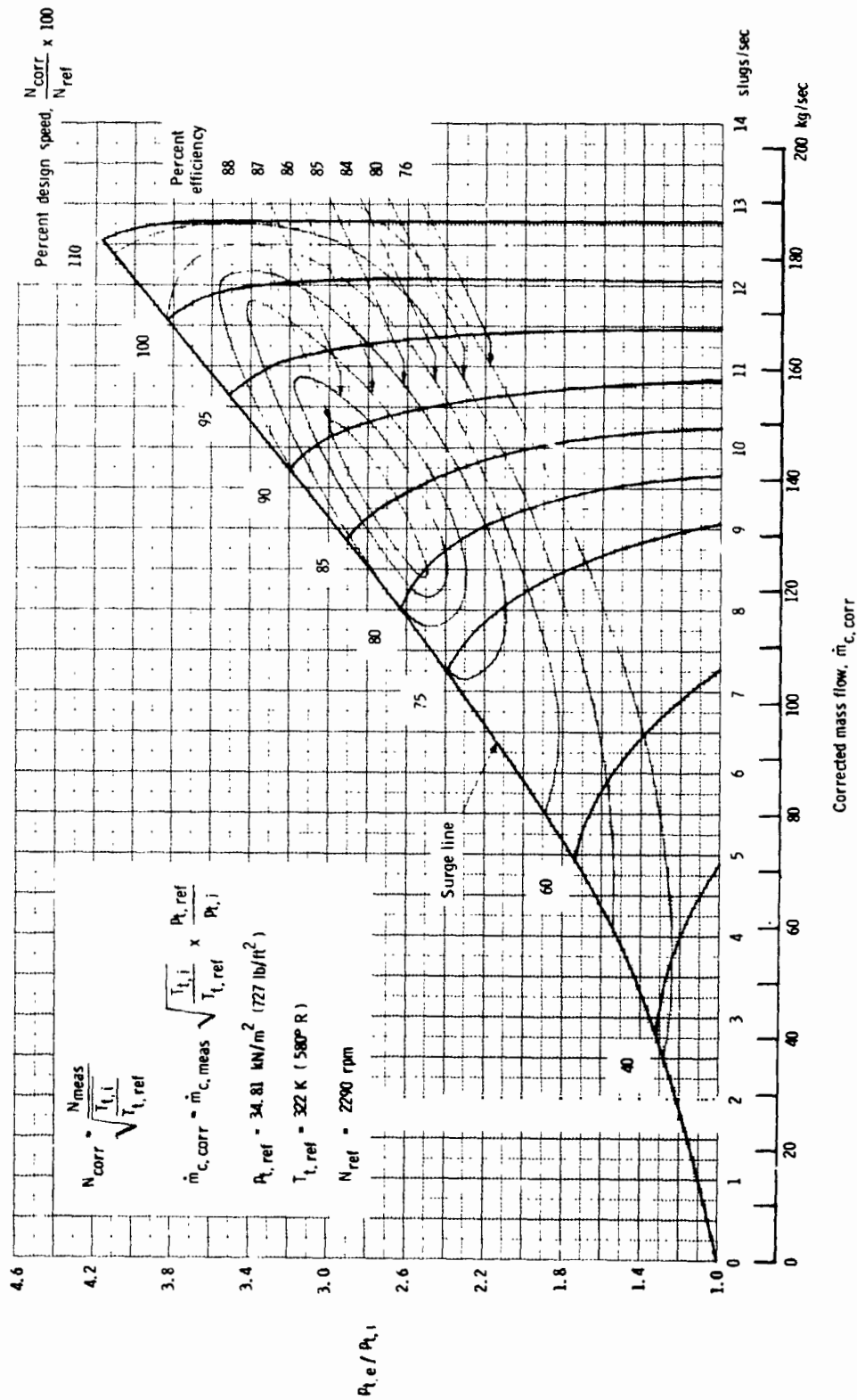
Figure 14. - Performance curves for air removal compressor in Langley 16-foot transonic tunnel.

$$N_{corr} = \frac{N_{meas}}{\sqrt{\dfrac{T_{t,i}}{T_{t,ref}}}}$$

$$\dot{m}_{c,corr} = \dot{m}_{c,meas} \sqrt{\frac{T_{t,i}}{T_{t,ref}}} \times \frac{P_{t,ref}}{P_{t,i}}$$

$P_{t,ref} = 34.81$ kN/m^2 (727 lb/ft^2)

$T_{t,ref} = 322$ K (580° R)

$N_{ref} = 2290$ rpm

Percent design speed, $\dfrac{N_{corr}}{N_{ref}} \times 100$

Percent efficiency

88
87
86
85
84
80
76

Surge line

Corrected mass flow, $\dot{m}_{c,corr}$

$P_{t,e}/P_{t,i}$

slugs/sec

kg/sec
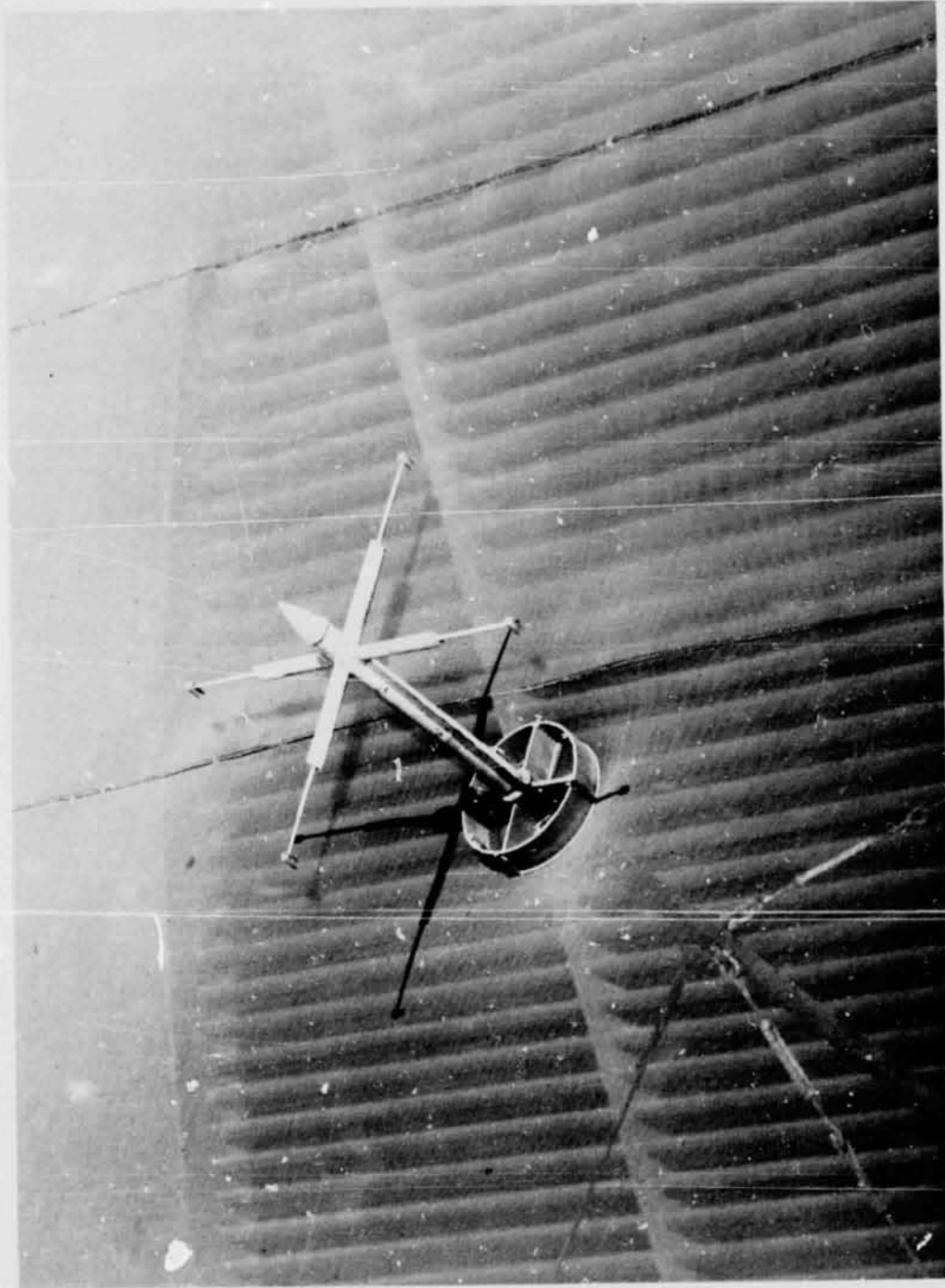
(a) Closeup view of stagnation-pressure-probe support.

Figure 15.- Airstream stagnation-pressure probes.

L-73-3791
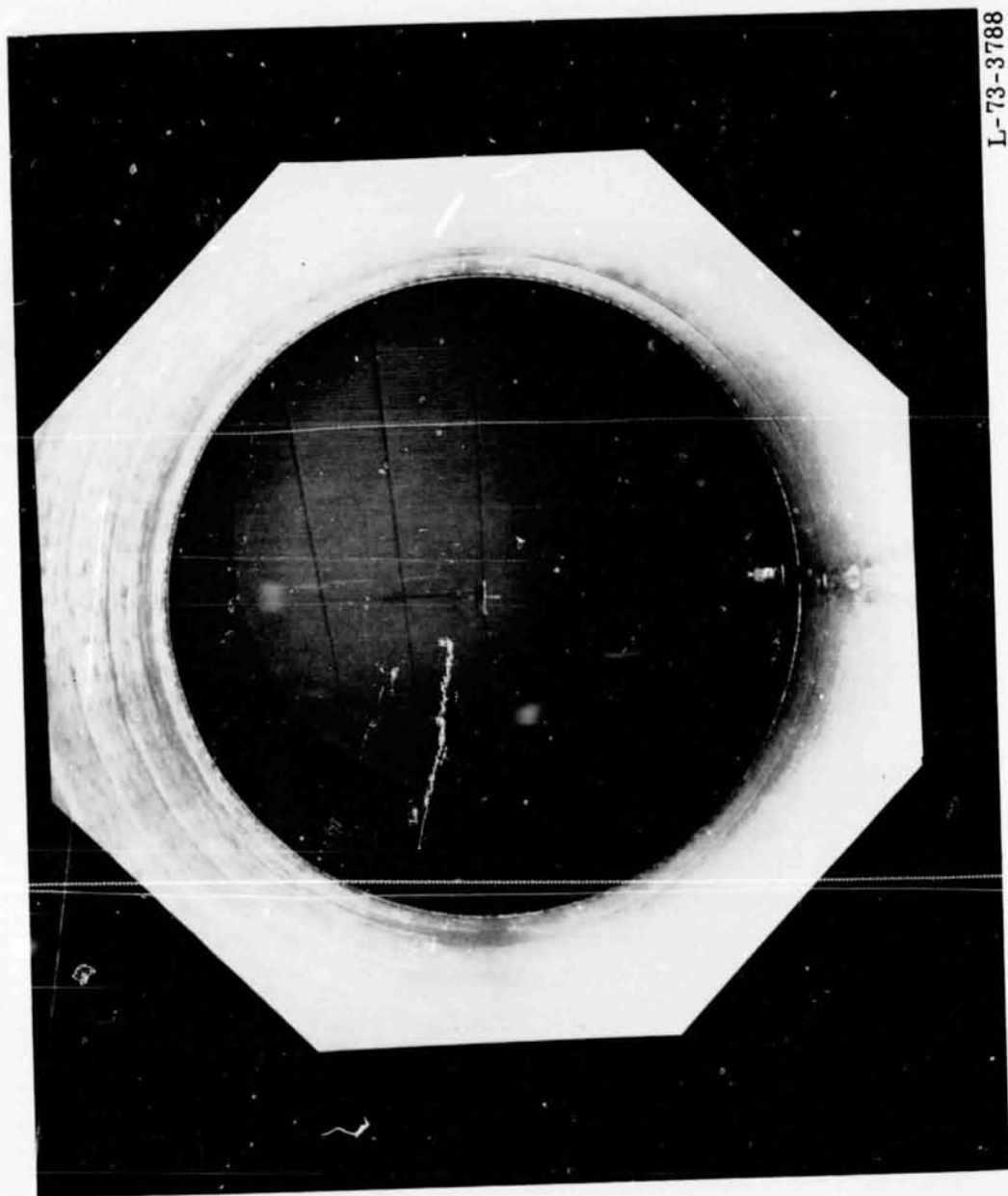
L-73-3788

(b) Stagnation-pressure-probe support viewed from test section.

Figure 15.- Concluded.
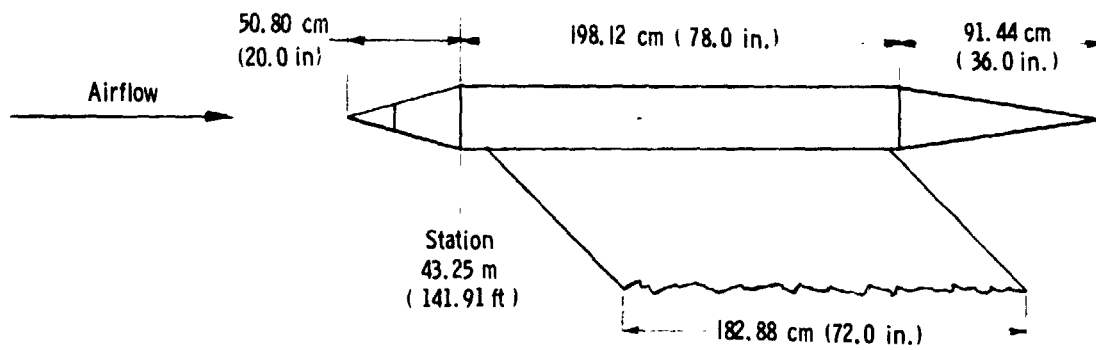
Conical nose fairing; survey tube removed; test section empty

27.31 cm (10.75 in.) diam.

- 10.16 cm (4.0 in.) diam.

30.48 cm (12.0 in.)

18.29 cm (7.2 in.)

Survey tube installed

140   142   144   146   148   150   152 ft

43   44   45   46 m
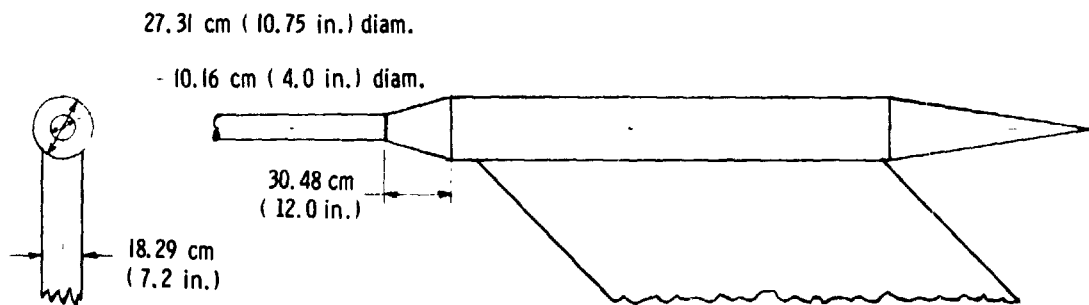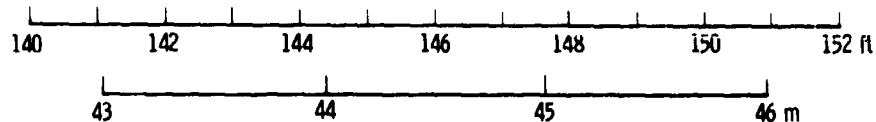
Tunnel station

Figure 16.- Strut head for center-line survey tube.

75
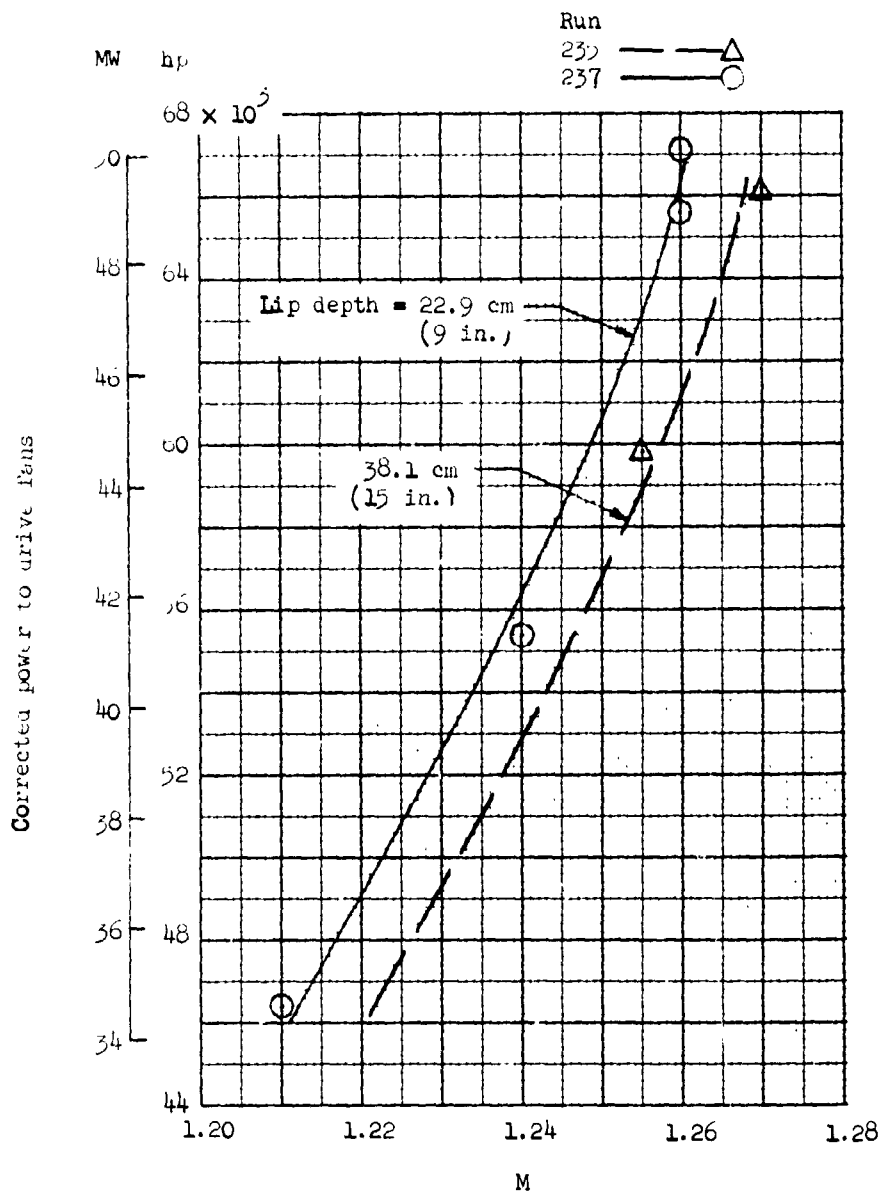
Figure 17.- Effect of diffuser entrance vane lip setting on wind-tunnel Mach number and power. Exploratory test; visual data; diffuser cracks not sealed; entrance vane lip angle, 20°; test section wall divergence angle, 0°5'.
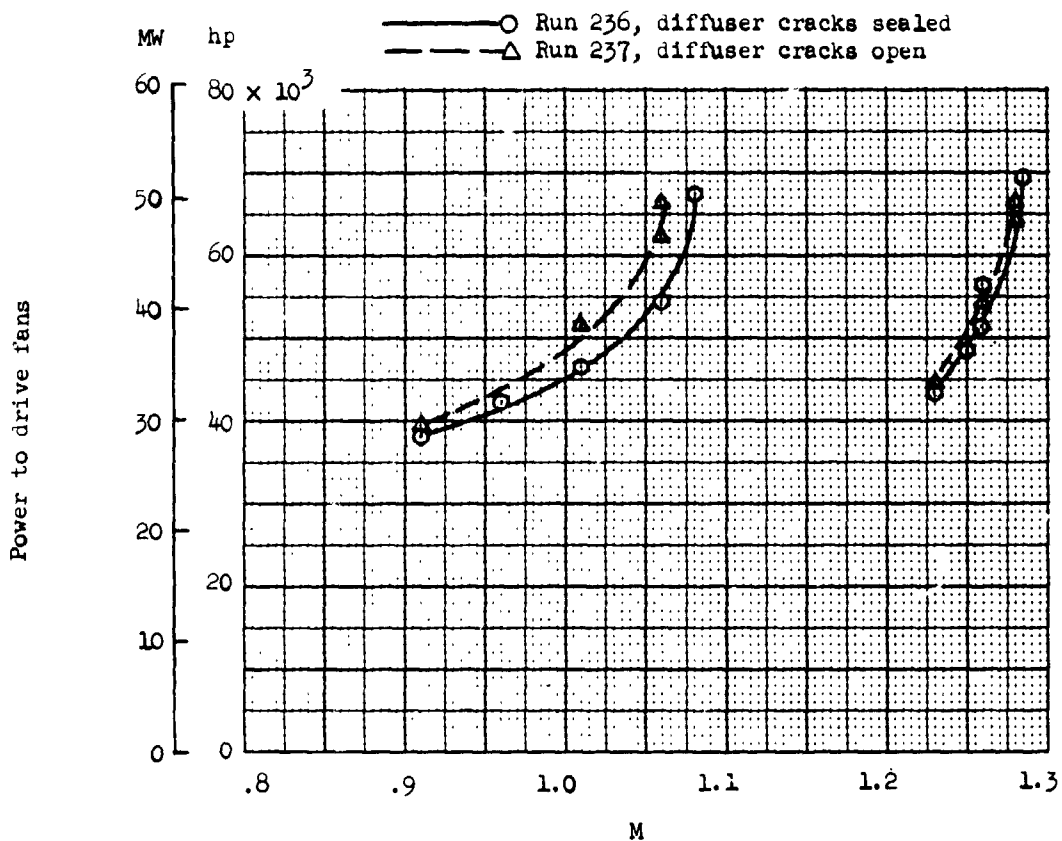
Figure 18.- Effect of diffuser joint seals on wind-tunnel Mach number and power. Exploratory test; visual data; wall divergence angle, $0^{o}5'$; entrance vane lip depth, 22.9 cm (9 in.); compressor motor speed, 550 rpm; power not corrected.
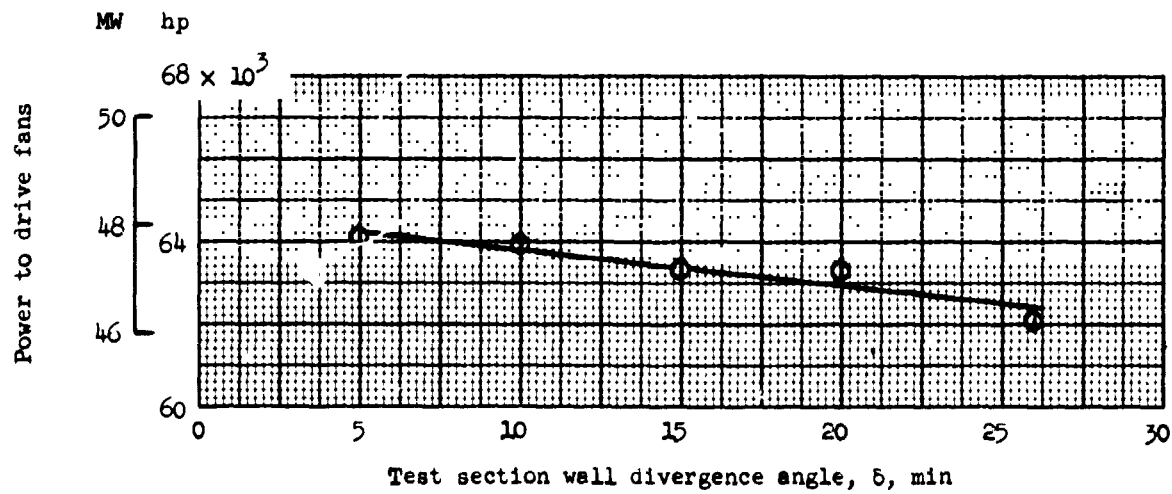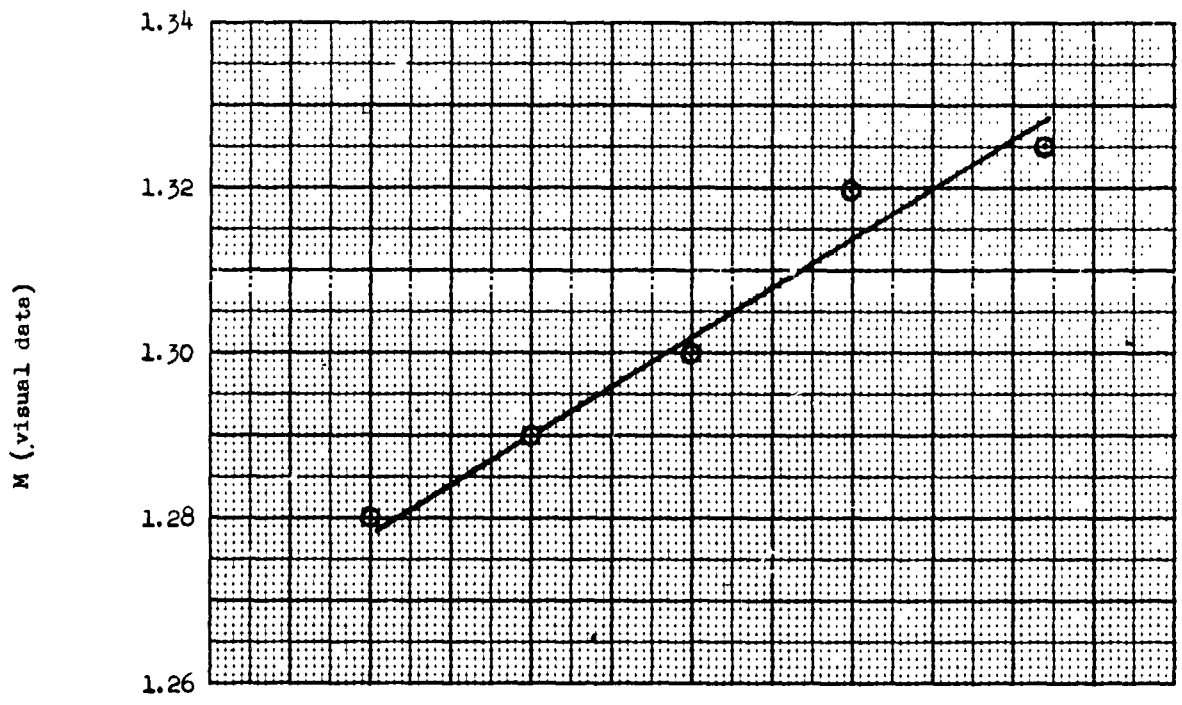
Figure 19.- Effect of test section wall divergence angle on wind-tunnel Mach number and power. Exploratory test; run 237; visual data; diffuser cracks not sealed; plenum valve full open; compressor speed, 552 rpm; power not corrected.

78
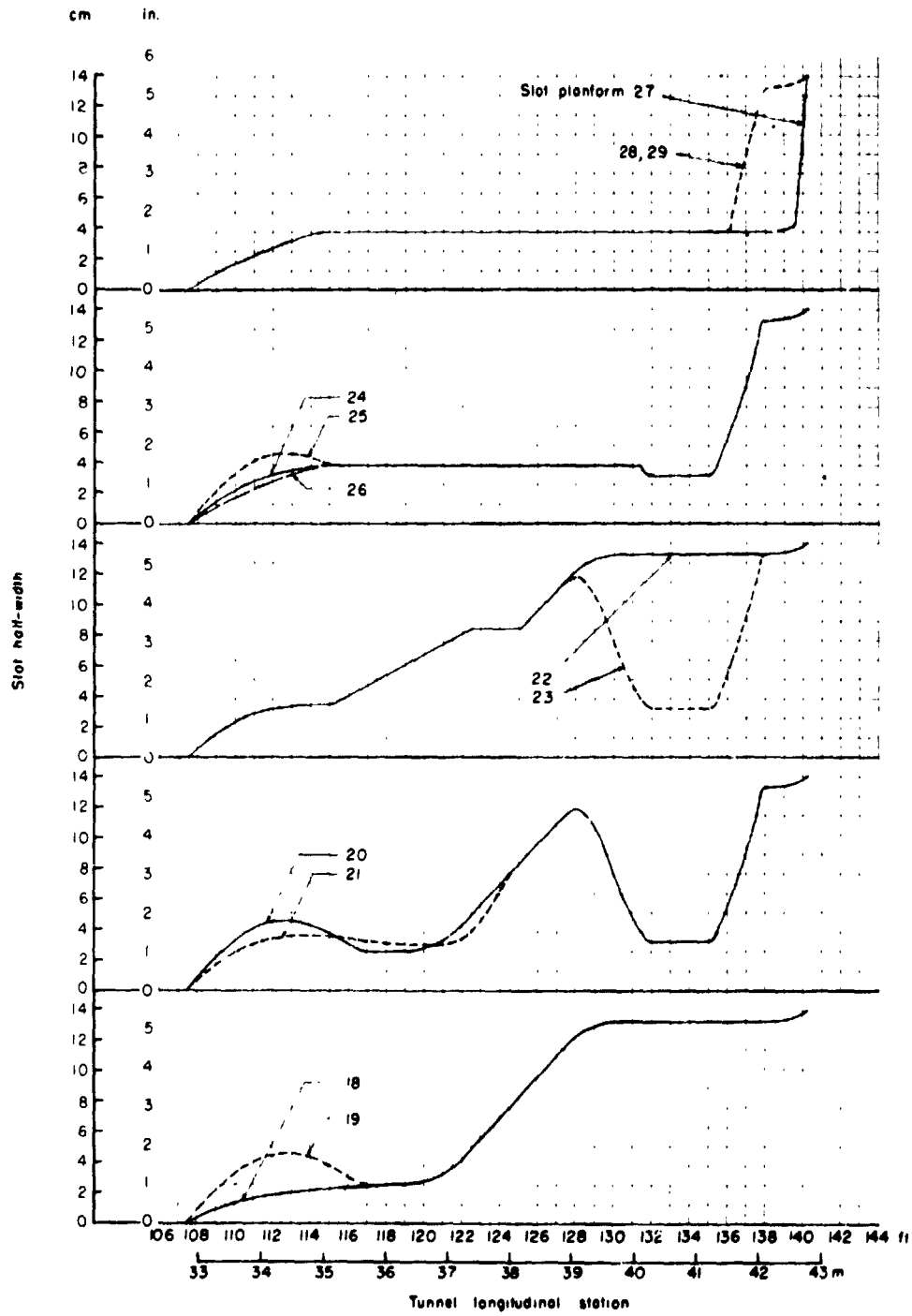
Figure 20.- Slot planforms investigated in the Langley 16-foot transonic tunnel. Slot half-width when test section wall divergence angle is $0^O0'$.

79
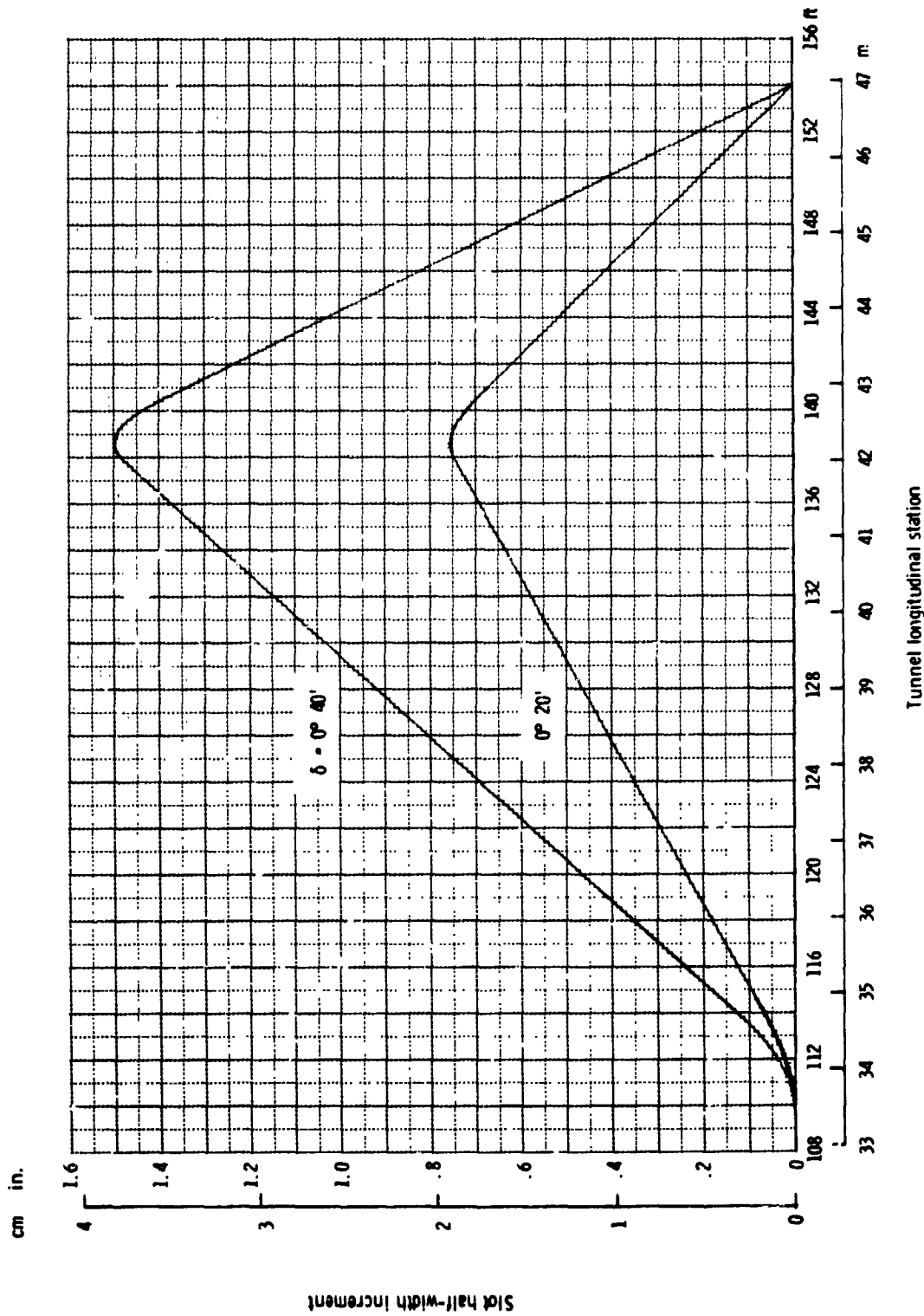
Figure 21.- Slot half-width increment variation with tunnel longitudinal station for test section
wall divergence angles of $0°20'$ and $0°40'$.

80
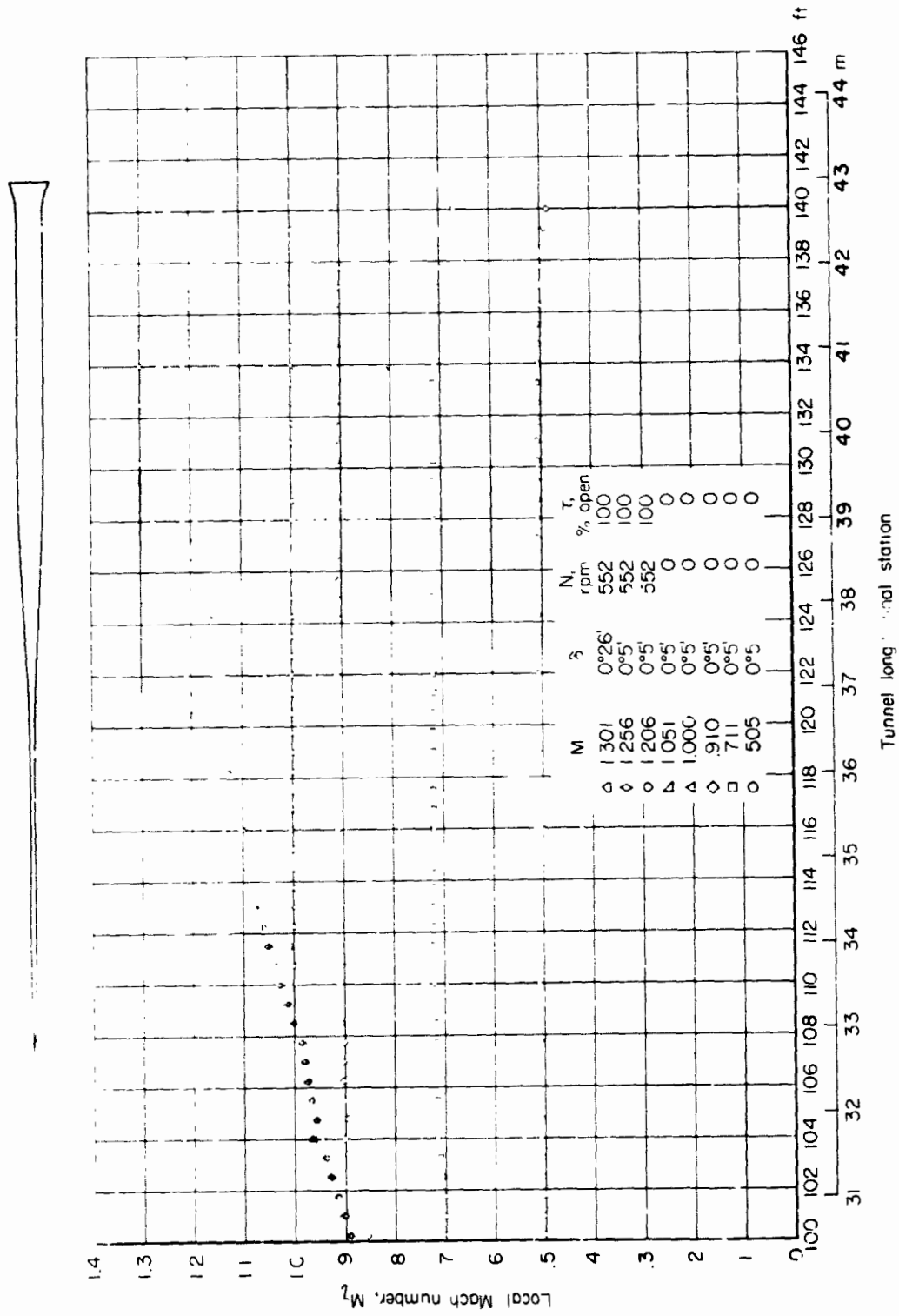
Figure 22.- Longitudinal Mach number distribution along center line of test section for slot shape 18.
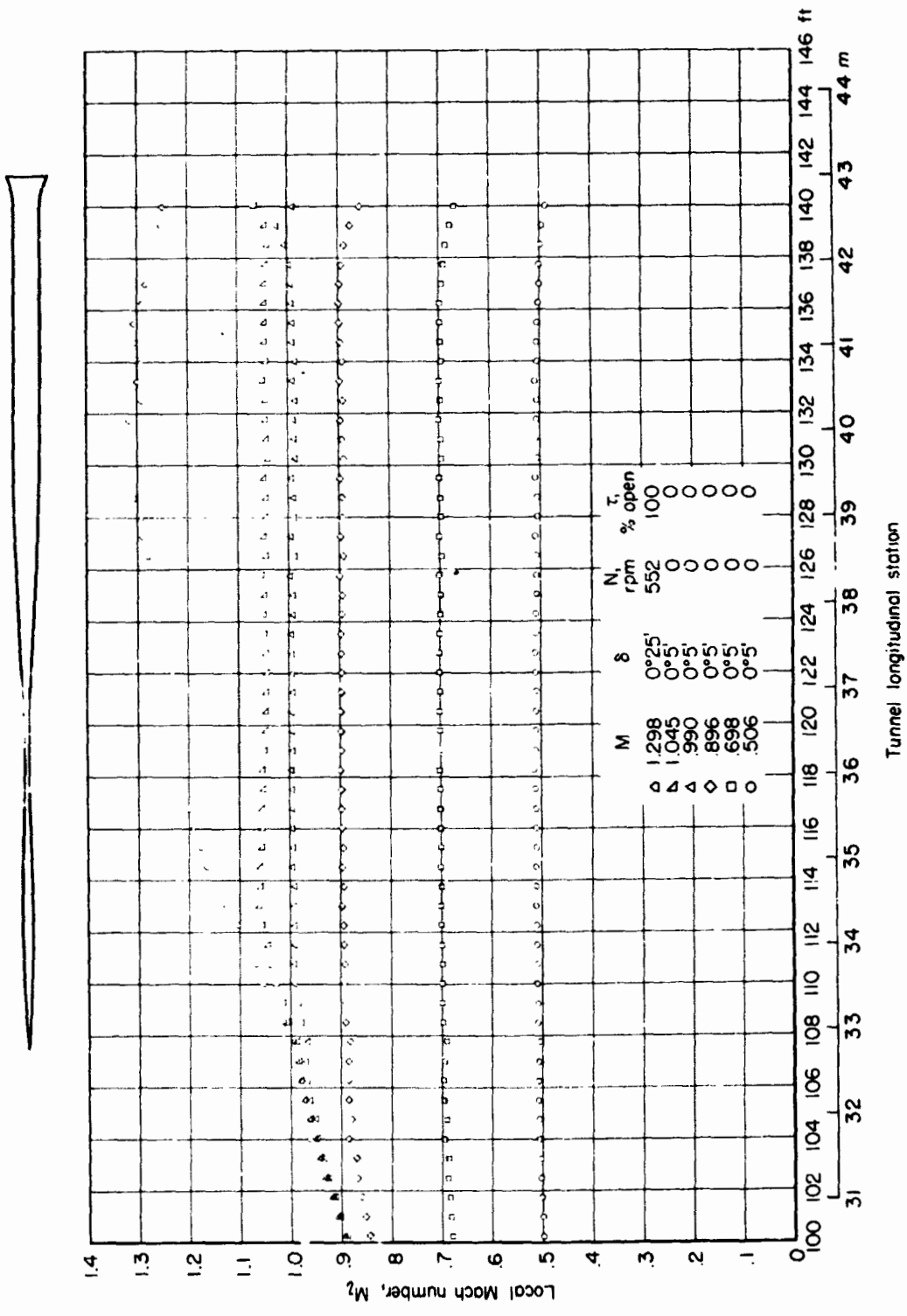
Figure 23.- Longitudinal Mach number distribution along center line of test section for slot shape 19.
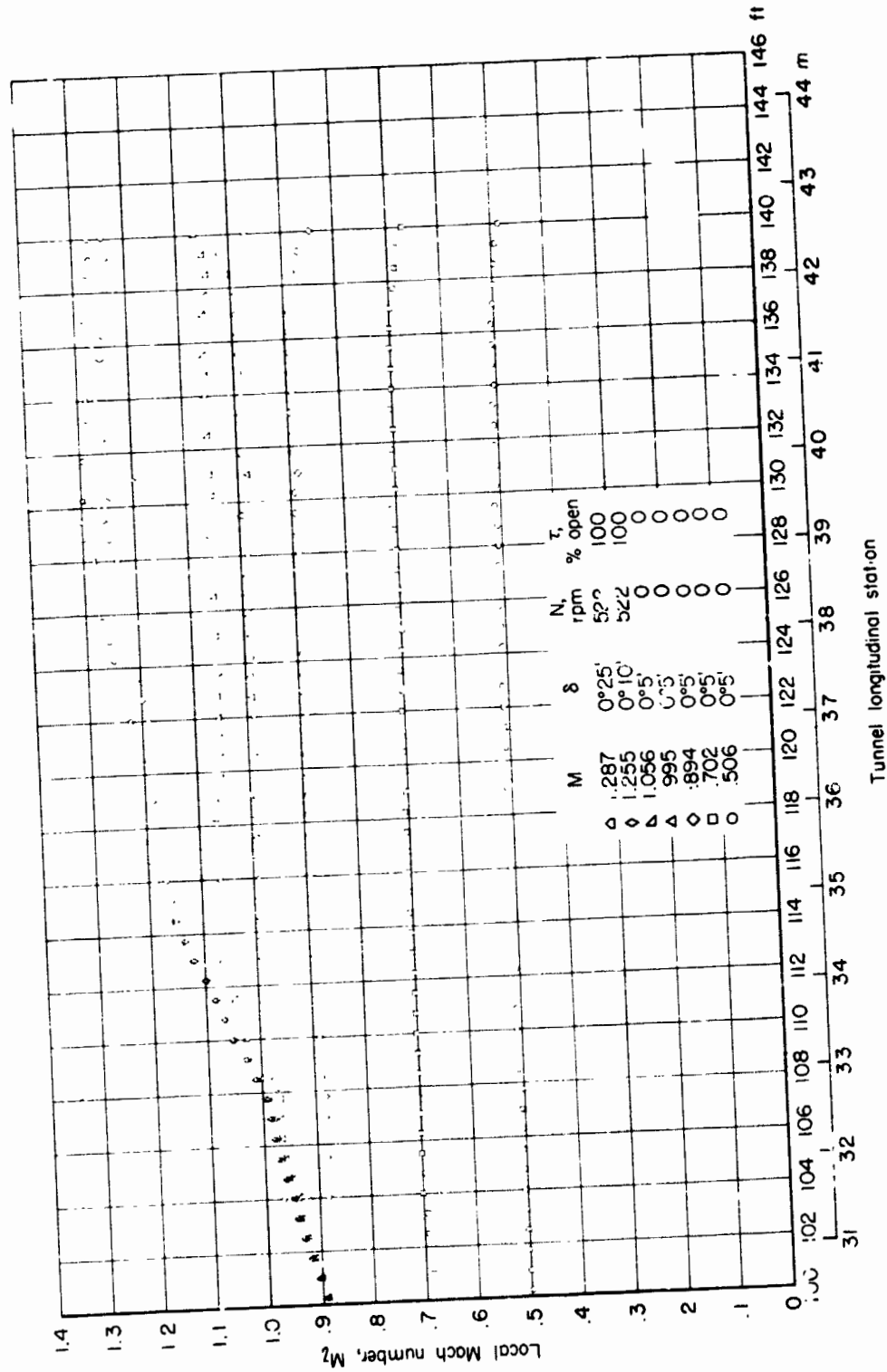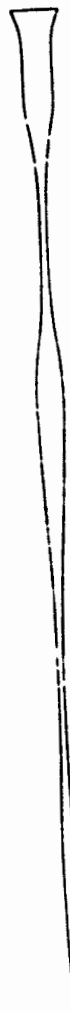
Figure 24. - Longitudinal Mach number distribution along center line of test section for slot shape 20.

83
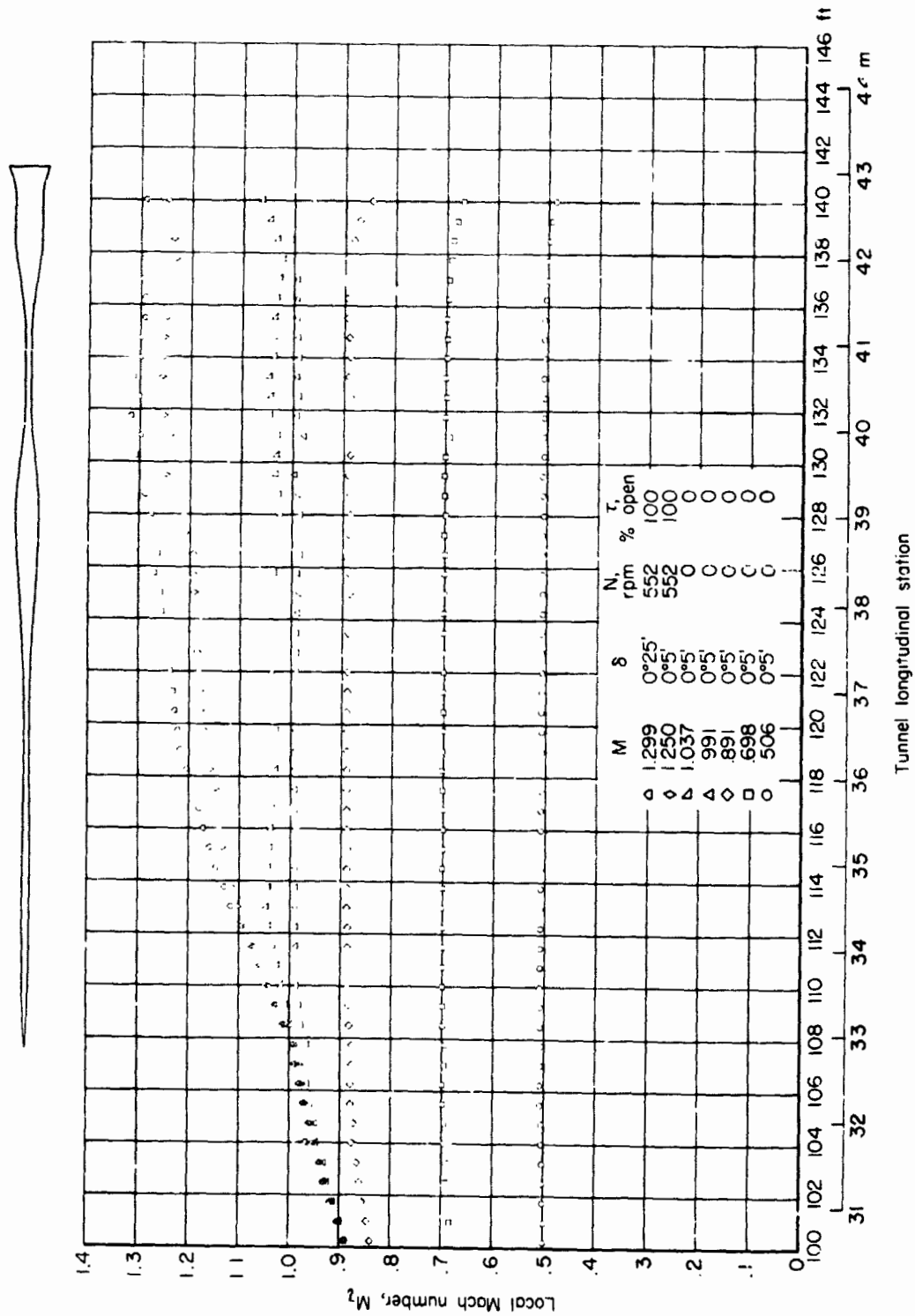
Figure 25.- Longitudinal Mach number distribution along center line of test section for slot shape 21.

84
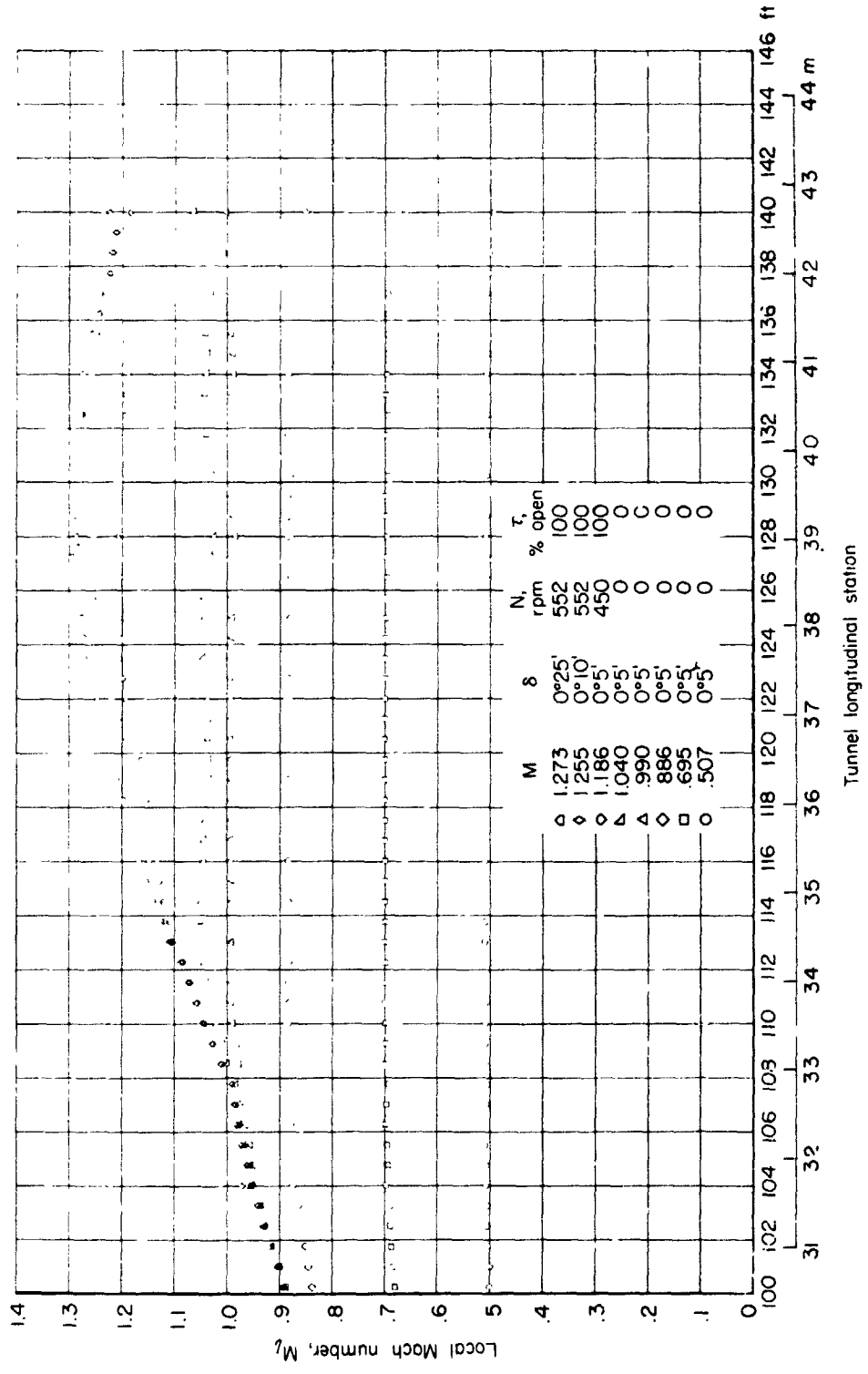
Figure 26.- Longitudinal Mach number distribution along center line of test section for slot shape 22.

Legend:

	M	δ	N, rpm	T, % open
◁	1.276	0°25'	552	100
◇	1.247	0°10'	552	100
◊	1.200	0°5'	552	60
◁	1.155	0°5'	552	40
△	1.050	0°5'	0	0
◁	.989	0°5'	0	0
◇	.898	0°5'	0	0
□	.695	0°5'	0	0
○	.503	0°5'	0	0

Local Mach number, M_z

Tunnel longitudinal station
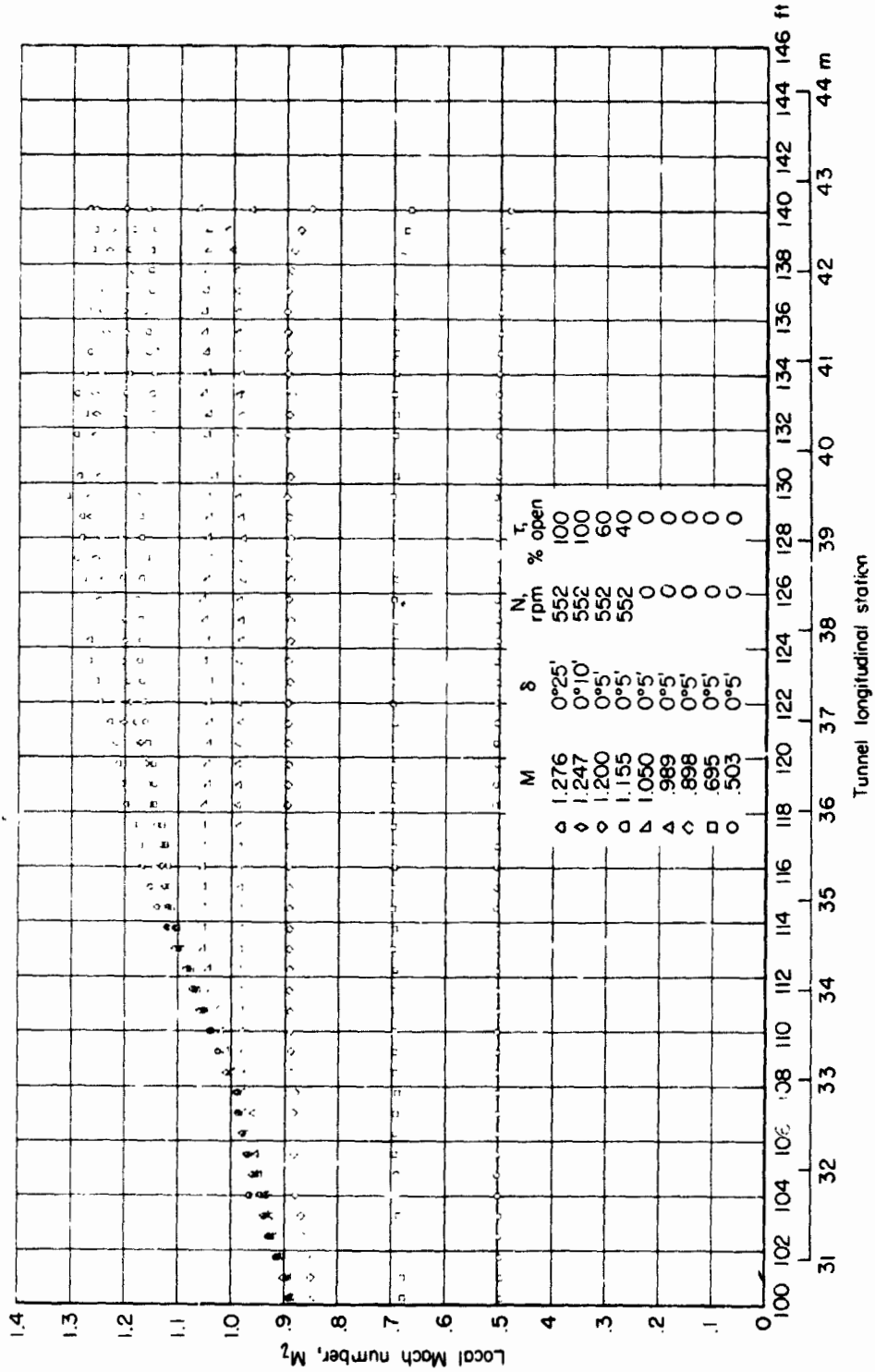
Figure 27.- Longitudinal Mach number distribution along center line of test section for slot shape 23.

86
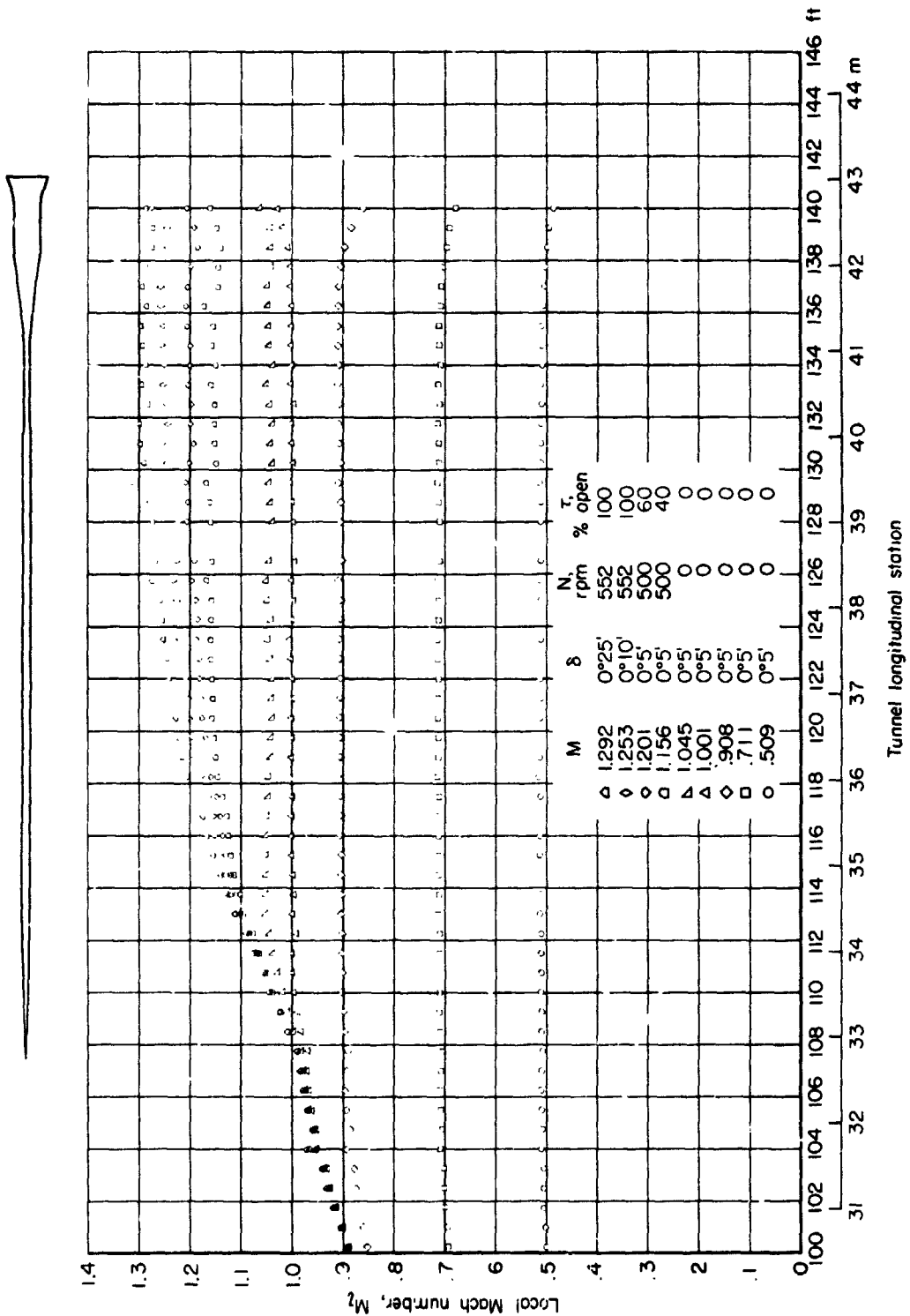
Figure 28. – Longitudinal Mach number distribution along center line of test section for slot shape 24.
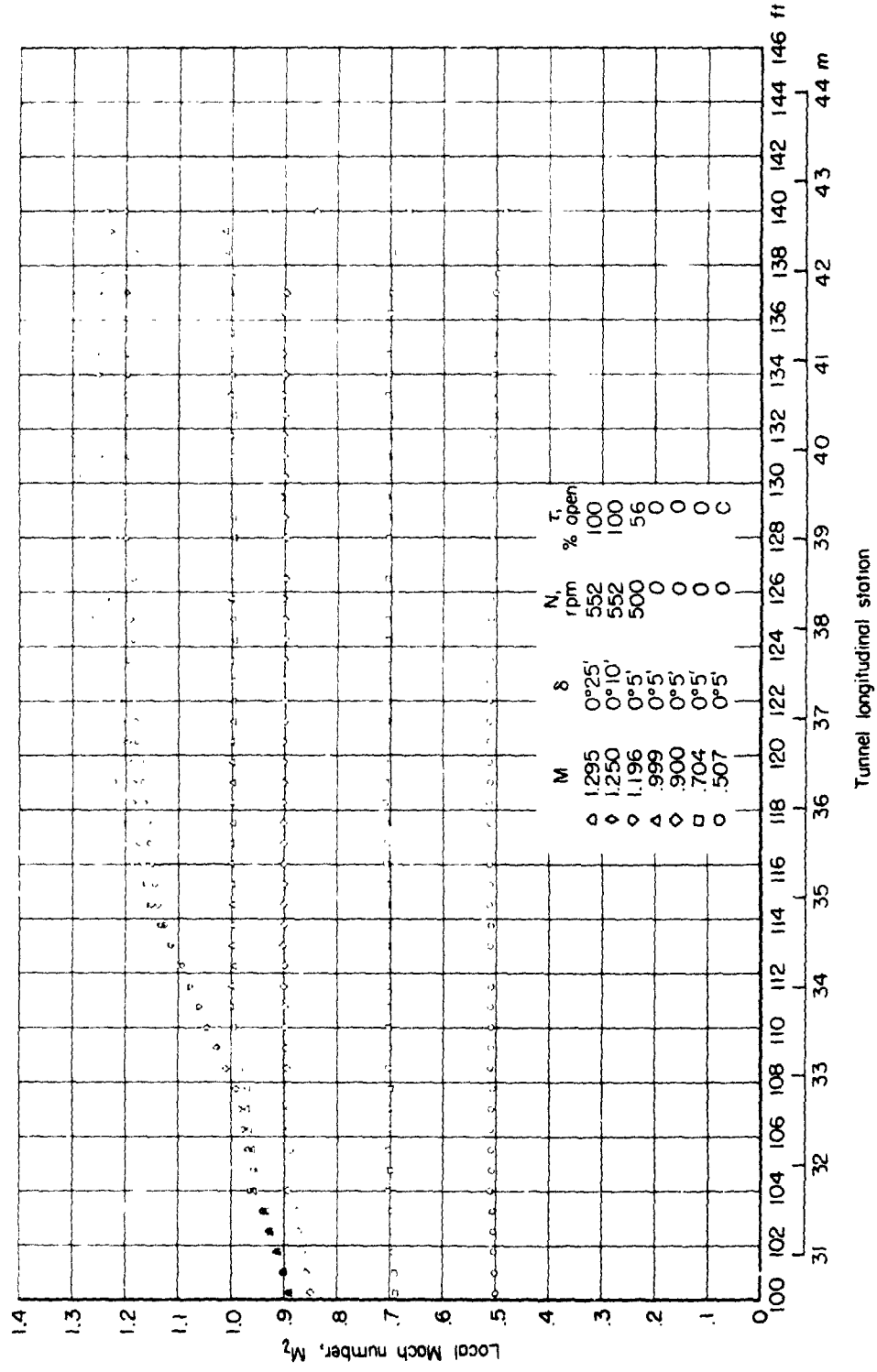
Figure 29.– Longitudinal Mach number distribution along center line of test section for slot shape 25.

88
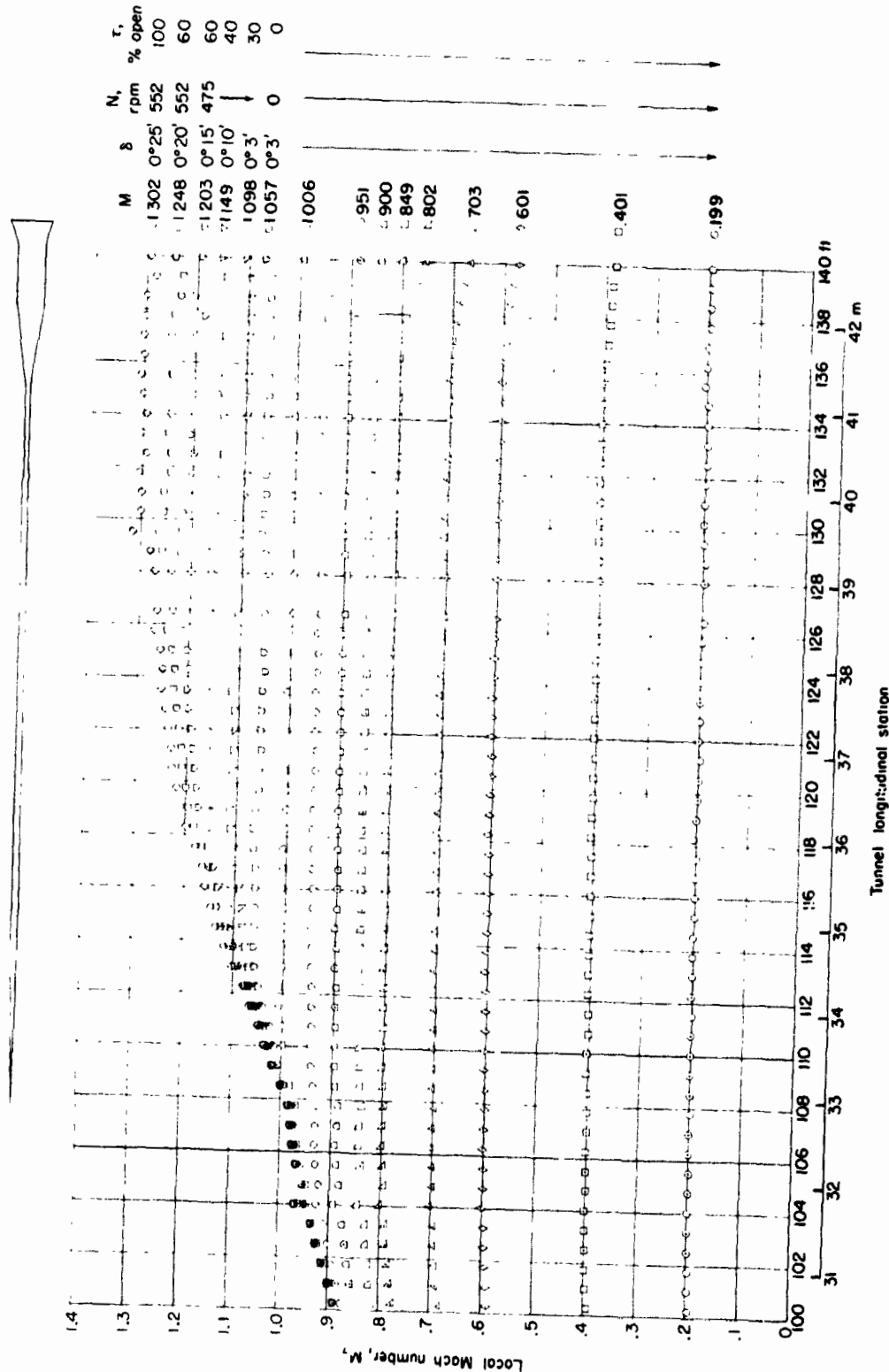
Figure 30.- Longitudinal Mach number distribution along center line of test section for slot shape 26.
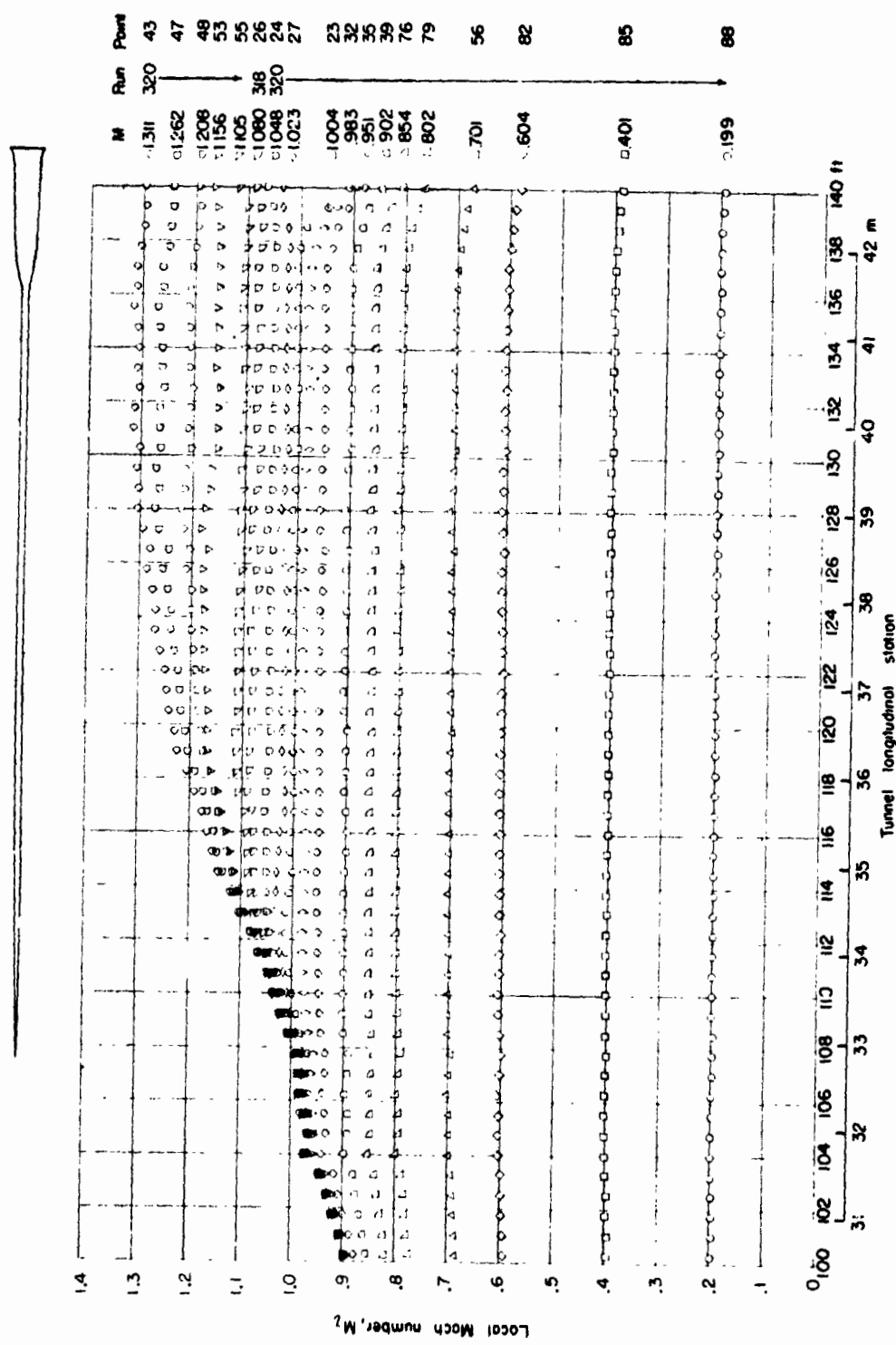
(a) Low dewpoint (2° to 4° C; 35° to 39° F).

Figure 31.- Longitudinal Mach number distribution along center line of test section for slot shape 29.
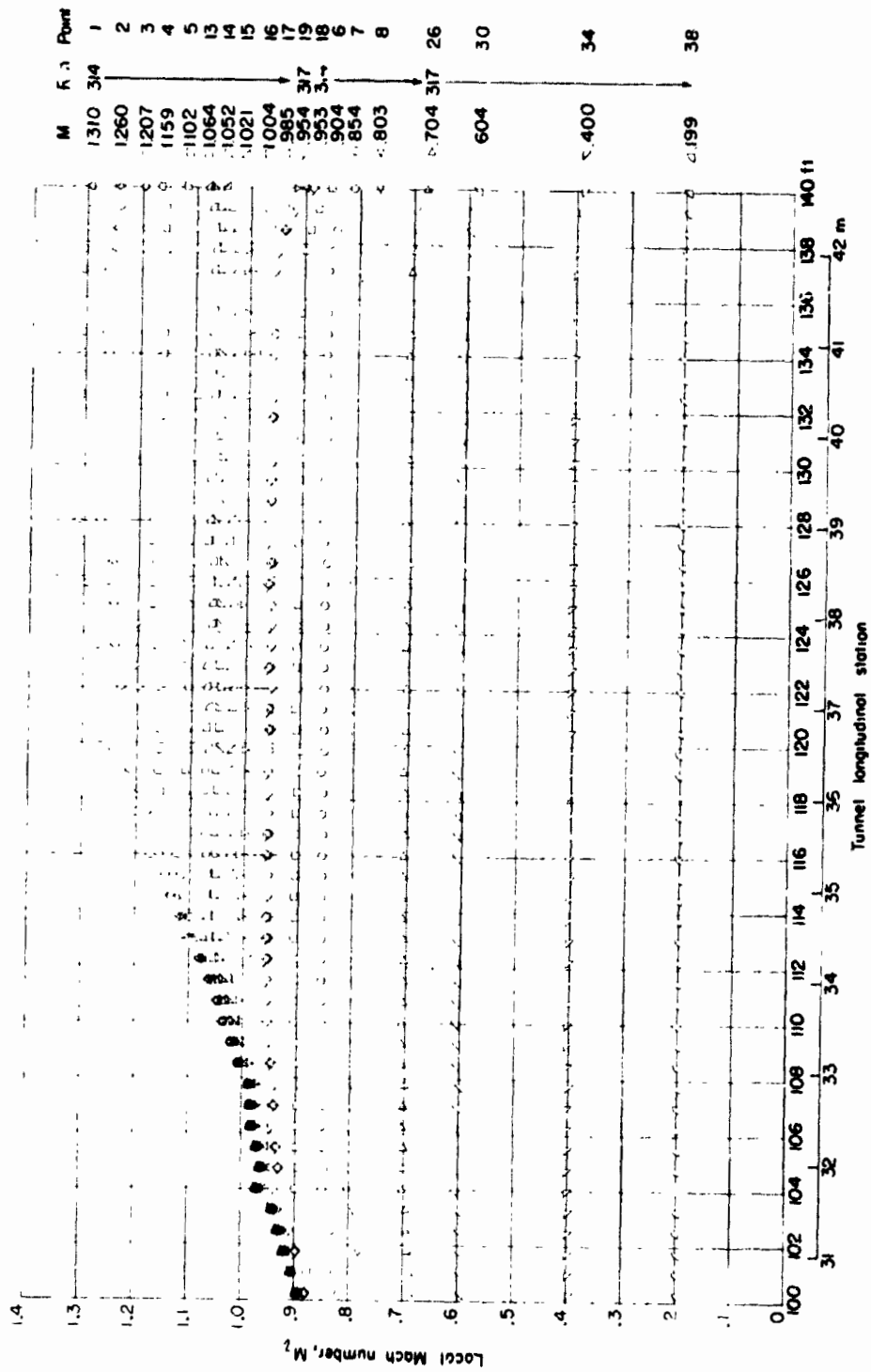
(b) High dewpoint (18° to 19° C; 64° to 66° F).

Figure 31.- Concluded.
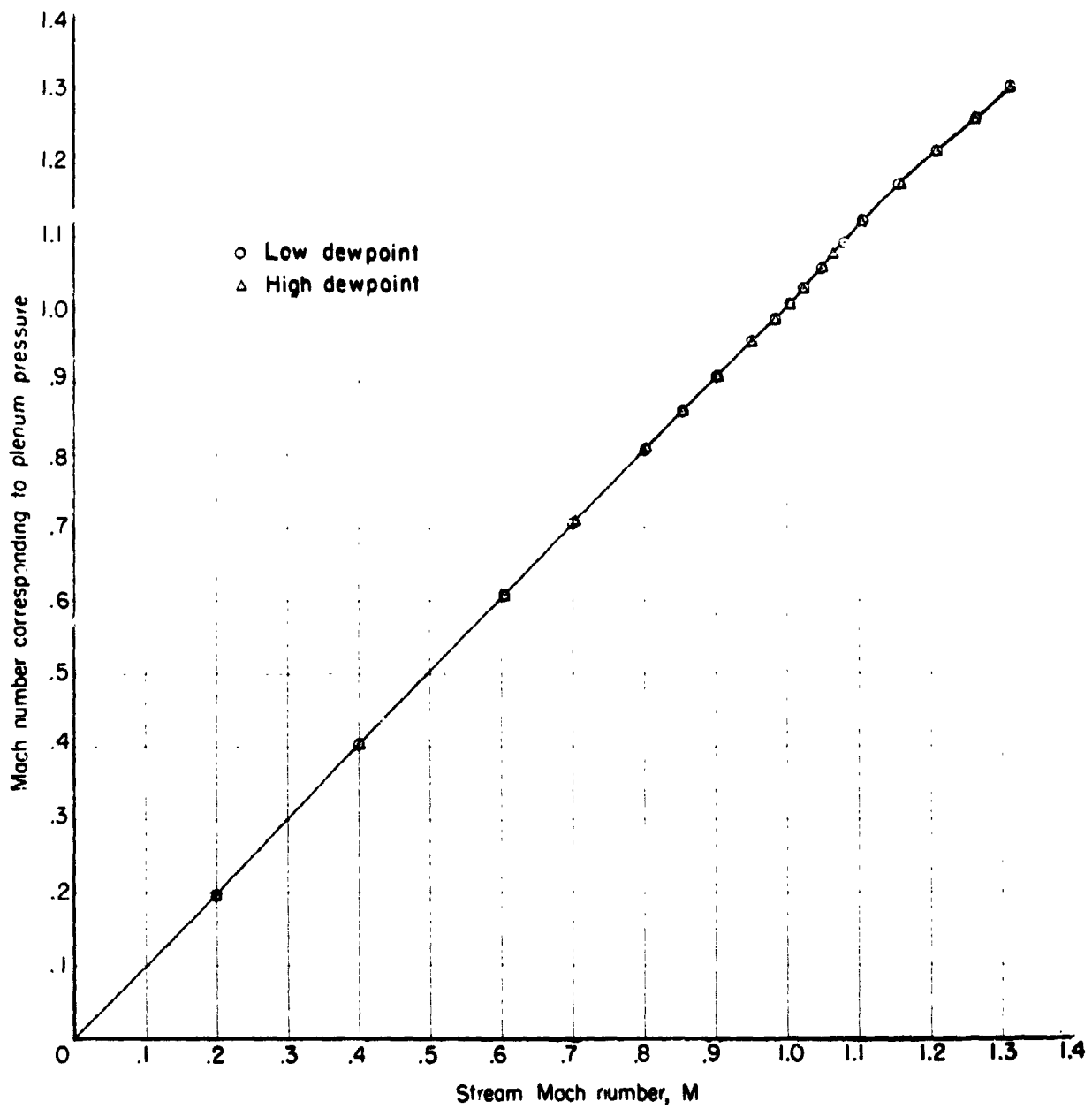
Figure 32.- Langley 16-foot transonic tunnel calibration with slot shape 29.
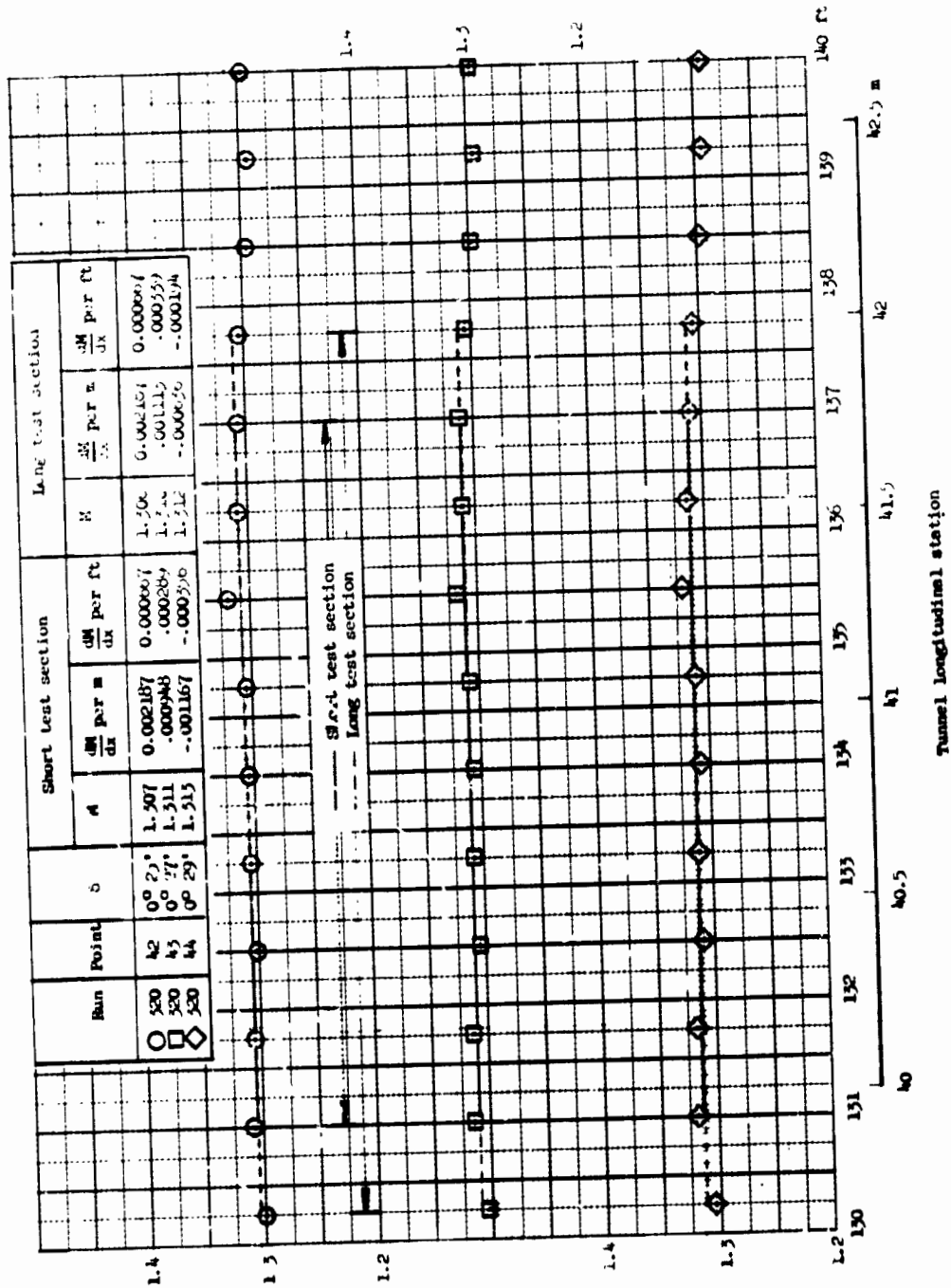
Figure 33.- Test section flow characteristics at $M \approx 1.3$. Low dewpoint.

93
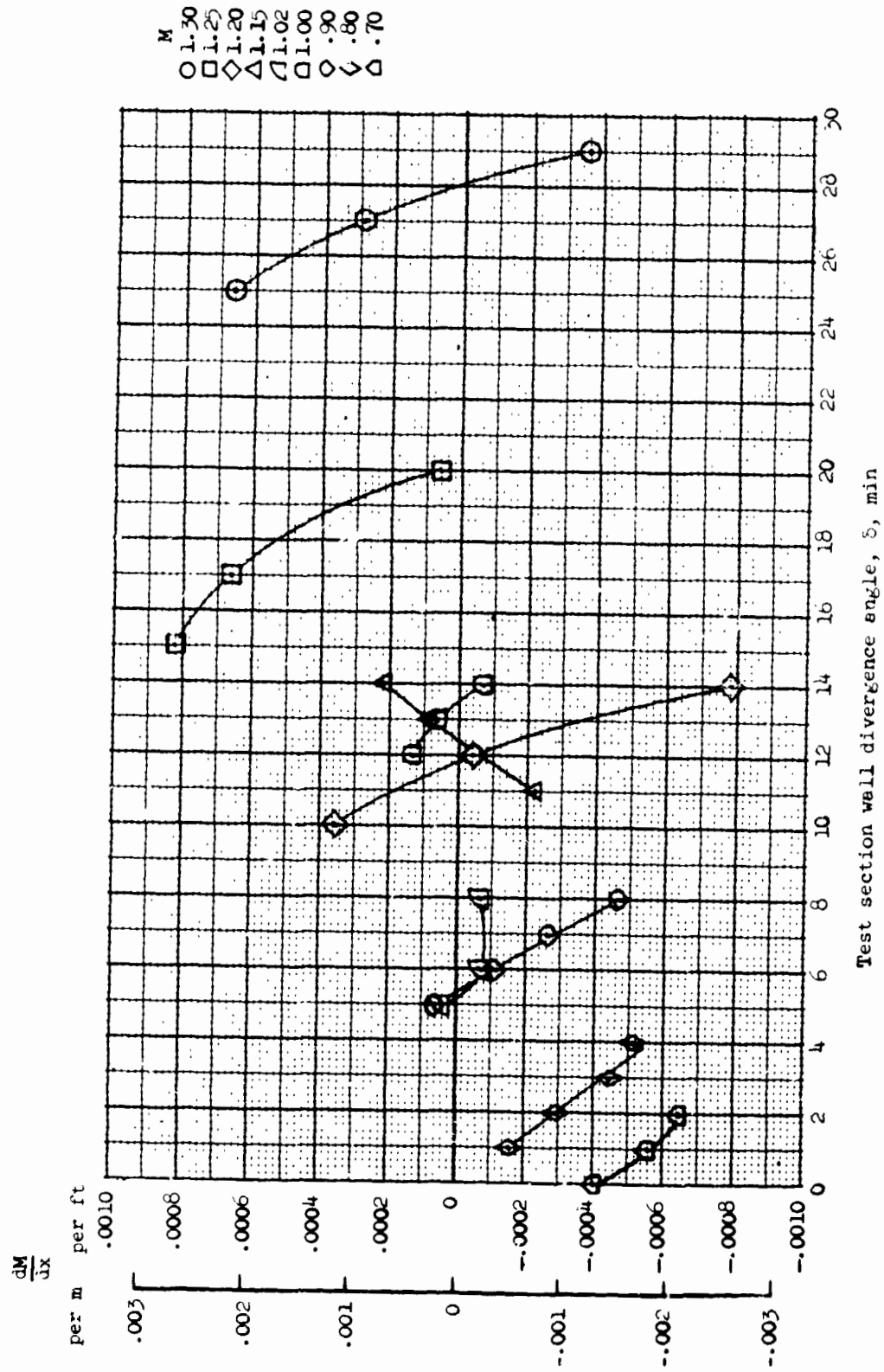
(a) Short test section.

Figure 34.- Variation of Mach number gradient with test section wall divergence angle. Low dewpoint.

94
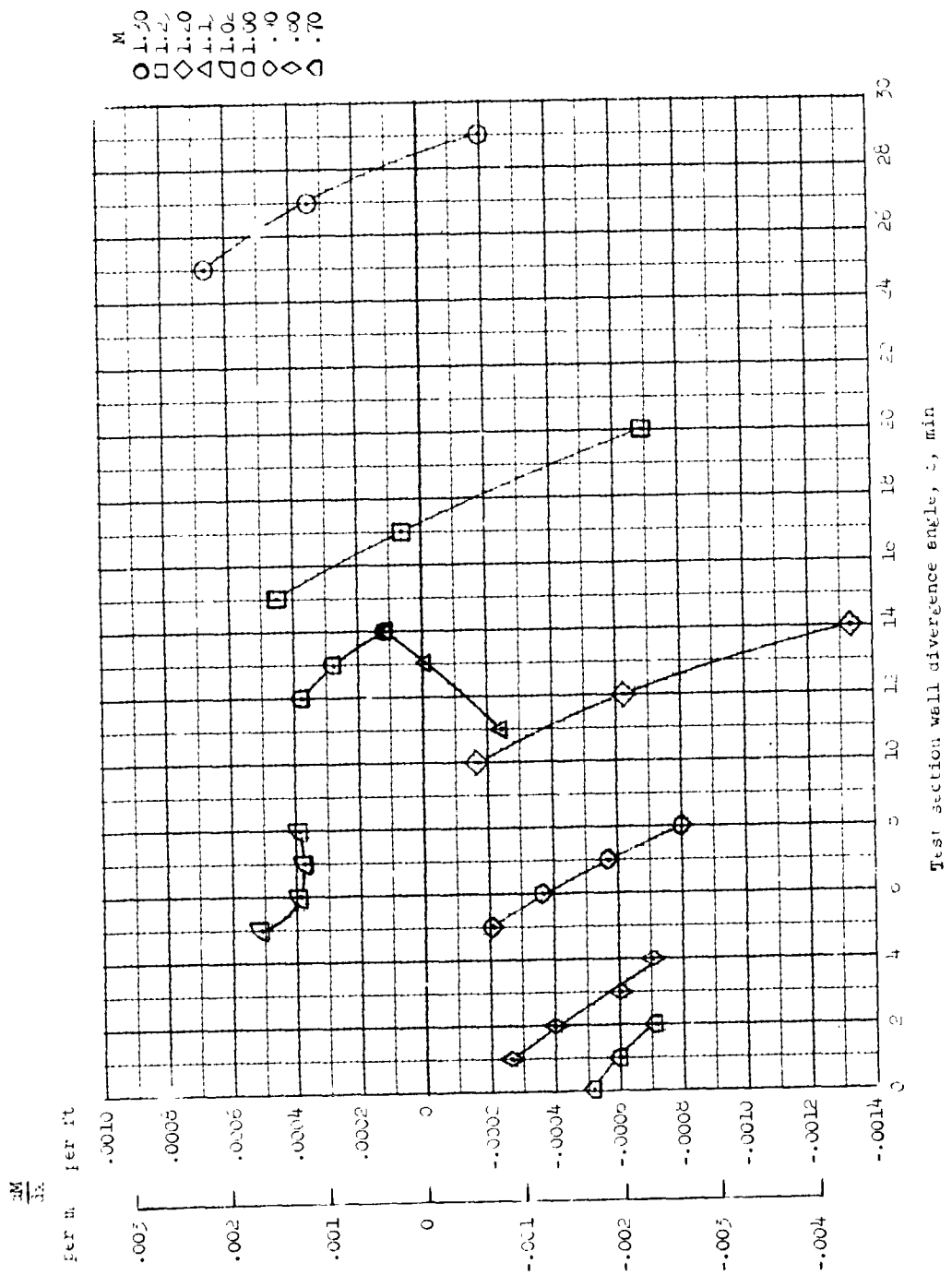
(b) Long test section.

Figure 34.- Concluded.

95
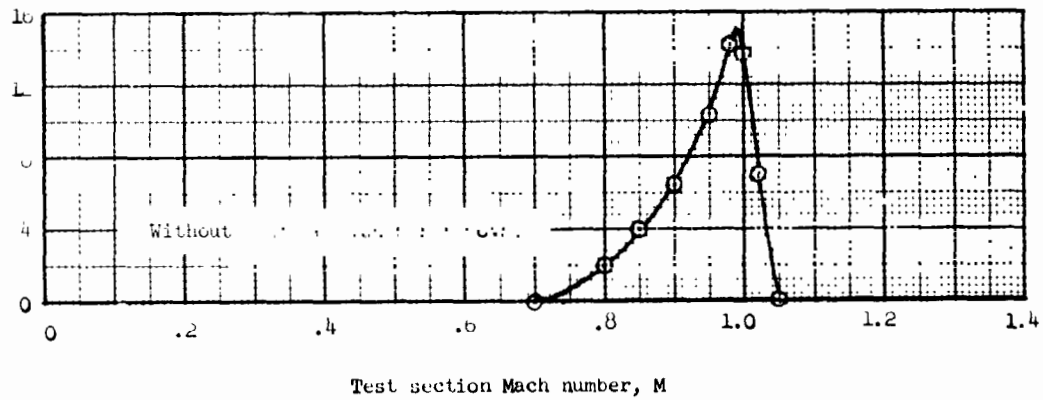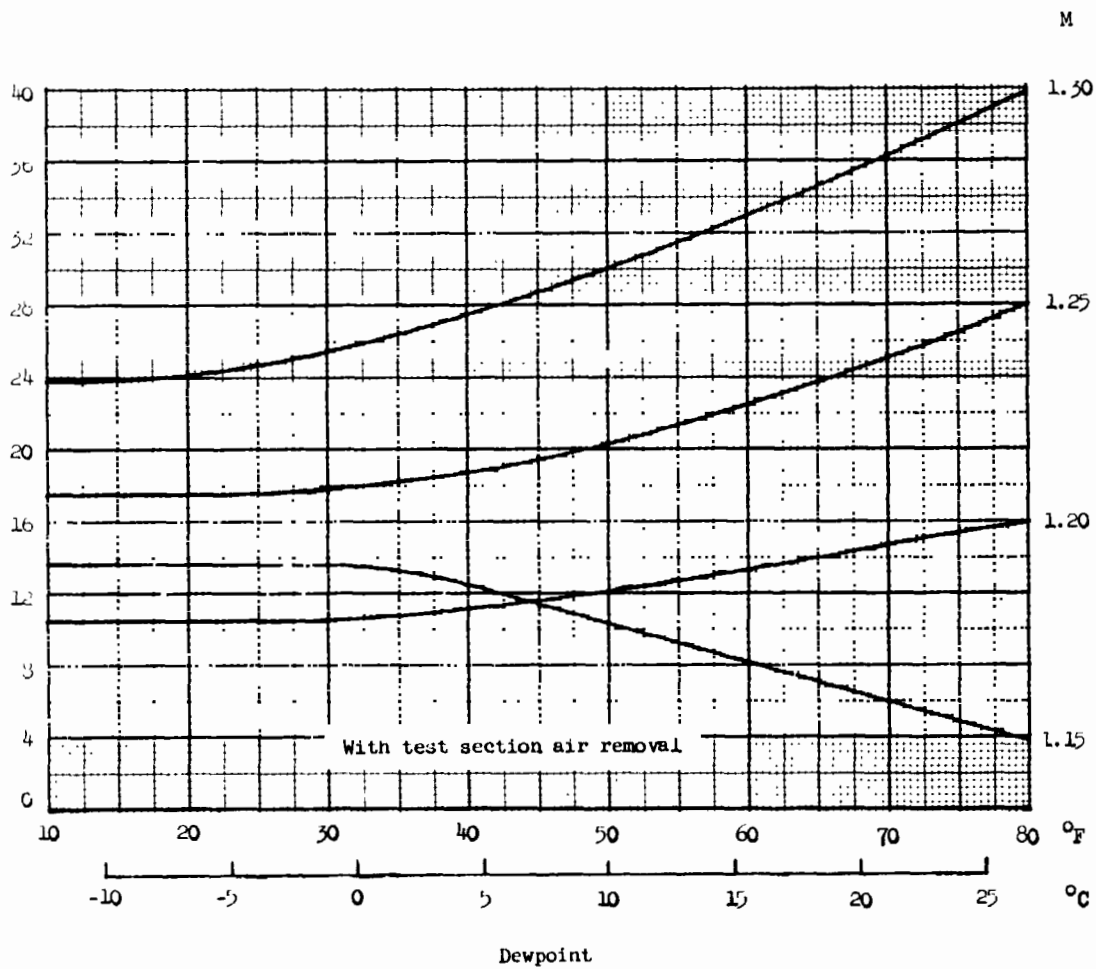
Figure 35.- Test section wall divergence angles for zero axial gradient of static pressure in the test section. (Calibration of October 1965.)
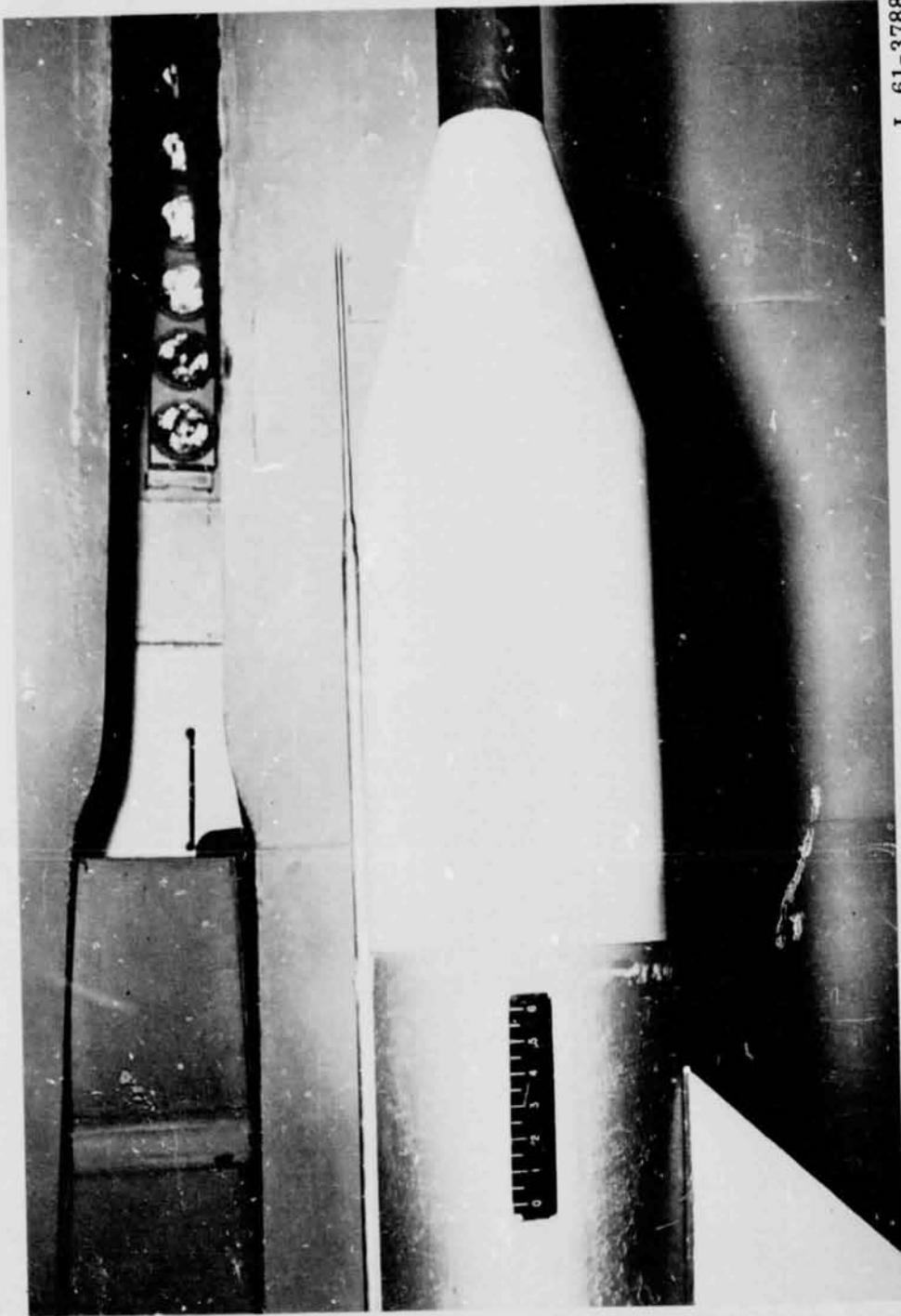
L-61-3788

Figure 36.- Strut head for center-line survey tube with dummy extension upstream.
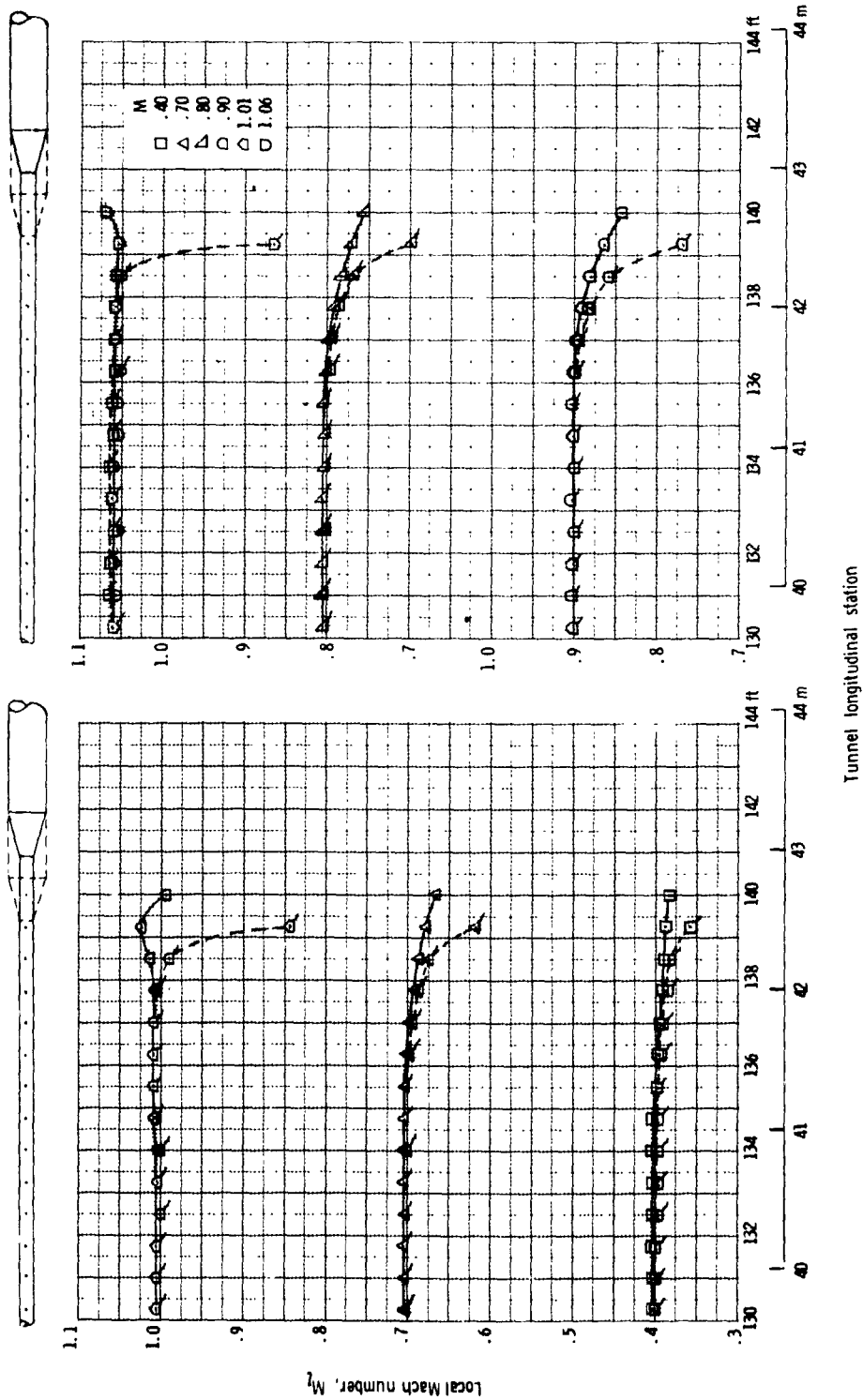
Figure 37.– Mach number distributions with and without strut-head dummy extension. Ticked symbols and dashed lines indicate data with strut-head extension.
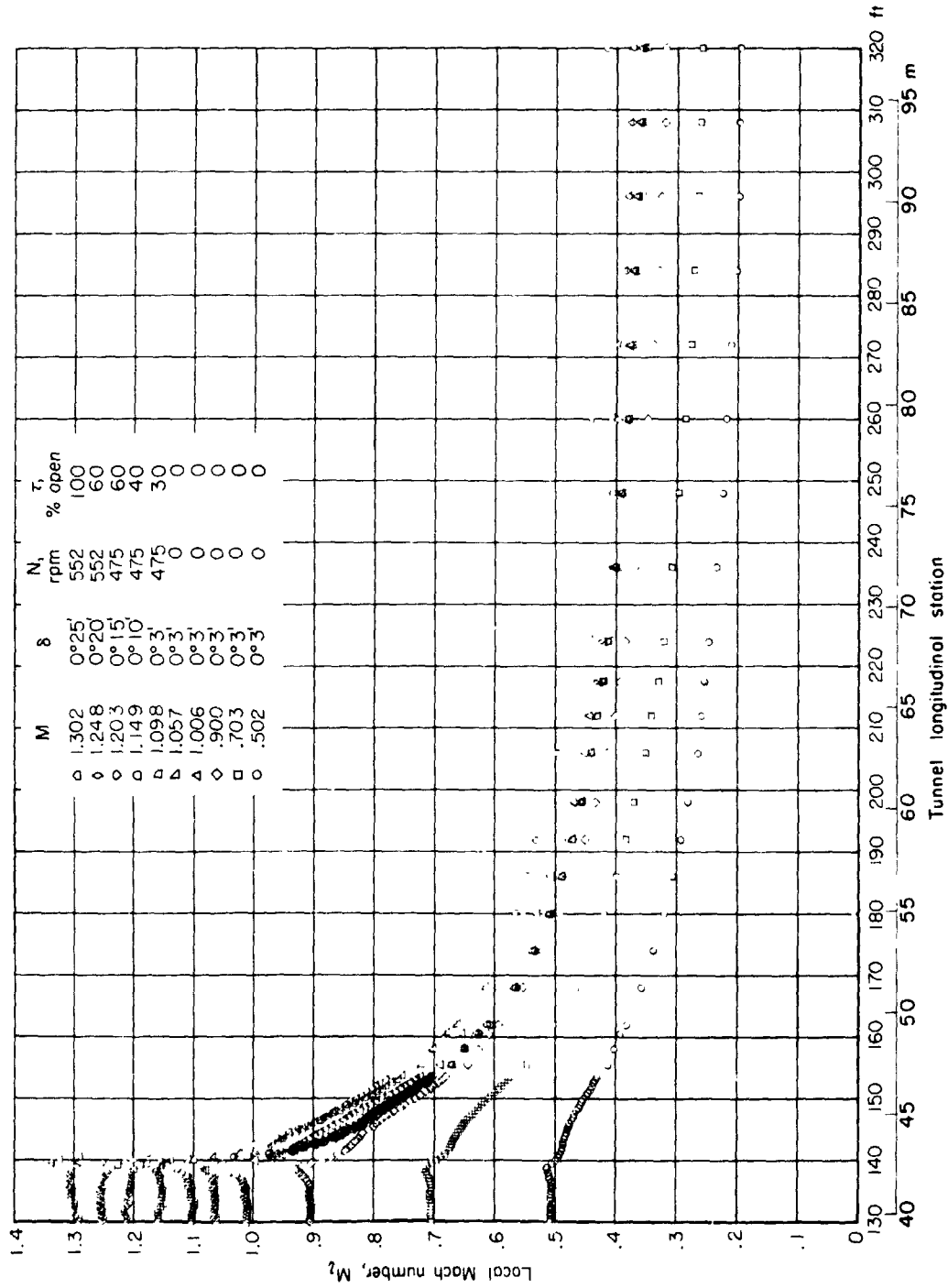
Figure 38.- Longitudinal distribution of Mach number in the diffuser of the Langley 16-foot transonic tunnel with slot shape 26.
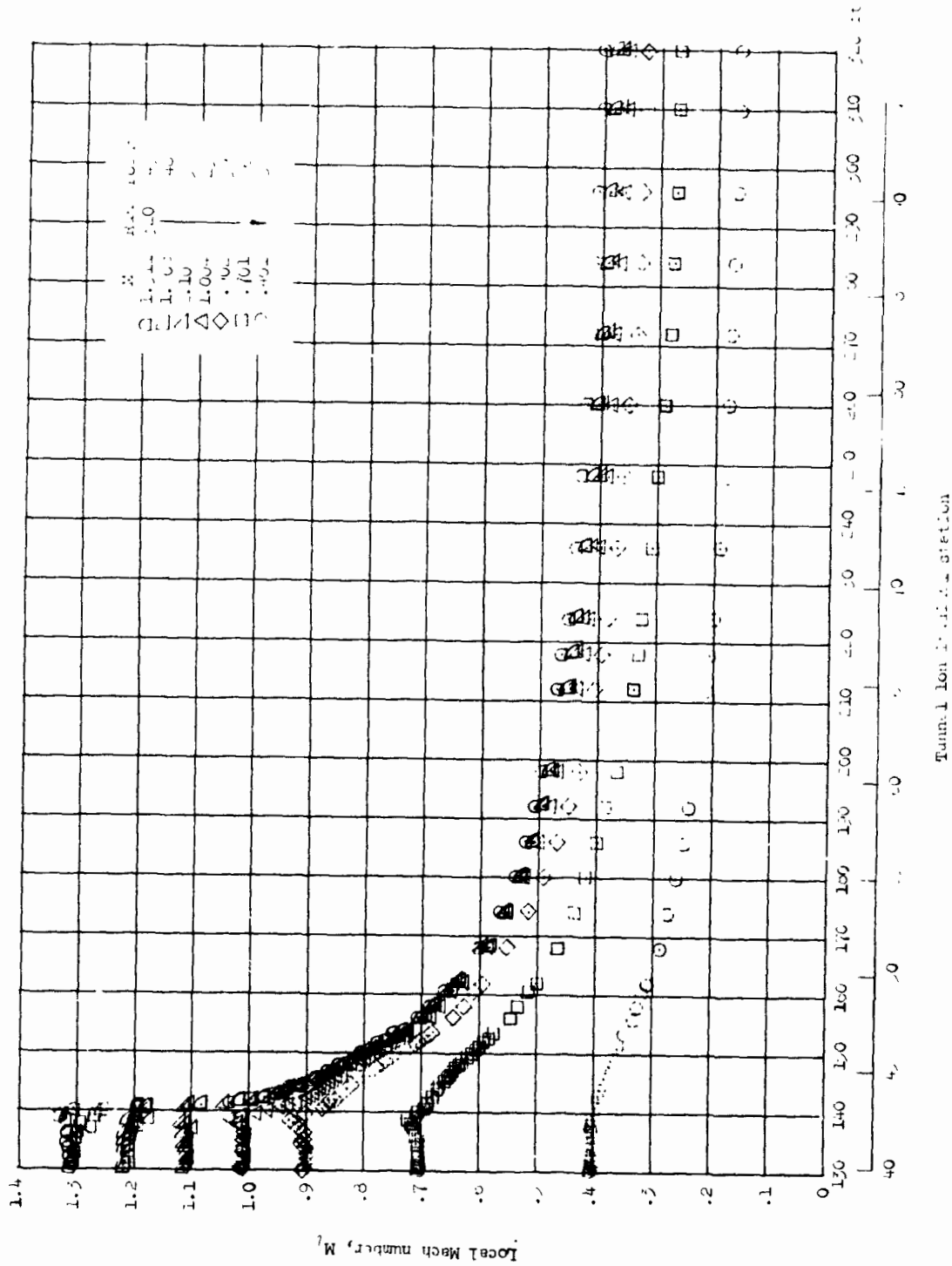
(a) Low dewpoint.

Figure 39.– Longitudinal distribution of Mach number in the diffuser of the Langley 16-foot transonic tunnel with slot shape 29.
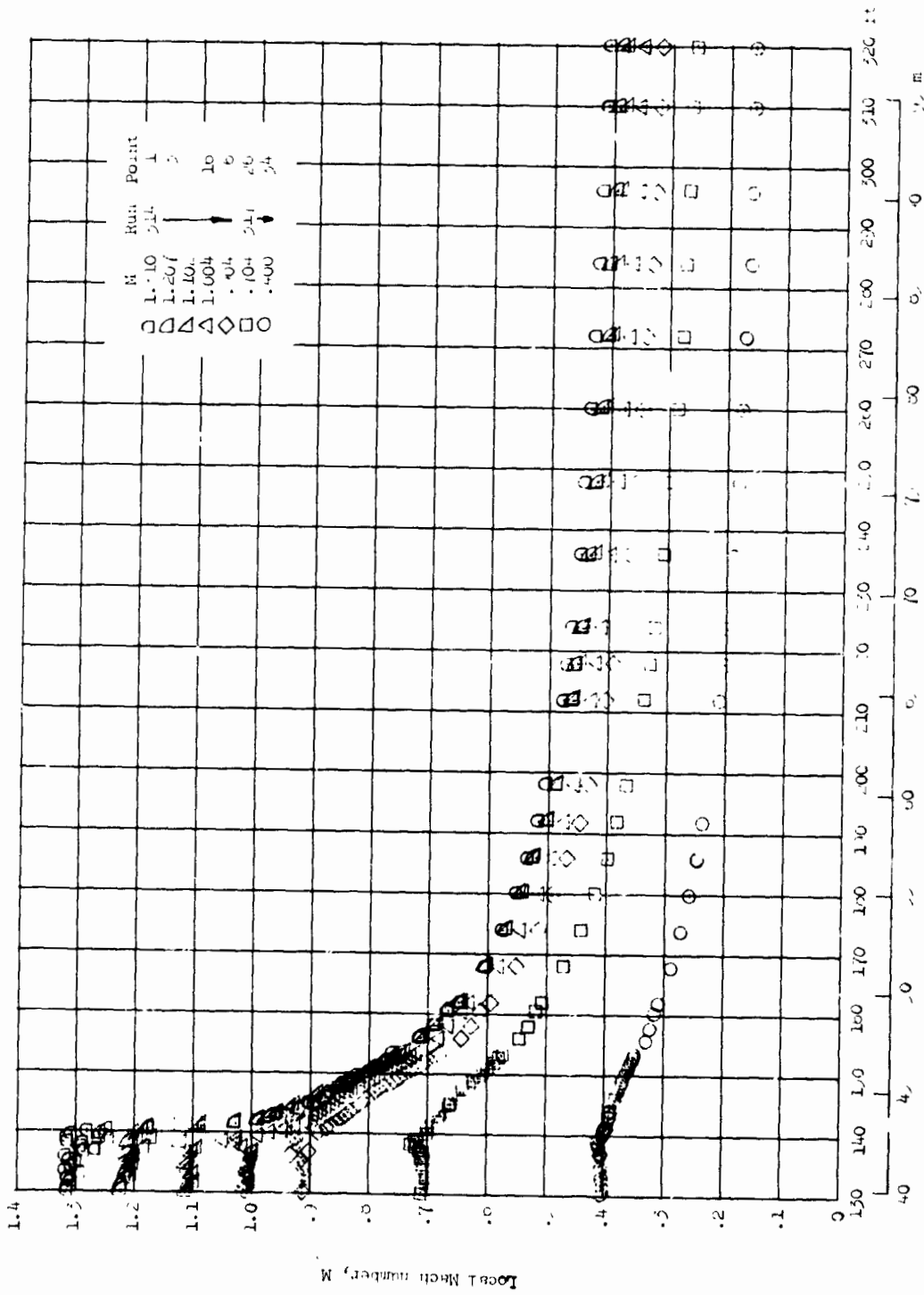
(b) High dewpoint.

Figure 39.- Concluded.
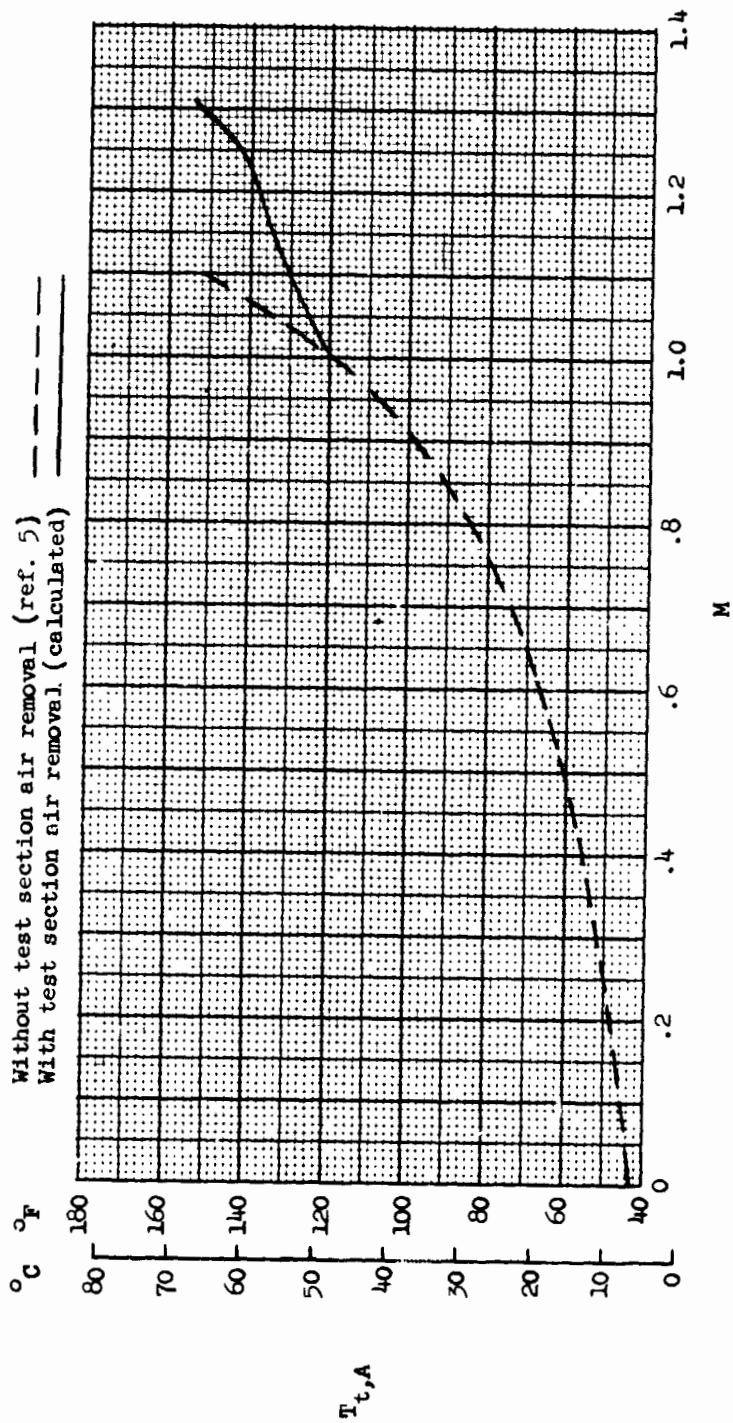
Figure 40.- Variation with Mach number of average stagnation temperature at station 0.
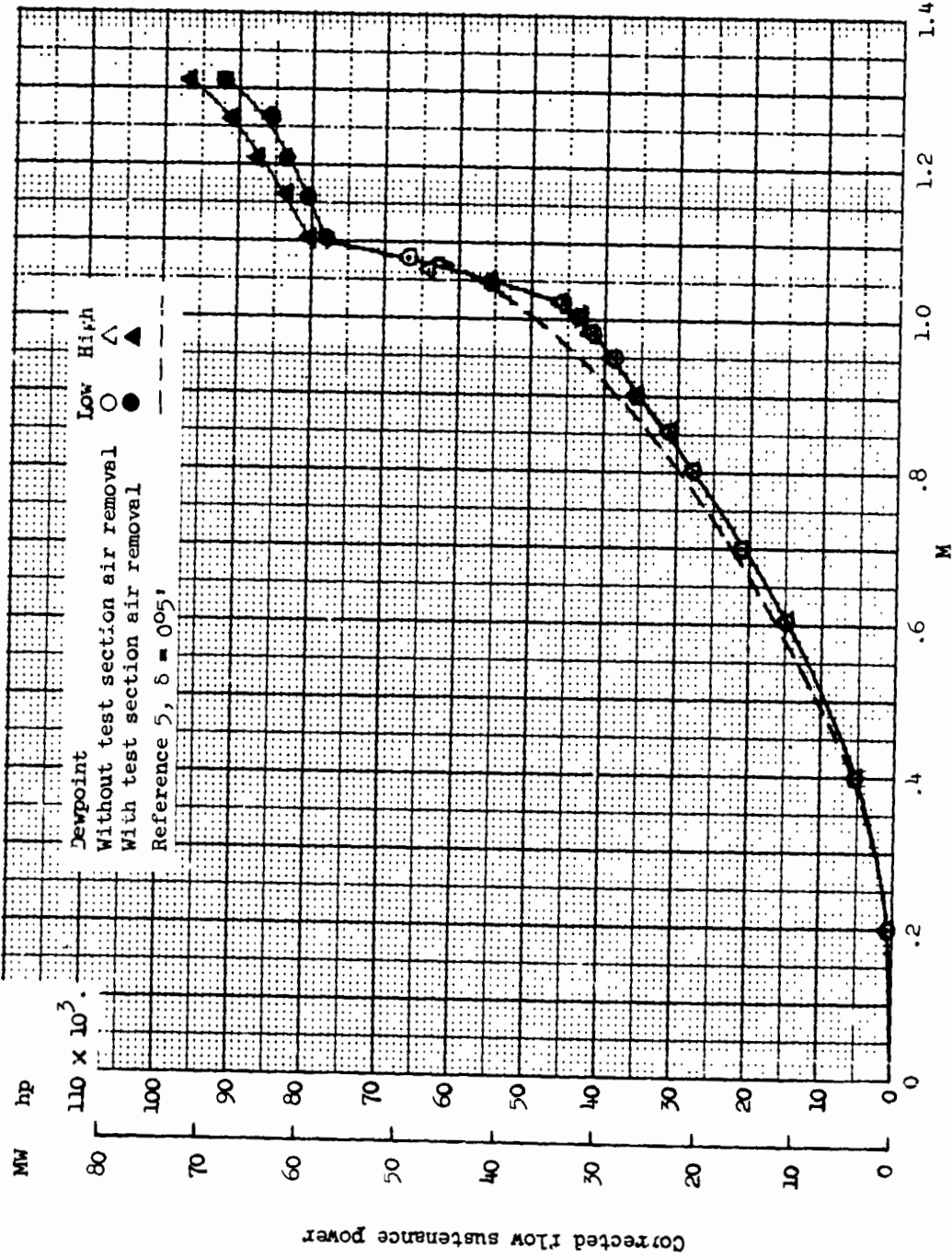
(a) Including power required to pump bypass air.

Figure 41.- Power required for flow sustenance, corrected to standard pressure and average stagnation temperature.
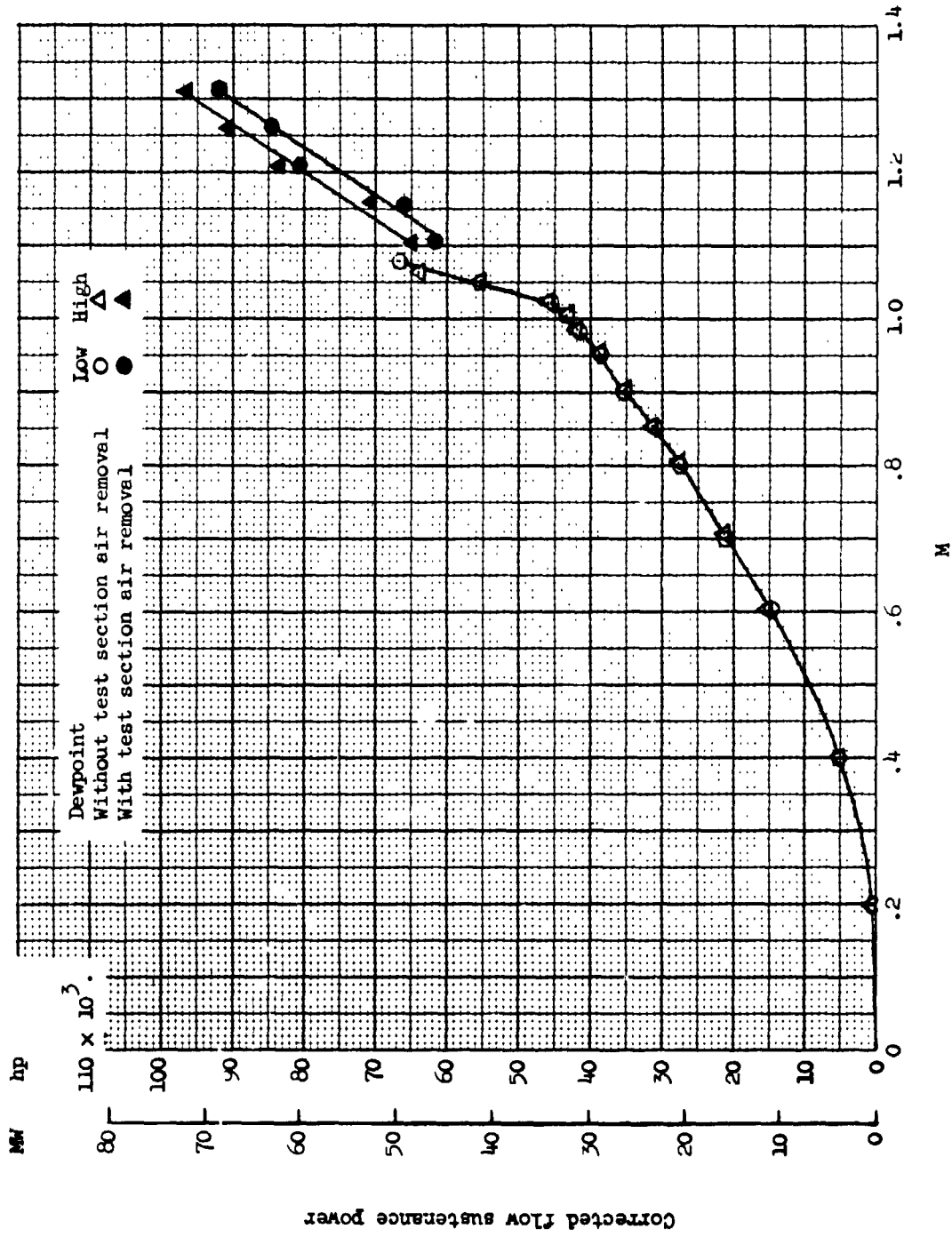
(b) Excluding power required to pump bypass air.

Figure 41.- Concluded.
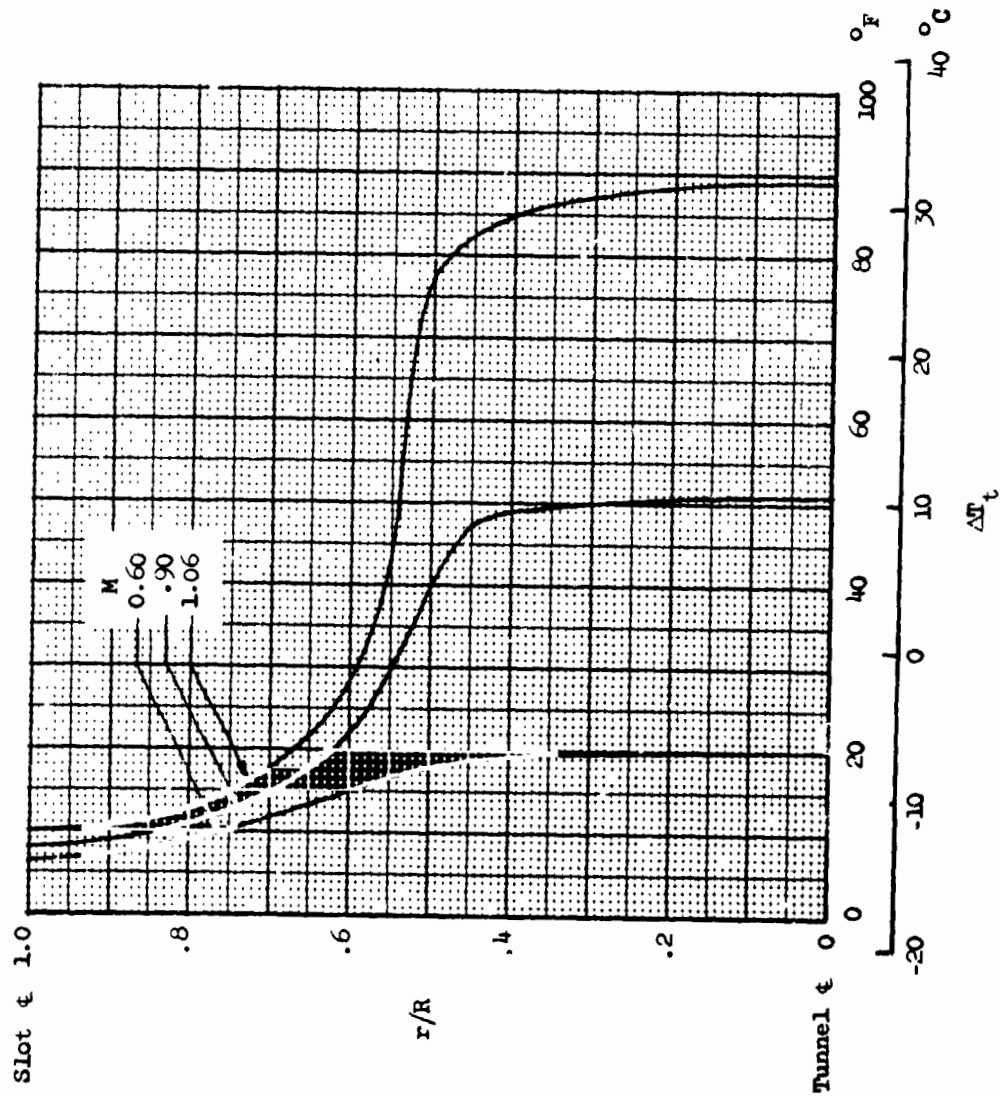
Figure 42.- Stagnation temperature rise above outside air temperature at station 38.71 m (127 ft) for slot shape 18. Air exchange full open.
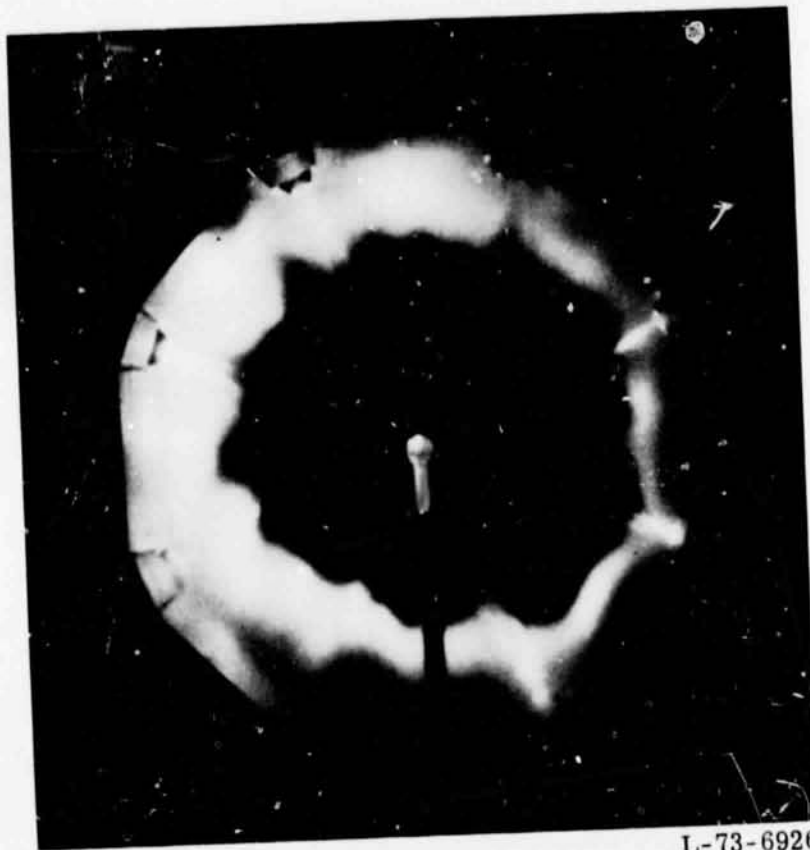
L-73-6926

(a) Condensation near wall; clear in central core.

Figure 43.- Air moisture condensation in the test section. (View looking upstream)

L-73-6925

(b) Condensation with extremely humid airstream.

Figure 43.- Concluded.
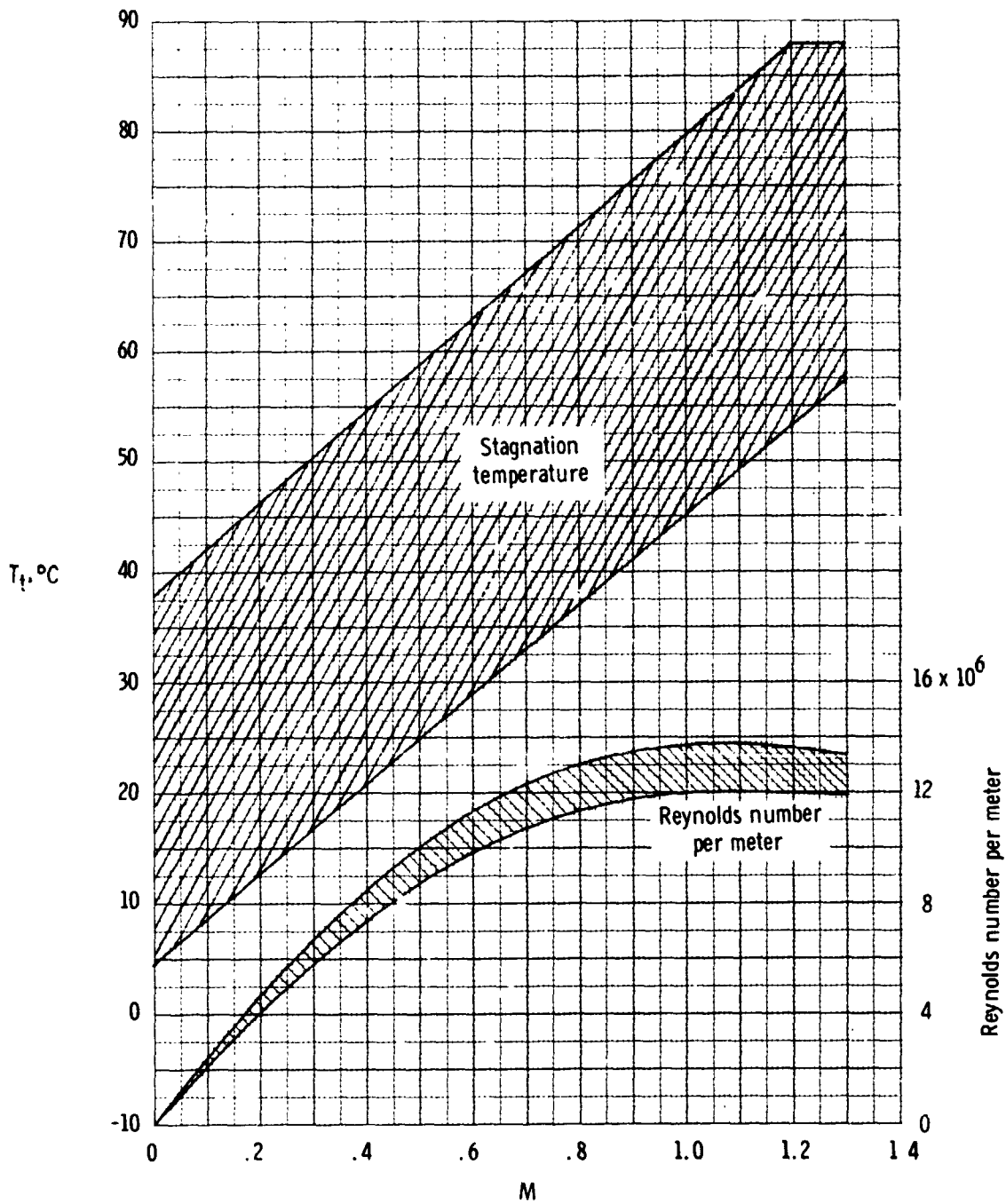
(a) $p_t = 101.32$ kN/m^2.

Figure 44.- Variation with Mach number of stagnation temperature
and Reynolds number per unit length.

108
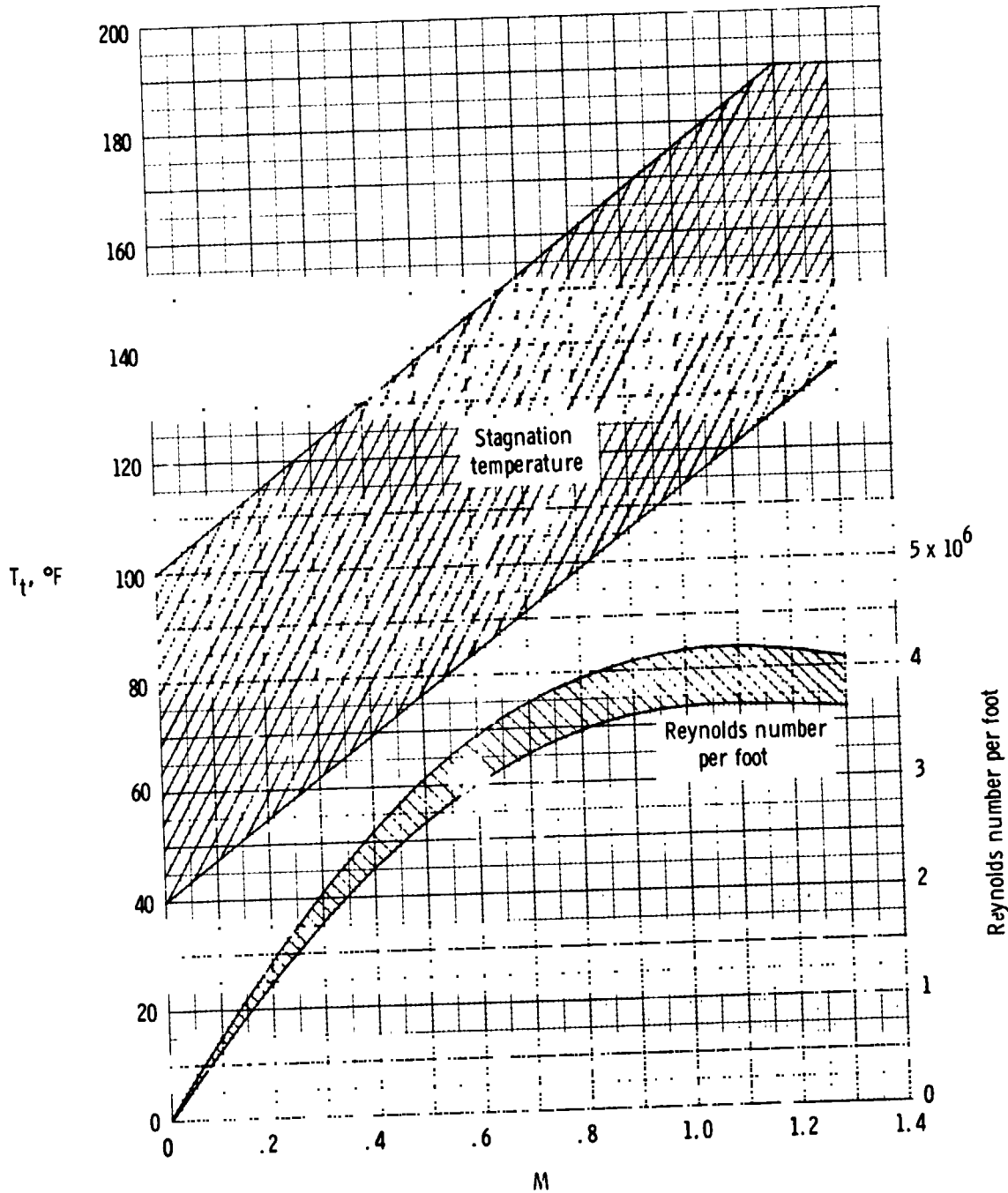
(b) $p_t = 2116 \text{ lb/ft}^2$.

Figure 44.- Concluded.
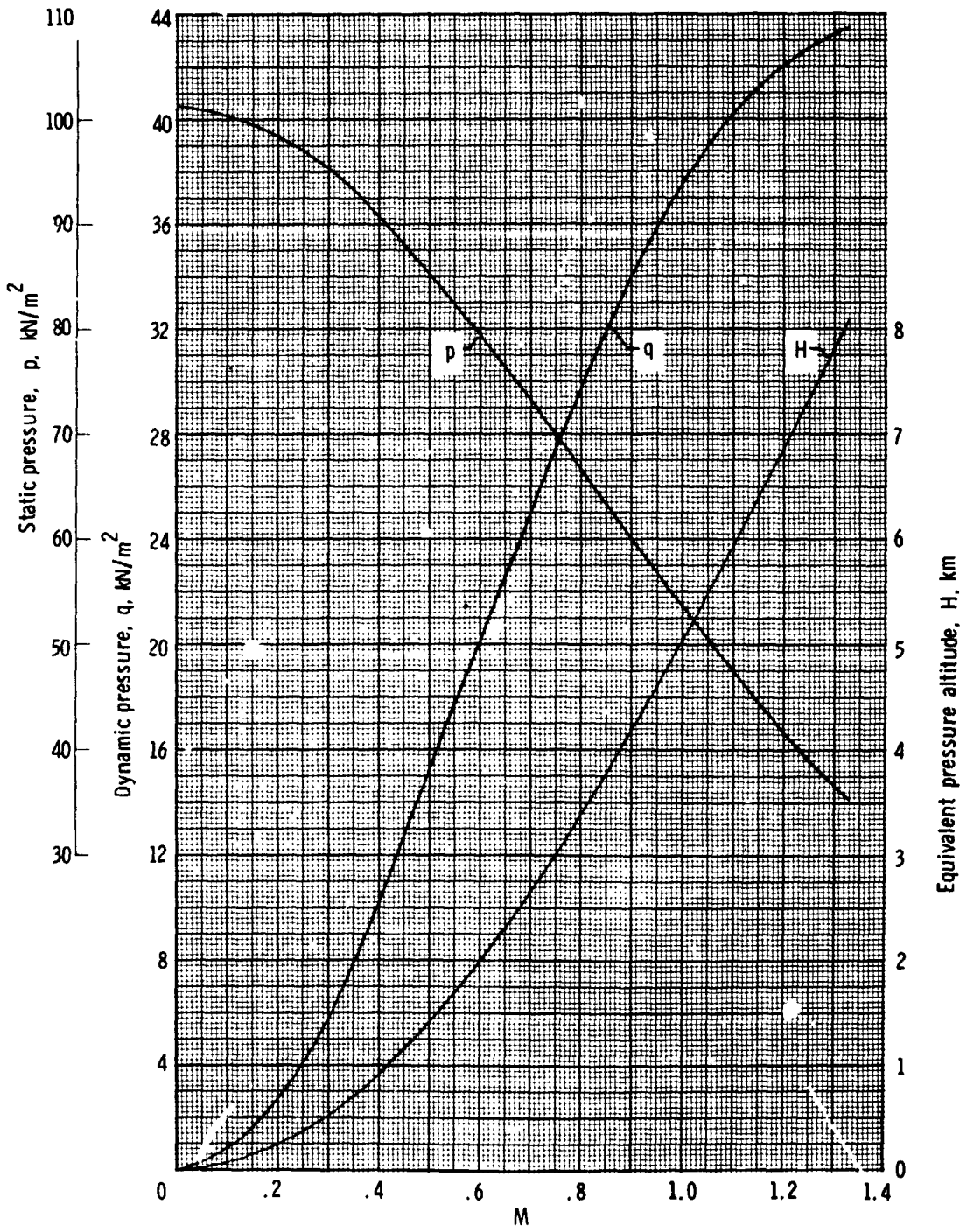
(a) $p_t = 101.32$ kN/m^2.

Figure 45.- Variation of static pressure, dynamic pressure, and equivalent pressure altitude with Mach number.
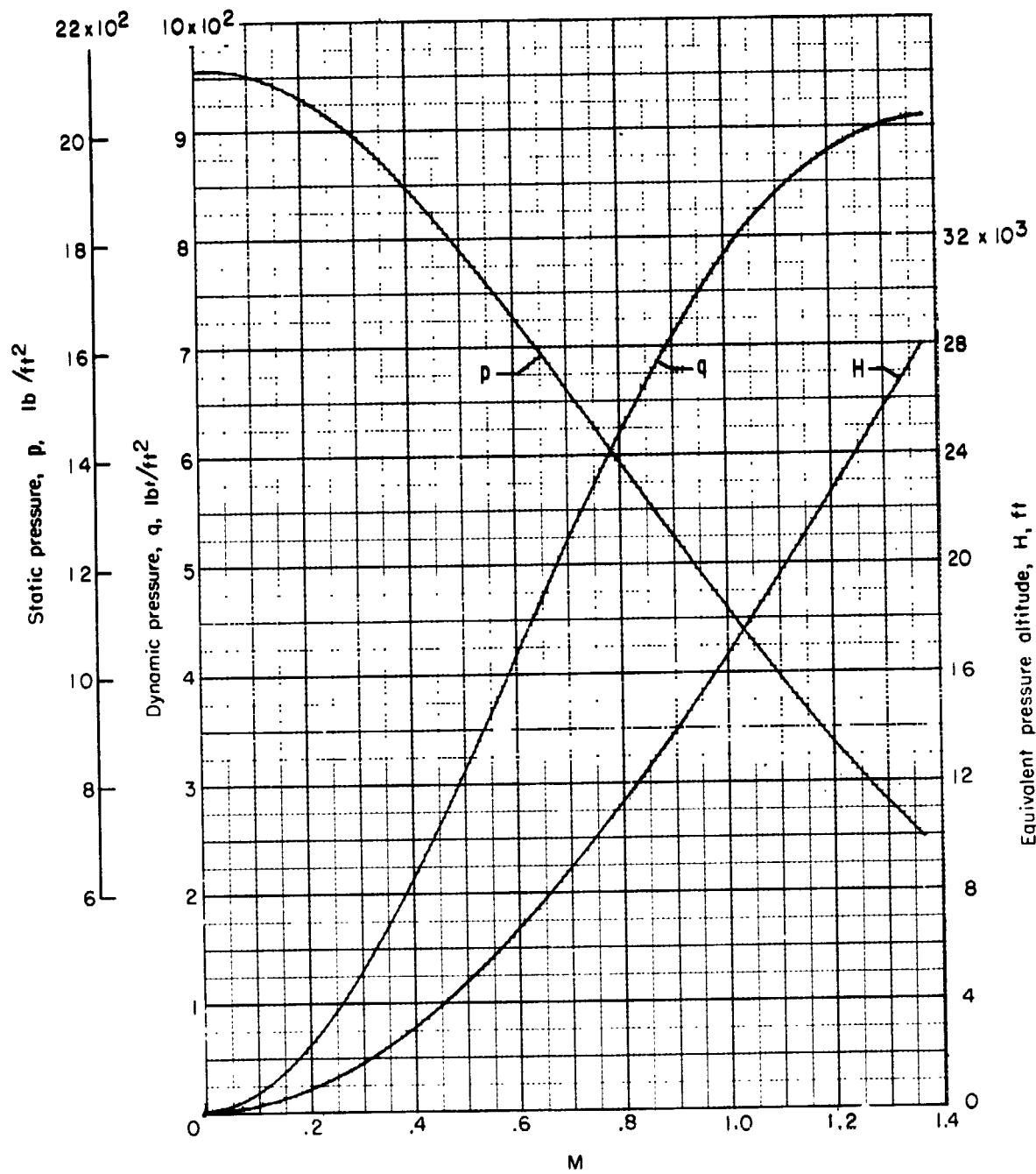
(b) $p_t = 2116$ lb/ft^2.

Figure 45.- Concluded.
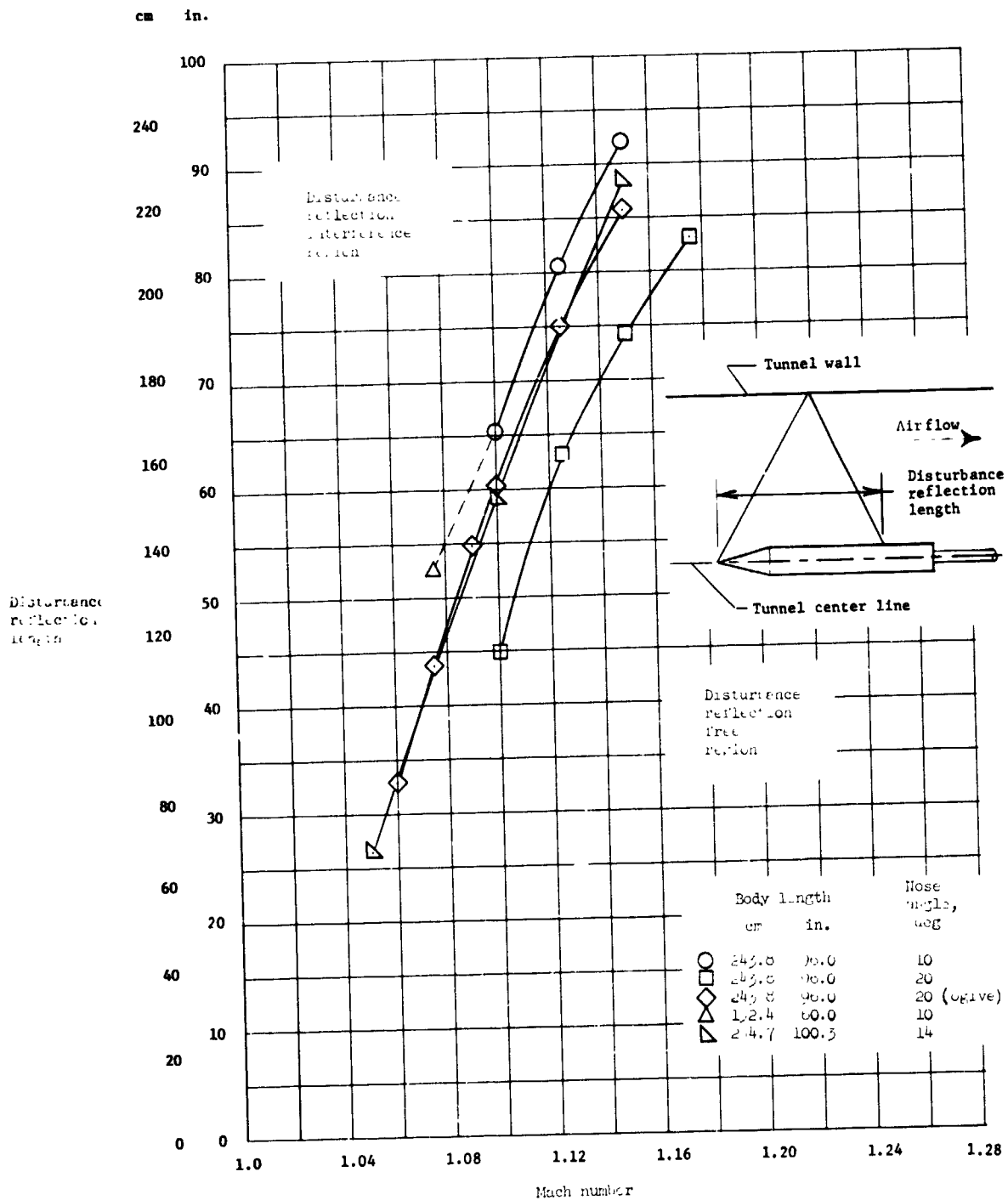
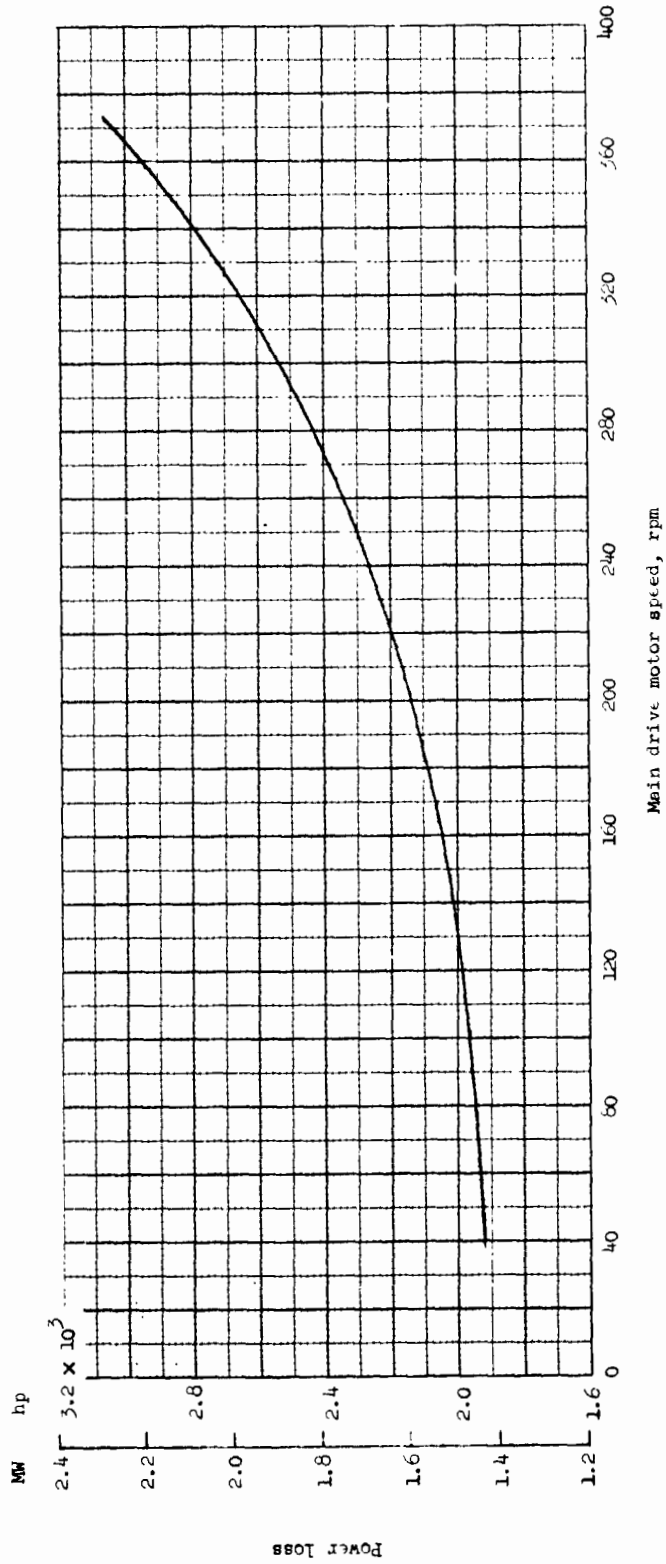Figure 46.- Boundary-reflected-disturbance lengths measured in the
Langley 16-foot transonic tunnel.

Figure 47. - Modified Kramer system power loss for each main drive motor based on maximum shaft power of 25.364 MW (34 000 hp) and synchronous speed of 400 rpm.
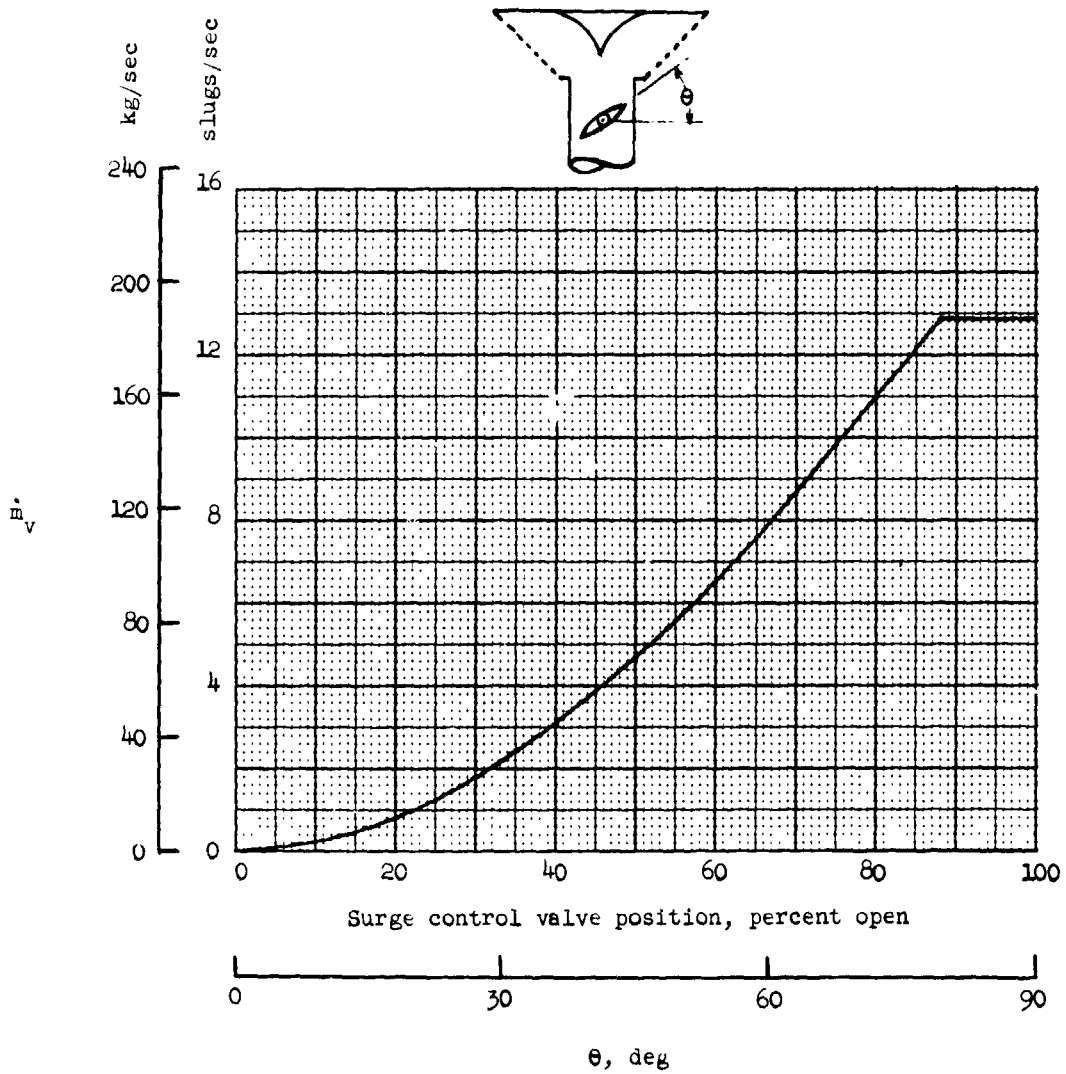
Figure 48.- Calculated mass flow through surge control valve.
$p_t = 101.32$ kN/m^2 (2116 lb/ft^2); $T_t = 15^o$ C (59° F).